DIGITAL COMPUTER LABORATORY
UNIVERSITY OF ILLINOIS
URBANA, ILLINOIS

REPORT NO. 137

PHASE PLANE THEORY OF TRANSISTOR BISTABLE CIRCUITS

by

Sergio Telles Ribeiro

June 6, 1963

(This work is being submitted in partial fulfillment of the requirements for the Degree of Doctor of Philosophy in Electrical Engineering, May, 1963, and was supported in part by the Office of Naval Research under contract Nonr-1834(15).)

DIGITAL COMPUTER LABORATORY
UNIVERSITY OF ILLINOIS
URBANA, ILLINOIS

REPORT NO. 137

PHASE PLANE THEORY OF TRANSISTOR BISTABLE CIRCUITS

by

Sergio Telles Ribeiro

June 6, 1963

(This work is being submitted in partial fulfillment of the requirements for the Degree of Doctor of Philosophy in Electrical Engineering, May, 1963, and was supported in part by the Office of Naval Research under contract Nonr-1834(15).)

ACKNOWLEDGMENTS

The author wishes to express his deep appreciation to his advisor, Professor W. J. Poppelbaum, for his advice, encouragement, and valuable suggestions to improve the manuscript. Thanks are also due to his colleagues Bruce E. Briley for his invaluable help with proofreading and Gabor K. Ujhelyi for his cooperation in the preparation of Chapter 6; to Mrs. Phyllis Olson for her unusual skill in typing this text, and to Kenneth C. Law and his draftsmen for their great ability and good will in the execution of the figures. Finally, the author wishes to thank his wife, Laura Beatriz, for her unconditional support, patience and understanding.

TABLE OF CONTENTS

TABLE OF CONTENTS (CONTINUED)

LIST OF TABLES

LIST OF ILLUSTRATIONS

A.1 Introduction

It is our purpose to establish a theory describing the state transition of transistor flipflops making use mostly of phase plane techniques, but using also a time or even frequency domain point of view whenever helpful. Based on such a theory, we further wish to devise practical engineering methods of analysis, design, and optimization of transistor flipflops.

We shall restrict ourselves to considering the asymmetric (Fig. A.1) and the Eccles-Jordan (Fig. A.2) flipflops, with constant current I_E fed into the common emitters, and except for a short discussion, we shall consider only the case of a rectangular trigger.

A.2 The Flipflop Differential Equation

Based on the differential equations relating terminal voltages with the charges at the junctions and diffusion tails in a transistor we obtain the transistor pair† characteristics below.

$$w_k = \frac{1}{2}[1 - (-1)^k \tanh x] \tag{A.1a}$$

$$z_k = \overset{o}{w}_k + \frac{1 - \alpha}{\alpha} w_k \tag{A.1b}$$

where k = 1, 2, is the transistor index used in Figs. 1 and 2, and the symbol $\overset{o}{x} = \frac{dx}{dt}$; besides,

$$x = x_1 - x_2 = \text{normalized base-to-base voltage}$$

† Throughout this volume the expression "transistor pair" refers to the pair of identical transistors with the constant current I_E fed into the common emitter, as in Figs. 1 and 2.

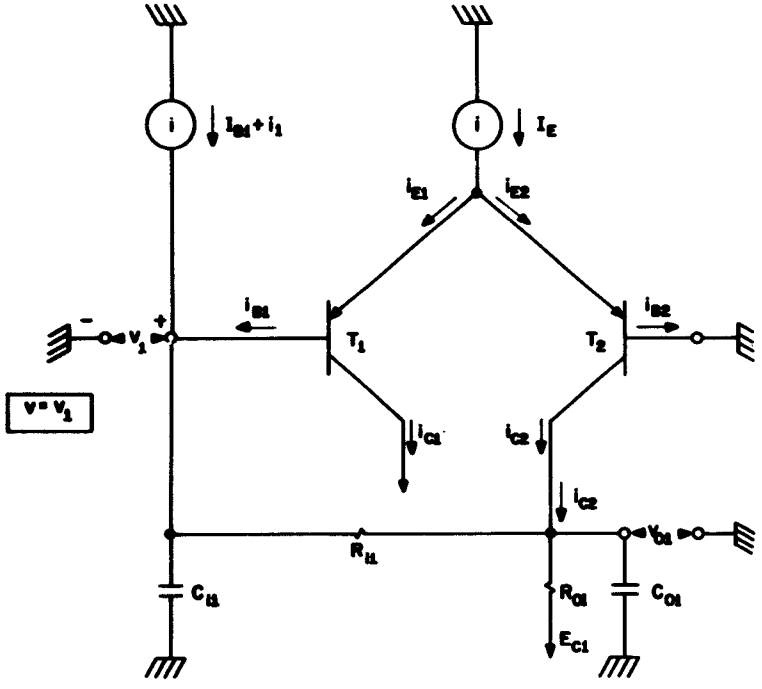

FIGURE A.1: THE ASYMMETRIC FLIPFLOP

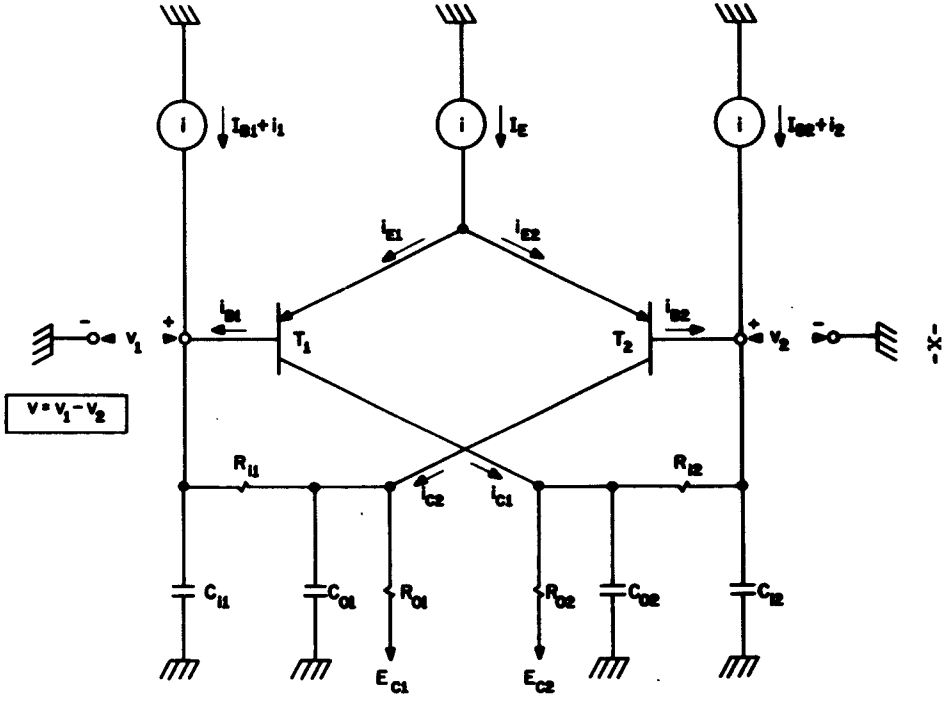

FIGURE A.2: THE ECCLES-JORDAN FLIPFLOP

$$x_k = \frac{qv_k}{2kT} = \text{normalized base voltages}^{\dagger}$$

$$w_k = \frac{i_{Ck}}{\alpha I_E} = \text{normalized collector current}$$

$$z_k = \frac{i_{Bk}}{\alpha I_E} = \text{normalized base current}$$

$$t = \frac{t'}{\tau} = \text{normalized time variable}$$

t' = real time variable

τ = collector time constant of the transistors

Equations (A.1) therefore, relate the collector and base currents of the transistor pair to the base-to-base voltage.

Analysis of the feedback networks yields a differential equation in the variable x_k for each value of k (k = 1, 2 for the Eccles-Jordan, but k = 1 for the asymmetric flipflop), respectively related to trigger plus base currents $(i_k + i_{Bk})$ and collector currents $i_{C\ell}$, $\ell \neq k$.

We shall concentrate our attention on the asymmetric flipflop. The result, after normalization, is:

$$\frac{\tau_i \tau_o}{\tau} \overset{oo}{x} + \frac{\tau_i + \tau_{oi} + \tau_o}{\tau} \overset{o}{x} + x = 2p \left\{ B + w_2 + \frac{\tau_{io}}{\tau} \left(\overset{o}{\theta}_1 + \overset{o}{z}_1 \right) + \frac{R_s}{R_o} \left(\theta_1 + z_1 \right) \right\} \tag{A.2}$$

where:

---

† The k in the denominator is the Boltzmann constant.

$$\left.\begin{aligned} \tau_i &= R_i C_i \\ \tau_{io} &= R_i C_o \\ \tau_{oi} &= R_o C_i \\ \tau_o &= R_o C_o \end{aligned}\right\} \text{ -- time constants}$$

$$B = \frac{I_B R_s + E_c}{\alpha I_E R_o} = \text{biasing condition}$$

$$\theta_1 = \frac{i_1}{\alpha I_E} = \text{normalized trigger current actually fed into the flipflop circuit}$$

Since θ_1 is the trigger current actually fed into the flipflop, it depends on the nature of the trigger circuit, and depends also on x itself.

In general, if the trigger circuit of transistor T_k is represented by a current source of intensity i_{tk} and shunt interval conductances G_k, we get

$$\theta_k = s_k - G_k x \qquad (A.3)$$

where,

$$s_k = \frac{i_{tk}}{\alpha I_E} = \text{normalized trigger current source intensity.}$$

Use of (A.1) with (A.2) and (A.3) will result in a second order non-linear differential equation in x containing terms in tanh x along with its first and second derivatives, and under a forcing function $s_1(t)$, and its first derivative $\overset{o}{s}_1(t)$. This equation shall be called "the flipflop equation."

A.3 Piecewise Linear Approximation

A general solution to the flipflop equation is not known. Let us consider, however, instead of (A.1), the characteristics below:

$$w_k = \frac{1}{2}[1 - (-1)^k \varphi(x)] \tag{A.4a}$$

$$z_k = \overset{o}{w}_k + \frac{1-\alpha}{\alpha} w_k, \text{ (as before)} \tag{A.4b}$$

where,

$$\varphi(x) = \begin{cases} -1, & x \leq -\frac{1}{\gamma} : \text{ region I} \\ \gamma x, & |x| \leq \frac{1}{\gamma} : \text{ region II} \\ +1, & x \geq +\frac{1}{\gamma} : \text{ region III} \end{cases} \tag{A.5}$$

and γ is selected so that $\varphi(x)$ is the best possible piecewise linear approximation to tanh x.† We are, therefore, considering an ideal transistor pair whose behavior approximates that of the real transistor pair, but whose characteristics are piecewise linear functions.

Equations (A.2), (A.3) and (A.4) will furnish equation (A.6), i.e., a second order differential equation in x, where the forcing functions $s_1(t)$ and $\overset{o}{s}_1(t)$, although nonlinear in the whole range of x, will be formed by three linear equations, respectively valid in the three regions as in equation (A.5) above. The second derivative of $\varphi(x)$ is a pair of impulse functions occurring in the transitions of x into and out of region II.

---

† With $\epsilon(x) = \varphi(x) - \tanh x$, both a criterion of getting γ such that $\max_x \epsilon(x)$ is minimum or γ such that $\int_0^\infty \epsilon(x)dx = 0$ will lead to $\gamma \approx 0.7$.

$$a\overset{oo}{x} + b\overset{o}{x} + cx = d + m\overset{o}{s} + ns + f(\overset{o}{x}) \cdot \delta(x \pm \frac{1}{\gamma}) \qquad (A.6)$$

where a, b, c, d, m depend on the region containing x, i.e., they are step functions of x, discontinuous at $x = \mp \frac{1}{\gamma}$.

A solution of (A.6) can be obtained by solving a second order linear differential equation in each region, using the final conditions in each region as the initial conditions of the next region. The impulse functions can be considered as discontinuities in the value of $\overset{o}{x}$.

A.4 The Rectangular Trigger and the Phase Plane Portrait

If $s_1(t)$ is a rectangular function of time, of duration T, then $\overset{o}{s}_o(t)$ is also a pair of impulse functions and can be taken account of as discontinuities of $\overset{o}{x}$, at t = 0 and t = T, whereas $s_1(t)$ itself can be represented as a constant equal to W if the trigger is ON and 0 (zero) if the trigger is OFF.

We have, so far, succeeded in reducing the analysis of a flipflop to the solution of three equations like (A.7) below:

$$a\overset{oo}{x} + b\overset{o}{x} + cx = D \qquad (A.7)$$

$$D = \begin{cases} d + W & \text{if the trigger is ON} \\ d & \text{if the trigger is OFF} \end{cases}$$

in three regions of values of x, matching their solutions in the boundaries $x = \mp \frac{1}{\gamma}$, and considering discontinuities of $\overset{o}{x}$ at t = 0, t = T, and at $x = \mp \frac{1}{\gamma}$.

The phase plane equation corresponding to (A.7) is

$$\frac{dy}{dx} = \frac{D - cx}{ay} - \frac{b}{a} \qquad (A.8)$$

where

$$y = \overset{o}{x}$$

The singular points (points of $\overset{o}{y} = y = 0$) are given by the solutions of

$$D - cx = 0 \tag{A.9}$$

i.e.,

$$x = \frac{D}{c} \tag{A.10}$$

and the nature of these singular points can be analyzed by studying the natural frequencies of the system (A.11) below in a neighborhood around each singularity.

$$\left.\begin{aligned} \overset{o}{x} &= y \\ \overset{o}{y} &= \frac{d}{a} - \frac{c}{a}x - \frac{b}{a}y \end{aligned}\right\} \tag{A.11}$$

This analysis shows that, if the trigger is OFF, and under proper biasing conditions, these singularities are two stable nodes,† one in each region I and III, and a saddle point†† in region II.

The action of a trigger of amplitude W is essentially to shift the stable nodes by an amount $\Delta x = \frac{nW}{c}$, and the saddle point by an amount $\Delta x = -\frac{nW}{c}$ (parameters always calculated in the correct regions!).

---

† In a neighborhood of a stable node both natural frequencies of the system are real and negative (by definition).

†† In a neighborhood of a saddle point the natural frequencies of the system are real and have opposite signs (by definition).

When a singular point is shifted out of its proper region we say it has become "virtual" because its nature still determines the behavior of the system in that region, but it does not really exist. There is a value of W above which the saddle point and one of the stable nodes become virtual. Then the representative point P of the system will describe a trajectory towards the remaining stable node. When the trigger is turned OFF this remaining stable node (and also the other two singularities) returns to its resting position; P will now move towards this point, which is, in effect, one of the two stable states of the flipflop. Figures A.3a, b, c, d illustrate a transition.

Clearly, improper biasing may result in other singularity configurations which will not correspond to flipflop behavior.

Study of some geometrical properties of the flipflop phase plane portrait, expecially the study of the separatrices and of certain properties of the trajectories can be made by analytical solutions to equation (A.8). The usefulness of this approach is limited, however, by the complexity of the algebraic expressions involved.

A.5 Engineering Methods for the Solution of Flipflop Problems

These methods consist essentially of the drawing of figures like A.3, i.e., phase plane portraits which are good approximations to the true phase plane portrait of a trajectory.

The time durations of any portion of a trajectory, say, between two points P_a and P_b is given by:

$$T_{ab} = t_b - t_a = \int_{x_a}^{x_b} \frac{1}{y(\xi)}\, d\xi$$

But if y(x) is a straight line,

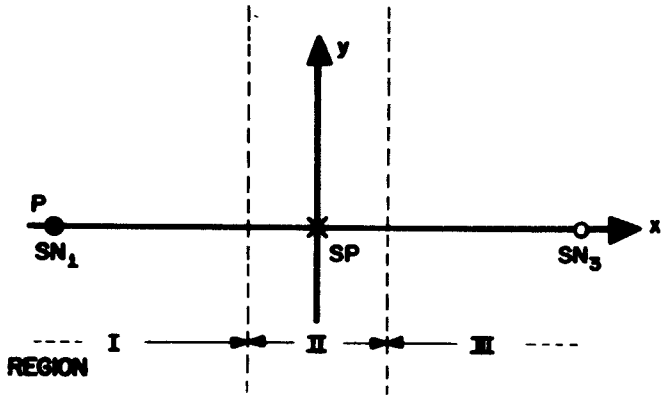

a) STATE 1: P IS IN SN_1

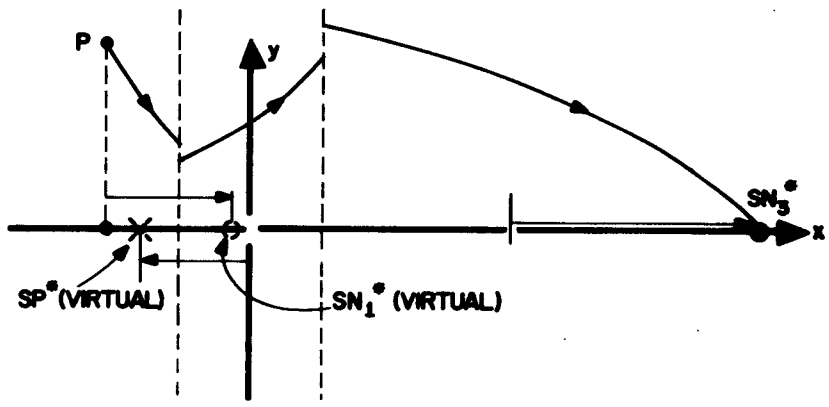

b) TRIGGER ON: P GOES TO SN_3^*

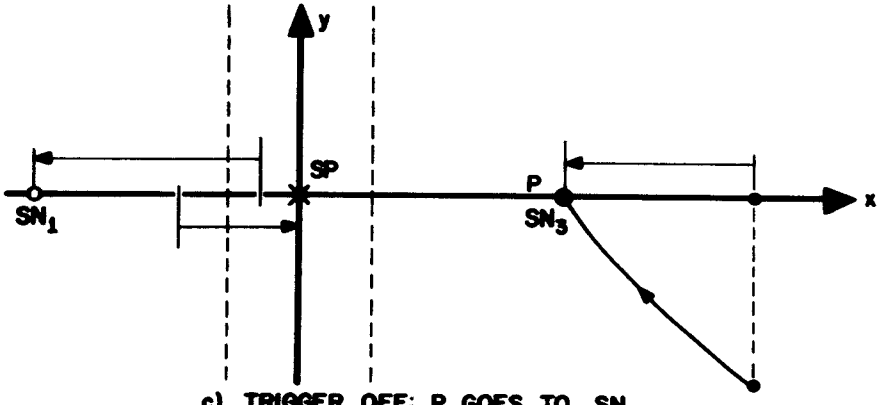

c) TRIGGER OFF: P GOES TO SN_3.

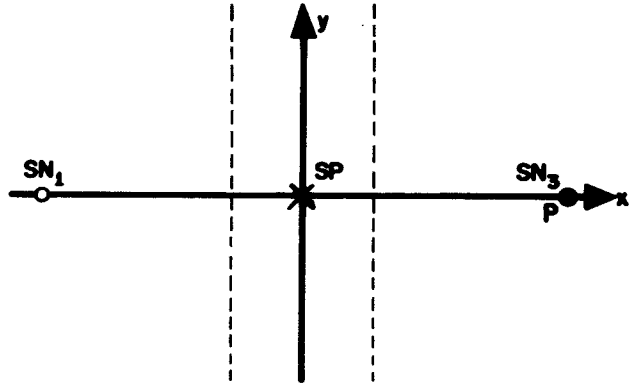

d) STATE 3: P IS IN SN_3.

FIGURE A.3: AN EXAMPLE OF A TRANSITION.

$$T_{ab} = t_a - t_b = \frac{\Delta x}{\Delta y} \ln \frac{y_b}{y_a}$$

Various procedures can be devised for the drawing of these approximate portraits once the coefficients of (A.8) are known in every region, both for trigger ON and OFF. From any approximate form of $y(x)$ it is a simple matter to obtain any waveform of interest, such as $x(t)$, $w_k(t)$, $z_k(t)$, etc., by very simple graphical constructions.

Even though only the asymmetrical flipflop is considered in this Abstract, it is very simple to show that the symmetric Eccles-Jordan flipflop is formally equivalent to the asymmetric circuit.

A.6 Extensions

A.6.1--Simple formulae for fast estimates of flipflop transition times can be derived from geometrical properties of the transition phase plane portraits.

A.6.2--The general (nonsymmetric) Eccles-Jordan flipflop can be treated by a modified phase plane which takes into account the two sets of variables (x_k, y_k), $k = 1, 2$, with some use of curves in the time domain $x_k(t)$, and of a plane (x_1, x_2). In some cases where there is a certain relationship between its parameters a nonsymmetric flipflop may be reduced to the asymmetric case.

A.6.3--Some degenerate cases, where one or more capacitances are zero can have $y(x)$ expressed in analytical and closed form.

A.6.4--Flipflops under other types of trigger can be studied by other techniques than phase plane techniques, such as frequency or time domain techniques.

A.7 Practical Results and Future Developments

Comparison of theoretical with experimental results indicates that an error of the order of $\pm$ 10 per cent is to be expected from the application of this theory.

There are strong indications that a large part of this error is caused by the fact that, although $\varphi(x) \approx \tanh x$, this is not so for the first and second derivatives of these functions. However, the results are satisfactory, and the theory could be extended in future to consider, for example: the non-linearity of the capacitances involved, inductances in the passive network, or perhaps the fact that these are distributed parameters. In another direction, it could be improved by a formal mathematical investigation of the piecewise linear approximation method for solving nonlinear differential equations.

1. INTRODUCTION

Many attempts have been made in the past to establish a theory of bistable systems. The nonlinear nature of bistable circuits (flipflops), however, makes it impractical to approach the analysis of such systems by means of mathematical techniques developed specially for the study of linear systems.

Nevertheless, several flipflop theories have been devised making use of strictly linear techniques [3, 16, 19, 23].† However, these theories, one way or another, had limited objectives. Typically, each of them aims at a specific problem among, for example, obtaining an approximation for the transition time, or finding minimum values for trigger duration and amplitude, or studying some aspect of stability, etc. These limited objectives could be, and were, attained with the linear techniques employed.

Adopting a quite different point of view, flipflop theory can be reduced to the study of nonlinear bistable equations or systems of equations (in general two first order equations) [26, 27]. The phase plane is the mathematical tool that immediately suggests itself for this type of problem [1, 26].

In the literature, authors are usually not concerned with the analysis of any specific physical problem, or mathematical model, but just with the development of the mathematical technique itself. Objectives here were also limited, since the establishment of a general theory was not aimed at, but it was desired to show that some results could be obtained by applying phase-plane methods to certain types of equations [26, 27].

It seems natural to attempt a general analysis of bistable physical systems using the phase-plane as the main technique. However, a general analysis of this kind would be of very little use (if it could be made at all)

---

† A square-bracketed set of numbers refers to works listed under "Bibliography" at the end of this dissertation.

first because nonlinear systems do not lend themselves too easily to generalization and second, because whatever generalization we would achieve, we would pay by not being specific about the most important of all electric bistable systems (we consider the common switch as being a mechanical bistable system...) and the only one in which we are really interested, namely, the transistor flipflop.

Thus the analysis of transistor flipflops--and of these only--appears to be attractive, since specific results and methods can be obtained and applied immediately. This is the objective of this report: a general analysis of transistor flipflops by phase-plane methods. It is general in the sense that any information about the flipflop behavior can be obtained from it, and also in the sense that the general (nonsymmetric) Eccles-Jordan flipflop is considered. Its differential equations are established along with the more important cases of the asymmetric (one base grounded) and the symmetric flipflops, and we go as far as suggesting means to analyze this general case on a special phase-plane.

Of course, phase-plane treatment practically outlaws any other but the rectangular trigger (as will be clear in the sequel). However, the equations established do not demand phase-plane treatment; in fact, for other types of trigger, numeric solutions may be necessary. But we shall concentrate our attention on the rectangular trigger case. The first part of the theory is concerned with the establishment of the general† dynamic transistor flipflop equations.

† In a common emitter coupling configuration, i.e., we consider a general Eccles-Jordan, and the asymmetric flipflops.

Next the problem of approximating the system is discussed; a set of approximate differential equations is established on a basis of piecewise linear approximation to the original system.

This set of approximate equations is then analyzed in the phase-plane using the time domain whenever expedient; this analysis includes the study of existence and nature of singular points and the description of separatrices. Then follows a discussion of triggering conditions, establishing their relationship with the system parameters. A specially detailed discussion of trajectories and their relation to parameters and trigger is presented. Some theorems about the geometry of the system phase-plane portrait are proved.

On the basis of the above analysis some techniques are described for the actual computation of trajectories, transition times, waveforms, or general characteristics of a given flipflop driven by a given triggering circuit. Especially simple formulae are presented with the purpose of better understanding the qualitative influence of the various parameters; these formulae are also useful when a quick estimate of some transition characteristics is needed.

Several extensions to the theory are also discussed, such as three degenerate cases, the nonsymmetric Eccles-Jordan, and other types of trigger.

Finally, some experiments are reported on and their results compared with the theoretical results.

2. THE FLIPFLOP DIFFERENTIAL EQUATION

2.1 Introduction

We shall try to find an equation which will not only describe the flipflop behavior but which is also relatively simple. This is a rather difficult task, since the number of equations describing such a circuit is not finite. However, if we add the further requirement that the state variable be a natural circuit variable, i.e., either a node-to-node voltage or a branch current, then the possible number of such equations is reduced to about a dozen possibilities.

A comparison among the most promising ones leads us to select the base-to-base voltage as the circuit state variable. The ensuing analysis illustrates the relative simplicity of such a choice.

2.2 The Transistor Pair Transfer Equation

Analysis of the transistor pair presented in Fig. 1 furnishes the following system of equations, which represents an entirely general description of the circuit both statically and dynamically [2, 15].

$$i_{E1} = \overset{\circ}{q}_{E1} + \overset{\circ}{q}_{B1} + j_{E1}(\exp\eta v_{E1} - 1) - \alpha_{C1} j_{C1}(\exp\eta v_{C1} - 1) \qquad (2.1)$$

$$i_{E2} = \overset{\circ}{q}_{E2} + \overset{\circ}{q}_{B2} + j_{E2}(\exp\eta v_{E2} - 1) - \alpha_{C2} j_{C2}(\exp\eta v_{C2} - 1) \qquad (2.2)$$

$$i_{C1} = -\overset{\circ}{q}_{C1} + \alpha_{E1} j_{E1}(\exp\eta v_{E1} - 1) - j_{C1}(\exp\eta v_{C1} - 1) \qquad (2.3)$$

$$i_{C2} = -\overset{\circ}{q}_{C2} + \alpha_{E2} j_{E2}(\exp\eta v_{E2} - 1) - j_{C2}(\exp\eta v_{C2} - 1) \qquad (2.4)$$

$$i_{B1} = \overset{\circ}{q}_{E1} + \overset{\circ}{q}_{B1} + \overset{\circ}{q}_{C1} + (1 - \alpha_{E1}) j_{E1}(\exp\eta v_{E1} - 1) - (1 - \alpha_{C1}) j_{C1}(\exp\eta v_{C1} - 1) \qquad (2.5)$$

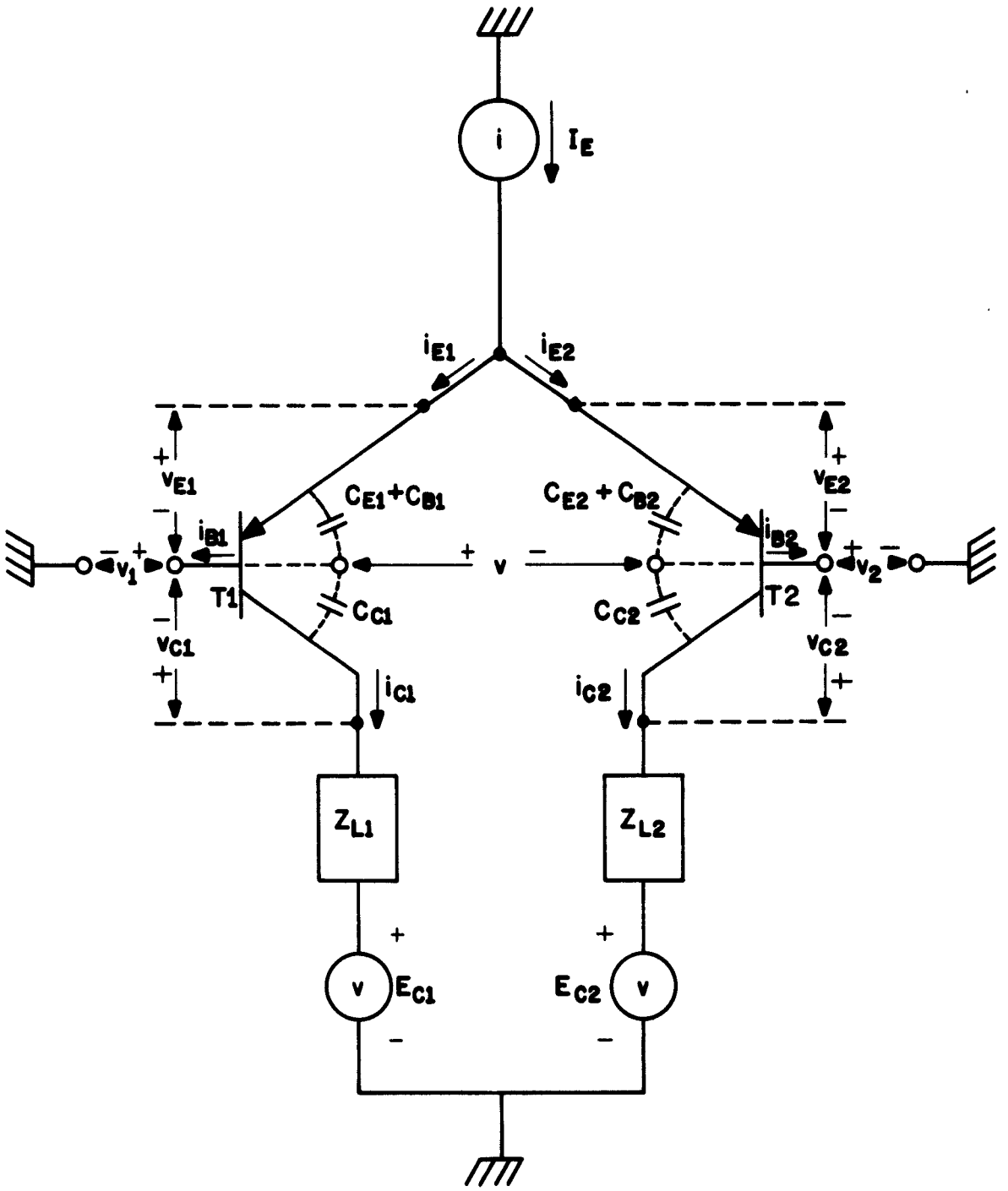

FIGURE 1: LOADED COMMON EMITTER COUPLED TRANSISTOR PAIR.

$$i_{B2} = \overset{\circ}{q}_{E2} + \overset{\circ}{q}_{B2} + \overset{\circ}{q}_{C2} + (1 - \alpha_{E2})j_{E2}(\exp\eta v_{E2} - 1) - (1 - \alpha_{C2})j_{C2}(\exp\eta v_{C2} - 1) \tag{2.6}$$

$$i_{E1} + i_{E2} = I_E \tag{2.7}$$

$$v_{E2} - v_{E1} = v \tag{2.8}$$

$$v_{C1} = E_{C1} + R_{L1}i_{C1} - v_1 \tag{2.9}$$

$$v_{C2} = E_{C2} + R_{L2}i_{C2} - v_2 \tag{2.10}$$

$$v_1 - v_2 = v \tag{2.11}$$

In the system above:

a) The symbol $\overset{\circ}{x}$ means $\frac{dx}{dt'}$, and t' is the time variable.

b) $\eta = \frac{\epsilon}{kT}$, with $\begin{cases} \epsilon = \text{electron charge} \\ k = \text{Boltzmann constant} \\ T = \text{absolute temperature} \end{cases}$

c) R_{L1}, R_{L2} are the load resistances.

d) q_{Ek}, q_{Bk}, q_{Ck} are the charges stored in transistor T_k capacitances:

q_{Ek} at emitter diffusion tail and depletion layer of the emitter-base junction.

q_{Bk} at the base diffusion capacitance.

q_{Ck} at the depletion layer of the collector to base junction.

e) j_{Ek}, j_{Ck} are the saturation currents of transistor T_k, respectively of its emitter-base and collector-base junctions, measured with the opposite terminal short circuited to the base.

f) α_{Ek}, α_{Ck} the normal and inverse alphas of transistor T_k respectively from emitter to collector and from collector to emitter.

Obs.: Notice the unusual convention of signs, which has been adopted in this report for convenience only.

Comments: The system has 11 equations and 13 variables; usually variables v_1 and v_2 would be independent, and then any other variable can be expressed as functions of them.

However, this system of equations can be considerably reduced by making the following simplifying assumptions (see Fig. 2).

The transistors and operation points are such that the following relations hold, accordingly simplifying equations (2.1) through (2.6):

$$j_{E1}(\exp\eta v_{E1} - 1) \gg \alpha_{C1} j_{C1}(\exp\eta v_{C1} - 1) \approx -\alpha_{C1} j_{C1} \tag{2.12}$$

$$j_{E2}(\exp\eta v_{E2} - 1) \gg \alpha_{C2} j_{C2}(\exp\eta v_{C2} - 1) \approx -\alpha_{C2} j_{C2} \tag{2.13}$$

$$\alpha_{E1} j_{E1}(\exp\eta v_{E1} - 1) \gg j_{C1}(\exp\eta v_{C1} - 1) \approx -j_{C1} \tag{2.14}$$

$$\alpha_{E2} j_{E2}(\exp\eta v_{E2} - 1) \gg j_{C2}(\exp\eta v_{C2} - 1) \approx -j_{C2} \tag{2.15}$$

$$(1 - \alpha_{E1}) j_{E1}(\exp\eta v_{E1} - 1) \gg (1 - \alpha_{C1}) j_{C1}(\exp\eta v_{C1} - 1) \approx -(1 - \alpha_{C1}) j_{C1} \tag{2.16}$$

$$(1 - \alpha_{E2}) j_{E2}(\exp\eta v_{E2} - 1) \gg (1 - \alpha_{C2}) j_{C2}(\exp\eta v_{C2} - 1) \approx -(1 - \alpha_{C2}) j_{C2} \tag{2.17}$$

For each transistor, the following relations hold, accordingly simplifying equations (2.1) through (2.6):

$$q_{E1} \ll q_{B1} \quad \text{and} \quad q_{C1} \ll q_{B1} \tag{2.18}$$

$$q_{E2} \ll q_{B2} \quad \text{and} \quad q_{C2} \ll q_{B2} \tag{2.19}$$

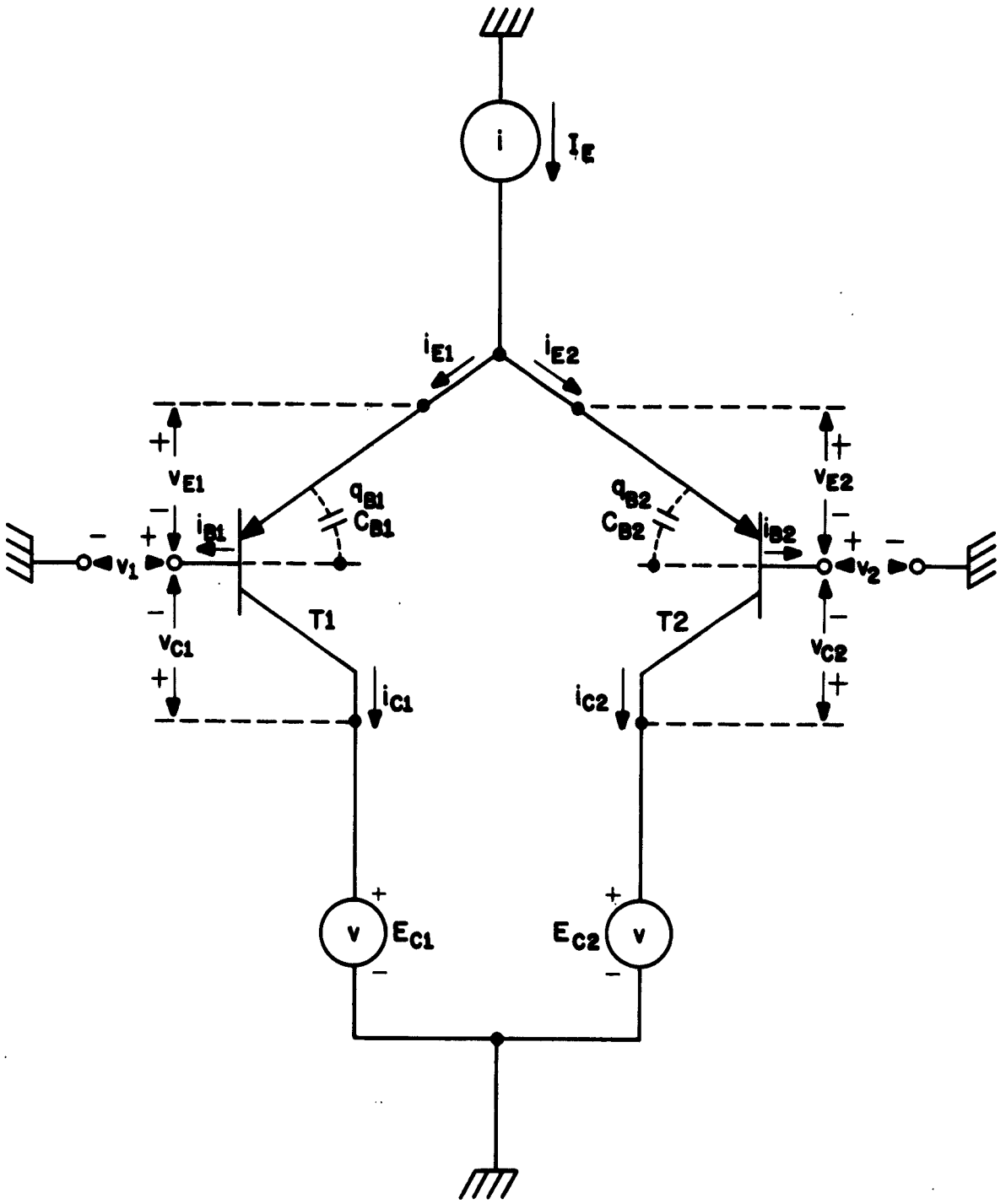

FIGURE 2: UNLOADED TRANSISTOR PAIR, WITH JUNCTION CAPACITANCES NEGLECTED.

$$q_{B1} = \tau_{C1} i_{C1} \quad \text{and} \quad q_{B2} = \tau_{C2} i_{C2} \tag{2.20}$$

where τ_{Cj} is the "collector time constant" of transistor T_j. The transistors are such that the following relations hold, accordingly modifying equations (2.1) through (2.6):

$$\tau_{C1} = \tau_{C2} = \tau \tag{2.21}$$

$$\alpha_{E1} = \alpha_{E2} = \alpha \tag{2.22}$$

$$j_{E1} = j_{E2} = j \tag{2.23}$$

τ, α, j independent of any system variable. (2.24)

Assumptions (2.12) through (2.17) divide the system (2.1) through (2.11) into two interdependent systems, namely (2.1) through (2.8) and (2.9) through (2.11). The first has eight equations and nine variables, so that all variables are determined if one of them is given; v is the "natural" independent variable. The second system has three equations and seven variables, so that four variables must be specified; in general, v_1 and v_2 would be given (thus specifying v by (2.11)) and also i_{C1} and i_{C2} which are solutions of the first system of equations.

These approximations restrict our analysis to nonsaturating matched transistors. Constancy of parameters with respect to system variables as well as negligible junction capacitances are fairly strong assumptions, since they cannot occur in practice [15]; however, we feel that the increased complexity involved in trying to take into account such things is too high a price to pay for the small increase in accuracy to be obtained.

We obtain the system of equations below by substituting (2.12) through (2.24) into equations (2.1) through (2.8):

$$i_{E1} = \tau i^{\circ}_{C1} + \frac{1}{\alpha} i_{C1} \tag{2.25}$$

$$i_{E2} = \tau i^{\circ}_{C2} + \frac{1}{\alpha} i_{C2} \tag{2.26}$$

$$i_{C1} = \alpha j_E \exp \eta v_{E1} \tag{2.27}$$

$$i_{C2} = \alpha j_E \exp \eta v_{E2} \tag{2.28}$$

$$i_{B1} = \tau i_{C1} + \frac{1 - \alpha}{\alpha} i_{C1} \tag{2.29}$$

$$i_{B2} = \tau i_{C2} + \frac{1 - \alpha}{\alpha} i_{C2} \tag{2.30}$$

$$i_{E1} + i_{E2} = I_E \tag{2.31}$$

$$v_{E2} - v_{E1} = v \tag{2.32}$$

Here we have neglected all terms j_{Ck}, $\alpha_{Ck} j_{Ck}$, $(1 - \alpha_{Ck}) j_{Ck}$; in the same spirit we have used the approximation

$$j_{Ek} \exp \eta v_{Ek} \approx j_{Ek} (\exp \eta v_{Ek} - 1) \tag{2.33}$$

which is not strictly valid. Actually, it is only valid as long as v_{E1} is positive, but not if v_{E1} is negative. However, to use this approximation (or should we call it a substitution!) for all the range of v_{Ek} is equivalent to connecting a current source of strength j_{Ek} in parallel with the emitter-base junction of T_k, in a direction such as to yield input current zero when $v_{Ek} \to -\infty$.

This will make very little difference as far as results are concerned, but will considerably simplify the algebra involved. To be sure, it will tend to compensate for the fact that we have already neglected the collector-base junction saturation current, yielding even a better composite characteristic for the transistor pair.

Equations (2.9) through (2.11) are now irrelevant since we seek to express the currents as functions of v, which can be obtained just by solving system of equations (2.25) through (2.32).

For convenience, we apply the following transformations of variables to this system:

$$t = \frac{t'}{\tau} \tag{2.34}$$

$$w_k = \frac{i_{Ck}}{\alpha I_E}, \qquad k = 1, 2 \tag{2.35}$$

$$z_k = \frac{i_{Bk}}{\alpha I_E}, \qquad k = 1, 2 \tag{2.36}$$

$$x = \frac{1}{2}\eta v \tag{2.37}$$

R_0 is the output resistor as shown in Fig. 3.

From now on, the symbol $\overset{o}{x}$ will be used for $\frac{dx}{dt}$, unless otherwise specified. We obtain:

$$\alpha(\overset{o}{w}_1 + \overset{o}{w}_2) + (w_1 + w_2) = 1 \tag{2.38}$$

$$w_2 = w_1 \exp 2x \tag{2.39}$$

$$\overset{o}{w}_2 = (\overset{o}{w}_1 + 2\overset{o}{x}w_1)\exp 2x \tag{2.40}$$

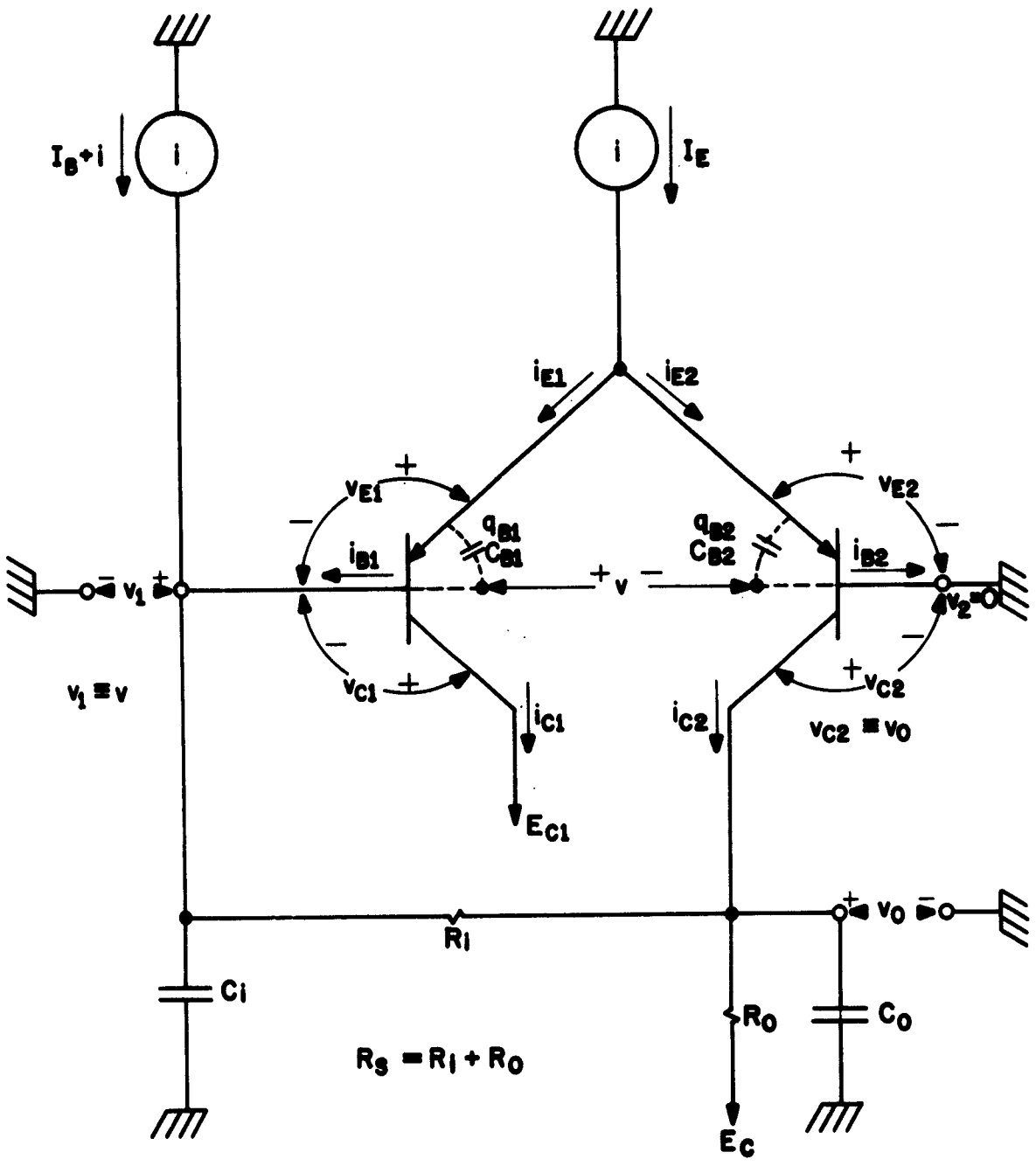

FIGURE 3: ASYMMETRIC FLIPFLOP

$$z_1 = \overset{o}{w}_1 + \frac{1 - \alpha}{\alpha} w_1 \tag{2.41}$$

$$z_2 = \overset{o}{w}_2 + \frac{1 - \alpha}{\alpha} w_2 \tag{2.42}$$

from which we get, using (2.38), (2.39) and (2.40):

$$\overset{o}{w}_1 + \left\{\frac{1}{\alpha} + \overset{o}{x}(1 + \tanh x)\right\} w_1 = \frac{1}{2}(1 - \tanh x) \tag{2.43}$$

This equation can be written in the form:

$$M dt + N dw_1 = 0 \tag{2.44}$$

If this is done, then we have:

$$\frac{1}{N}\left(\frac{\partial M}{\partial w_1} - \frac{\partial N}{\partial t}\right) = \left\{\frac{1}{\alpha} + \overset{o}{x}(1 + \tanh x)\right\} = g(t) \tag{2.45}$$

where $g(t)$ is only a function of t, i.e., it is independent of w_1; here we assume that $x = x(t)$ is a given function of t, independent of w_1.

Then $\mu(t) = \exp\left[\int g(t)dt\right]$ is an integrating factor for equation (2.43) [8]. We have then:

$$\mu(t) = \exp\left\{\frac{t}{\alpha} + \int (1 + \tanh x)\overset{o}{x}dt\right\} \tag{2.46}$$

But

$$\int (1 + \tanh x)\overset{o}{x}dt = \int (1 + \tanh x)dx = x + \ell n(\cosh x) + \text{const.} \tag{2.47}$$

Hence, ignoring the constant,

$$\mu(t) = \exp\left(\frac{t}{\alpha} + x\right) \cdot \cosh x = \frac{\exp\frac{t}{\alpha}}{1 - \tanh x}. \tag{2.48}$$

The differential equation can now be easily solved.

Let $F(w_1,t) = 0$ be the solution; then:

$$\left.\begin{aligned} &\frac{\partial F}{\partial w_1} = \mu(t) \qquad \text{(since M = 1)} \\ &\text{and} \\ &\frac{\partial F}{\partial u} = N\mu(t) \end{aligned}\right\} \tag{2.49}$$

We get from (2.46):

$$F(w_1,t) = w_1 \cdot \mu(t) + f(t) = 0 \tag{2.50}$$

and from (2.49) and (2.50):

$$N\mu(t) = w_2 \cdot \overset{o}{\mu}(t) + \overset{o}{f}(t) \tag{2.51}$$

Therefore

$$\overset{o}{f}(t) = -\frac{1}{2}(1 - \tanh x)\mu(t) \tag{2.52}$$

So:

$$f(t) = -\frac{1}{2}\int(1 - \tanh x) \cdot \mu(t)dt \tag{2.53}$$

From (2.48) into (2.53):

$$f(t) = -(\frac{\alpha}{2} \exp \frac{t}{\alpha} + \text{const.}) \tag{2.54}$$

From (2.50), explicitating w_1, we finally get:

$$w_1 = \frac{1}{2}(1 - \tanh x)[1 + C\exp(-\frac{t}{\alpha})] \tag{2.55}$$

where C is an arbitrary constant determined by some initial charge stored in the bases prior to the moment $t = t_0$ when the circuit takes on the configuration described by (2.43). Therefore, for all practical purpose $C\exp(-\frac{t}{\alpha})$ is zero, since we can assume this configuration to be in existence for an arbitrarily long time; we finally have, using (2.56), (2.39), (2.41) and (2.42):

The "transfer functions":

$$w_1 = \frac{1}{2}(1 - \tanh x) \tag{2.56}$$

$$w_2 = \frac{1}{2}(1 + \tanh x) \tag{2.57}$$

and the "input functions":

$$z_1 = \frac{1}{2}\left\{\frac{1-\alpha}{\alpha}(1 - \tanh x) - \overset{o}{x} \cdot \operatorname{sech}^2 x\right\} \tag{2.58}$$

$$z_2 = \frac{1}{2}\left\{\frac{1-\alpha}{\alpha}(1 + \tanh x) + \overset{o}{x} \cdot \operatorname{sech}^2 x\right\} \tag{2.59}$$

For completion, we have, with k = 1, 2

$$\overset{o}{z}_k = (-1)^k \frac{1}{2}\left[\frac{1-\alpha}{\alpha}\overset{o}{x} + \overset{oo}{x} - 2(\overset{o}{x})^2 \tanh x\right] \cdot \operatorname{sech}^2 x \tag{2.60}$$

which are the characteristic functions for a transistor pair connected as in Fig. 2.

As a corollary of this solution, we notice that, at all times, the following relations hold:

$$\left.\begin{aligned} w_1 + w_2 = 1 \quad &\Longrightarrow \quad i_{C1} + i_{C2} = \alpha I_E \\ z_1 + z_2 = \frac{(1-\alpha)}{\alpha} \quad &\Longrightarrow \quad i_{B1} + i_{B2} = (1-\alpha) I_E \end{aligned}\right\} \qquad (2.61)$$

which check with (2.7): $i_{E1} + i_{E2} = I_E$.

2.3 The Asymmetric Flipflop

The asymmetric flipflop shown in Fig. 3 has a feedback network whose configuration depends on the trigger circuit, as shown in Figs. 4a and 4b.

However, we can obtain the equilibrium equation for this network assuming an arbitrary trigger current i, which can be replaced by its value when a trigger is specified (see section 2.5).

Analysis of the circuit of Fig. 4a yields:

$$\tau_i \tau_o \overset{\infty}{v}_i + (\tau_i + \tau_{oi} + \tau_o)\overset{\circ}{v}_1 + v_1 = R_o i_{C2} + I_B R_s + E_C + R_o \tau_{io}(\overset{\circ}{i} + \overset{\circ}{i}_{B1}) + R_s(i + i_{B1}) \qquad (2.62)$$

where:

$$\text{a)} \quad \tau_i = R_i C_i \qquad (2.63a)$$

$$\text{b)} \quad \tau_o = R_o C_o \qquad (2.63b)$$

$$\text{c)} \quad \tau_{io} = R_i C_o \qquad (2.63c)$$

$$\text{d)} \quad \tau_{oi} = R_o C_i \qquad (2.63d)$$

$$\text{e)} \quad R_s = R_i + R_o \qquad (2.63e)$$

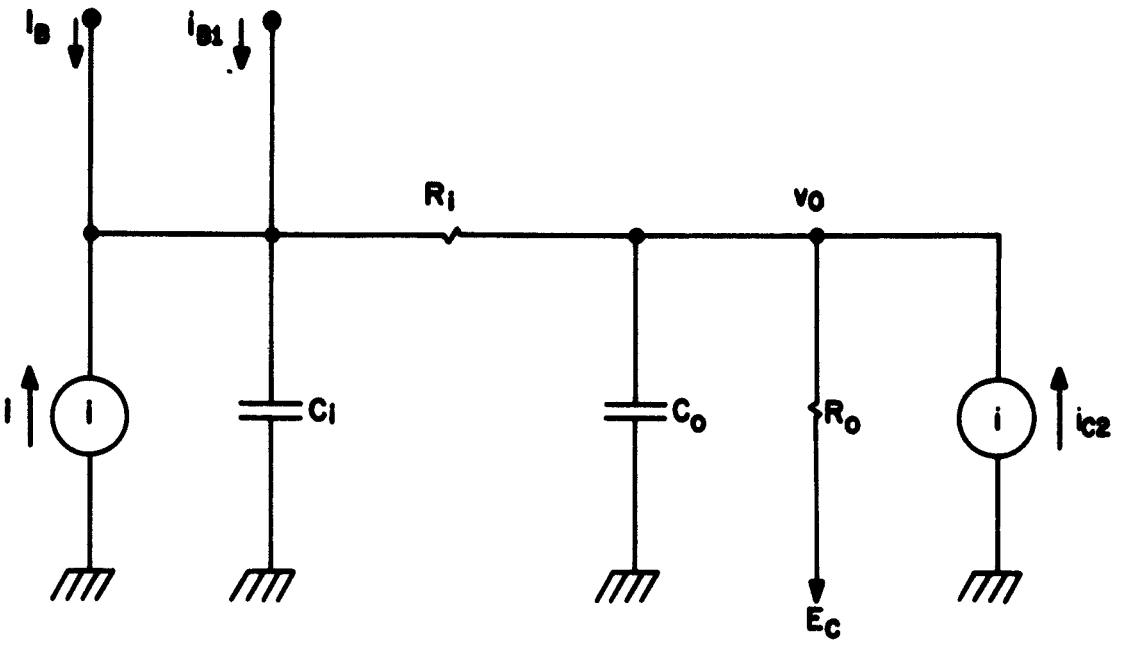

a) FEEDBACK NETWORK AND EQUIVALENT CURRENT SOURCE FEEDING TRIGGER CURRENT i_t.

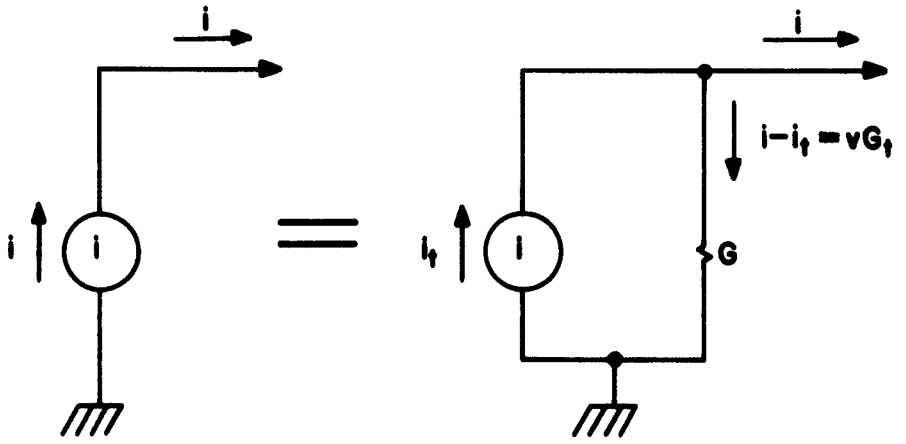

b) THE CURRENT SOURCE WITH AN INTERNAL CONDUCTANCE G IS REPLACED BY AN IDEAL VOLTAGE SOURCE WHOSE OUTPUT IS i.

FIGURE 4: TRIGGER SOURCES

Notice that in this asymmetric flipflop (Fig. 3) $v_1 \equiv v$. Let us apply to (2.62) the same transformations of variables used in section 2.2, i.e., equations (2.34) through (2.37), and also (2.64) below (a similar transformation for the trigger current):

$$\theta = \frac{i}{\alpha I_E} \tag{2.64}$$

The result, with $\overset{o}{x}$ again standing for $\frac{dx}{dt}$, will be:

$$\frac{\tau_i \tau_o}{\tau^2} \overset{oo}{x} + \frac{\tau_i + \tau_{oi} + \tau_o}{\tau} \overset{o}{x} + x = p \left\{ 2B + 2w_2 + 2 \frac{\tau_{io}}{\tau} (\overset{o}{\theta} + \overset{o}{z}_1) + 2 \frac{R_s}{R_o} (\theta + z_1) \right\} \tag{2.65}$$

where

$$\text{a)} \quad B = \frac{I_B R_s + E_C}{\alpha I_E R_o} \tag{2.66a}$$

$$\text{b)} \quad \rho = \frac{1 - \alpha}{\alpha} \frac{R_s}{R_o} \qquad \text{(not explicit above)} \tag{2.66b}$$

$$\text{c)} \quad p = \frac{1}{4} \eta \alpha I_E R_o \tag{2.66c}$$

If we expand (2.65) by replacing z_1 according to (2.58) we get:

$$\frac{\tau_i \tau_o}{\tau^2} \overset{oo}{x} + \frac{\tau_i + \tau_{oi} + \tau_o}{\tau} \overset{o}{x} + x \tag{2.67}$$

$$= p \left\{ (1 + 2B + \rho) + (1 - \rho) \tanh x + 2 \frac{\tau_{io}}{\tau} (\overset{o}{\theta} + \overset{o}{z}_1) + 2 \frac{R_s}{R_o} (\theta - z_o) \right\}$$

where

$$z_0 = \frac{1}{2}\overset{o}{x}\,\mathrm{sech}^2 x \tag{2.68}$$

The condition given by

$$1 + 2B + \rho = 0 \tag{2.69}$$

is called "state-symmetry."

In practice the effect of the base current on biasing, represented by the term ρp,† is usually small (see (2.66b)), so that the state-symmetry condition can be approximated by setting $1 + 2B = 0$. Of course the larger α is (closer to 1), the better this approximation will be.

Equation (2.65), whether in this form or its more explicit form (2.67), is the general asymmetric transistor flipflop equation.

2.4. The Eccles-Jordan Flipflop

Analysis of the two feed-back circuits of the flipflop of Fig. 5 leads to the following pair of differential equations:

$$\frac{\tau_{ik}\tau_{ok}}{\tau^2}\overset{oo}{x}_k + \frac{\tau_{ik} + \tau_{oik} + \tau_{ok}}{\tau}\overset{o}{x}_k + x_k$$

$$= p_k\left\{2B_k + 2w_\ell + 2\frac{\tau_{iok}}{\tau}\left(\overset{o}{\theta}_k + \overset{o}{z}_k\right) + 2\frac{R_{sk}}{R_{ok}}\left(\theta_k + z_k\right)\right\} \tag{2.70}$$

with $k = 1, 2$; $\ell = 1, 2$; $\ell \neq k$; τ as in (14.1) and (14.4) and:

$$\text{a)}\quad \tau_{ik} = R_{ik}C_{ik} \tag{2.71a}$$

† Notice that this term implies that the base-to-base voltage v (in this case identical to v_1) will have a constant component equal to $\frac{1}{2}(1 - \alpha)I_E R_s$.

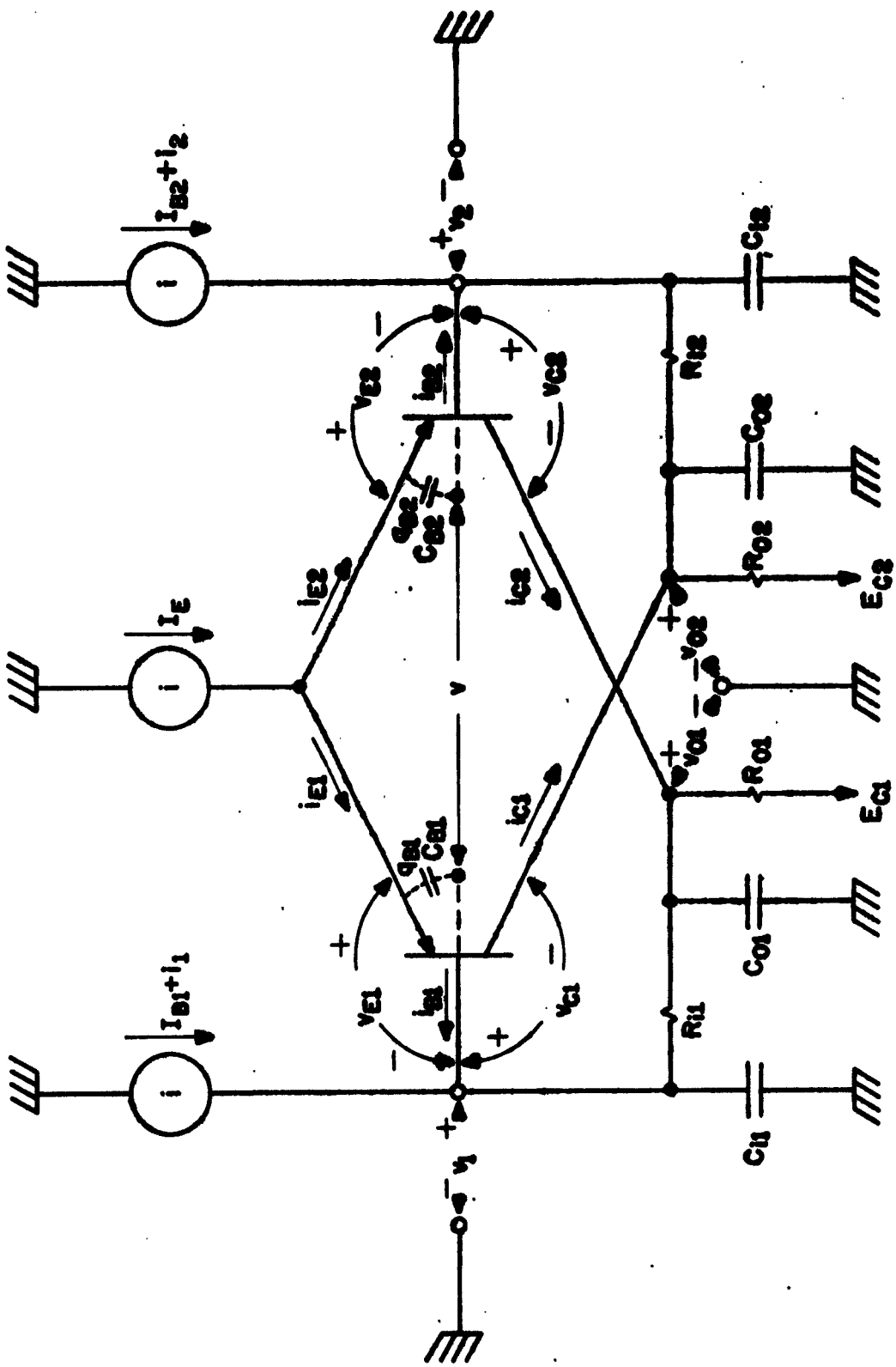

FIGURE 5: THE GENERAL ECCLES-JORDAN FLIPFLOP

b) $\tau_{ok} = R_{ok}C_{ok}$ (2.71b)

c) $\tau_{iok} = R_{ik}C_{ok}$ (2.71c)

d) $\tau_{oik} = R_{ok}C_{ik}$ (2.71d)

e) $R_{sk} = R_{ik} + R_{ok}$ (2.71e)

f) $B_k = \dfrac{I_{Bk}R_{sk} + E_{Ck}}{\frac{1}{2}\alpha I_E R_{ok}}$ (2.71f)

g) $x_k = \frac{1}{2}\eta v_k$ (2.71g)

h) $p_k = \frac{1}{4}\eta\alpha I_E R_{ok}$ (2.71h)

i) $\theta_k = \dfrac{i_k}{\alpha I_E}$ (2.71i)

j) w_k and z_k are given by equations (2.56) through (2.59) with x replaced by $(x_1 - x_2)$. (2.71j)

Notice that i_k is the trigger current actually fed into the flipflop; i_{tk} is the trigger current put out by the pure current sources (see Figs. 4).

Executing (2.71j), w_k and z_k turn out to be:

$$w_k = \frac{1}{2}\left\{1 + (-1)^k \tanh(x_1 - x_2)\right\} \tag{2.72}$$

$$z_k = \frac{1}{2}\left\{\frac{1-\alpha}{\alpha}\left[1 + (-1)^k \tanh(x_1 - x_2)\right] + (-1)^k(\overset{\circ}{x}_1 - \overset{\circ}{x}_2)\operatorname{sech}^2(x_1 - x_2)\right\} \tag{2.73}$$

Taking (2.72) and (2.73) into (2.70) we get:†

$$\frac{\tau_{ik}\tau_{ok}}{\tau^2}\overset{oo}{x}_k + \frac{\tau_{ik} + \tau_{oik} + \tau_{ok}}{\tau}\overset{o}{x}_k + x_k = p_k\left\{(1 + 2B_k + \rho_k)\right. \tag{2.74}$$

$$\left. - (-1)^k(1 - \rho_k)\tanh(x_1 - x_2) + 2\frac{\tau_{iok}}{\tau}(\overset{o}{\theta}_k + \overset{o}{z}_k) + 2\frac{R_{sk}}{R_{ok}}(\theta_k + (-1)^k z_o)\right\}$$

where, with k = 1, 2:

$$\text{a)}\quad \rho_k = \frac{1 - \alpha}{\alpha}\frac{R_{sk}}{R_{ok}} \tag{2.75a}$$

$$\text{b)}\quad z_o = \frac{1}{2}(\overset{o}{x}_1 - \overset{o}{x}_2)\operatorname{sech}^2(x_1 - x_2) \tag{2.75b}$$

Equations (2.74) describe a general Eccles-Jordan transistor flipflop. The asymmetric flipflop equation (2.67) is a special case of (2.74), and so is the symmetric flipflop, represented by equation (2.77), as follows:

Let us consider the case of a symmetric (but possibly unsymmetrically biased) flipflop. Subtraction of (2.70, k = 2) from (2.70, k = 1) yields:

$$\frac{\tau_i\tau_o}{\tau^2}\overset{oo}{x} + \frac{\tau_i + \tau_{oi} + \tau_o}{\tau}\overset{o}{x} + x = p\left\{2(B_1 - B_2) + 2(w_1 - w_2)\right. \tag{2.76}$$

$$\left. + 2\frac{\tau_{io}}{\tau}[(\overset{o}{\theta}_1 - \overset{o}{\theta}_2) + (\overset{o}{z}_1 - \overset{o}{z}_2)] + 2\frac{R_s}{R_o}[(\theta_1 - \theta_2) + (z_1 - z_2)]\right\}$$

This furnishes (2.76) below, which can also be obtained directly by subtraction of (2.74, k = 2) from (2.74, k = 1):

† Notice that $(-1)^k = -(-1)^\ell$.

$$\frac{\tau_i \tau_o}{\tau^2} \overset{oo}{x} + \frac{\tau_i + \tau_{oi} + \tau_o}{\tau} \overset{o}{x} + x$$

$$= p\left\{2(B_1 - B_2) + 2(1 - \rho)\tanh x + 2\frac{\tau_{io}}{\tau}\left[\overset{o}{\theta} + \overset{o}{z}\right] + 2\frac{R_s}{R_o}\left[\theta - 2z_o\right]\right\} \tag{2.77}$$

where the indices 1, 2 have been dropped from all parameters P whenever $P_1 = P_2$; in the case of the variables we have as before:

$$\text{a)}\quad x = x_1 - x_2 \tag{2.78a}$$

$$\text{b)}\quad \theta = \theta_1 - \theta_2 \tag{2.78b}$$

$$\text{c)}\quad z = z_1 - z_2 = -\left[\frac{1 - \alpha}{\alpha}\tanh x + 2z_o\right], \text{ from (2.73) and (2.78a)} \tag{2.78c}$$

$$\text{d)}\quad z_o = \frac{1}{2}\overset{o}{x}\,\operatorname{sech}^2 x \tag{2.78d}$$

Inspection of (2.74) and (2.75) shows that the symmetric flipflop is formally equivalent to the asymmetric† one. Furthermore, if it is biased in such a way that $B_1 = B_2$ (not necessarily symmetric biasing), then it is formally equivalent to a state-symmetric asymmetric flipflop.

We should stress the importance of this conclusion, since it actually doubles the effectiveness of the theory! But better yet, it allows us to compare the performance of any symmetric flipflop with its asymmetric counterpart, for we will actually be comparing formally equivalent things.

† In this report, the word "asymmetric" is reserved for the flipflop of Fig. 3. The Eccles-Jordan with different parameters on either side will be called "nonsymmetric."

We can anticipate here that (as will be seen in the following) that all other things being equal, the asymmetric flipflop besides being simpler, performs better than the symmetric flipflop with the same parameter values.

2.5 Triggering

The equations we have found so far take the trigger into account in a rather general form. Among the infinite possible trigger waveforms, however, we shall discuss only those which are the most important in practice, and study them in some detail.

First we consider the type of trigger circuit. It can be a:

a) Voltage source with negligible internal resistance.

b) Current source with negligible internal conductance.

c) Voltage source with considerable internal resistance.

d) Voltage source with considerable internal conductance.

So for the trigger current waveform, the following are three important types (see Fig. 6):

a) Rectangular.

b) Impulse.

c) Pair of rising and decaying exponentials.

d) Sinusoidal wave plus constant, simulating usual trigger.

We will study type a) in detail, and discuss types b), c) and d) (see section 5.5).

The asymmetric and symmetric flipflops will be treated together (since they are formally equivalent), and an indication will be given as to how a basically similar method applies to the more general nonsymmetric Eccles-Jordan flipflop. This is justified because of the much greater practical importance of the asymmetric and symmetric case, compared to the more academic importance of the nonsymmetric case.

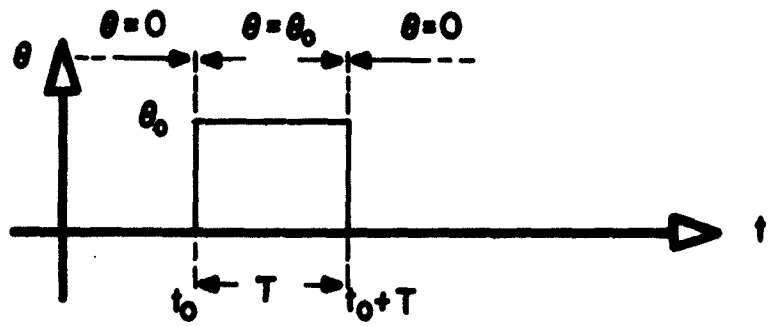

a) RECTANGULAR TRIGGER.

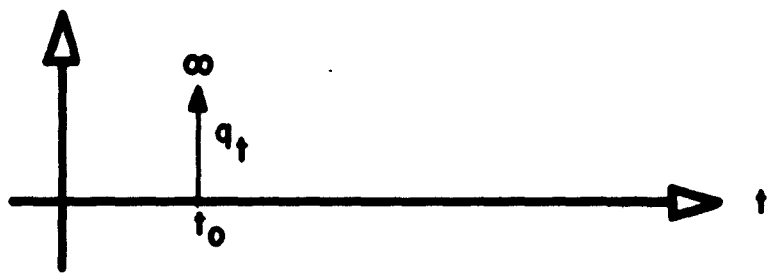

b) IMPULSE TRIGGER.

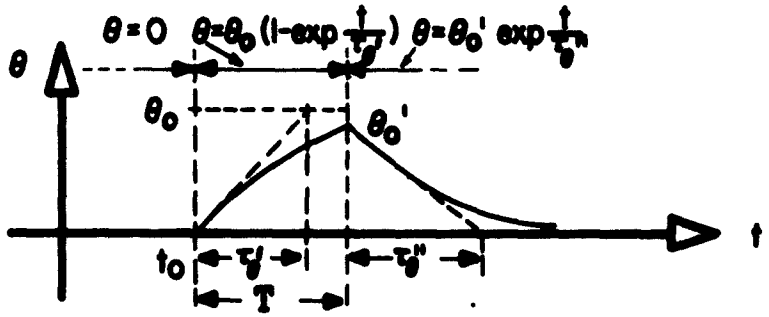

c) PAIR OF RISING AND DECAYING EXPONENTIALS.

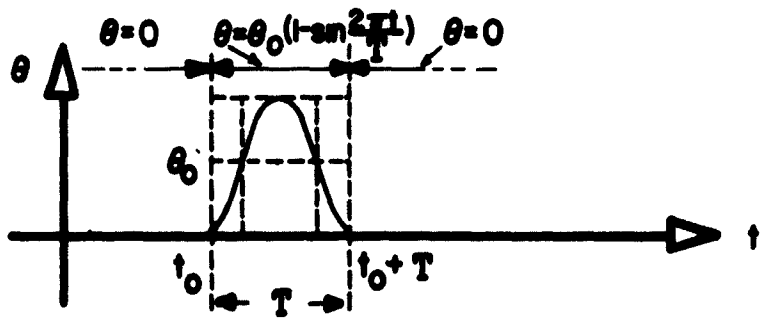

d) SINUSOIDAL WAVE PLUS CONSTANT, SIMULATING USUAL TRIGGER.

FIGURE 6: TRIGGER WAVEFORMS.

In the treatments of both voltage and current triggering sources, we will assume that the trigger has a definite duration, outside of which current sources have zero output current, and voltage sources are isolated from the input of the flipflop (say, by means of an open diode gate).

One way of simulating this condition is to require that, outside the duration of the trigger, the voltage or current of the triggering sources are such that the normalized trigger currents θ_k be zero, for any k.

Let us consider the various types of trigger: type a) is a trivial case, since the variable x is specified; case b) is both theoretically and formally a special case of d) and case c) is shown to be formally equivalent to d), which is not surprising since one case can be converted into the other by Thévenin or Norton transformations.

We will establish expressions for θ in each of the special cases mentioned above except case a).

Case b): See case c).

Case c): Let the trigger circuit be as shown in Fig. 7a. We get, with k = 1, 2:

$$\theta_k = \theta_{tk} - \frac{G_k R_{ok}}{2p_k} x_k \tag{2.79}$$

$$\overset{\circ}{\theta}_k = \overset{\circ}{\theta}_{tk} - \frac{G_k R_{ok}}{2p_k} \overset{\circ}{x}_k \tag{2.80}$$

where

$$\theta_{tk} = \frac{i_{tk}}{\alpha I_E}$$ is the normalized trigger current put out by the ideal current source. (2.81a)

$$\theta_k = \frac{i_k}{\alpha I_E}$$ is the normalized trigger current actually fed into the flipflop terminals. (2.81b)

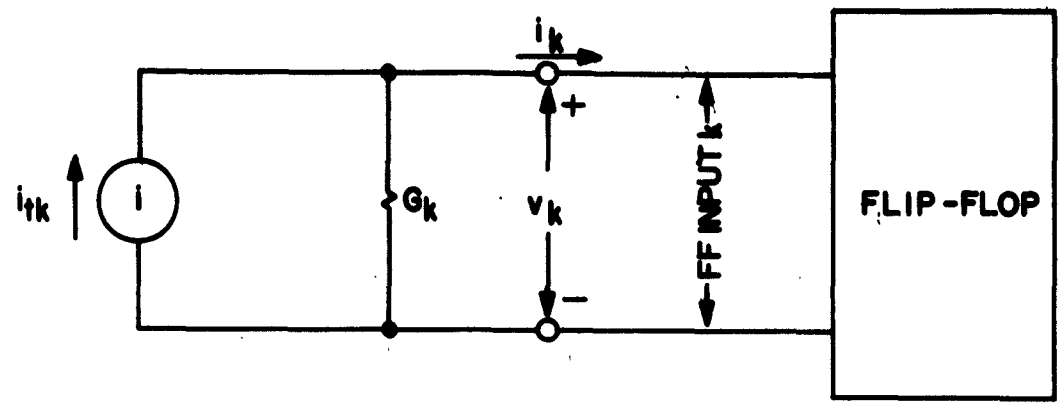

FIGURE 7a: TRIGGER CURRENT i_k PRODUCED BY CURRENT SOURCE. CLEARLY, $i_k = i_{tk} - G_k v_k$.

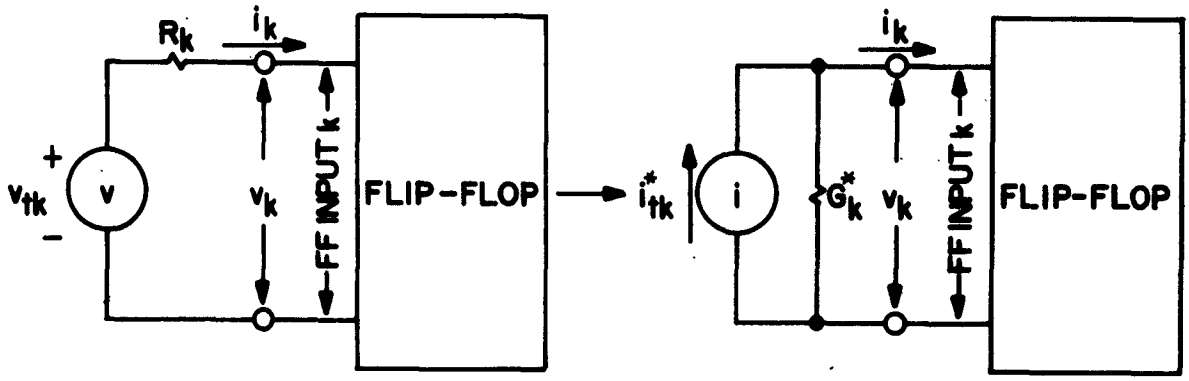

FIGURE 7b: TRIGGER CURRENT i_k PRODUCED BY VOLTAGE SOURCE. CLEARLY,

$$i_k = \frac{1}{R_k}(v_{tk} - v_k) = i^*_{tk} - G^*_k v_k$$

$$\text{IF } i^*_{tk} = G^*_k v_{tk} \quad \text{AND} \quad G^*_k = \frac{1}{R_k}$$

FIGURE 7: TRIGGER SOURCE

G_k is the trigger circuit internal conductance. (2.81c)

Now case b) is obtained by letting $G_k = 0$ in equations (2.79) and (2.80).

Case d): Let the trigger circuit be as shown in Fig. 7b. We get, with k = 1, 2:

$$\theta_k = \frac{R_{ok}}{2p_k R_k} x_{tk} - \frac{R_{ok}}{2p_k R_k} x_k \tag{2.82}$$

$$\overset{o}{\theta}_k = \frac{1}{\frac{1}{2}\eta R_k} \overset{o}{x}_{tk} - \frac{1}{\frac{1}{2}\eta R_k} \overset{o}{x}_k \tag{2.83}$$

where:

$x_{tk} = \frac{1}{2}\eta v_{tk}$ is the normalized source voltage. (2.84)

Hence, independently of the nature of the trigger circuit the form of θ_k is the same. In other words, the voltage source x_{tk} with internal resistance R_k can be converted into a current source of intensity θ^*_{tk} and internal conductance G^*_k given by:

$$\theta^*_{tk} = \frac{R_{ok}}{2p_k R_k} x_{tk} \tag{2.85}$$

$$G^*_k = \frac{1}{R_k} \tag{2.86}$$

From now on s_k will be used meaning either θ_{tk} or θ^*_{tk}, whatever the case may be.

Furthermore, we will require that whatever the waveform of s_k, it must be nonzero only for a time interval (t_{ak}, t_{bk}), being zero at any other time.

From now on we will use only s_k and G_k to describe the trigger.

For the asymmetric flipflop, we will have only s_1 and G_1; for the symmetric Eccles-Jordan $s_1 - s_2 = s$, and we require $G_1 = G_2 = G$. For the nonsymmetric Eccles-Jordan we will keep s_k and G_k, $k = 1, 2$, in their respective independent equations.

We can also account for the possibility that G_k has one value when the trigger is ON and another when it is OFF by using an index μ to indicate which case is being considered: Then $\mu = 0$ or 1 will indicate respectively trigger OFF or ON, and $G_{k\mu}$ will assume the appropriate one of its two possible values, G_{k0} or G_{k1}.

With this notation, the general flipflop equations are:

For the asymmetric case:

$$\frac{\tau_i \tau_o}{\tau^2} \overset{oo}{x} + \frac{\tau_i + \tau_{oi} + \tau_o + \tau_{io} R_o G_{t\mu}}{\tau} \overset{o}{x} + (1 + R_s G_\mu) x$$

$$= p \left\{ (1 + 2B + \rho) + (1 - \rho)\tanh x - \left[\frac{\tau_{io}}{\tau} \overset{oo}{x} + \left(\frac{(1 - \alpha)}{\alpha} \frac{\tau_{io}}{\tau} + \frac{R_s}{R_o} \right) \overset{o}{x} \right.\right.$$

$$\left.\left. - 2 \frac{\tau_{io}}{\tau} (\overset{o}{x})^2 \tanh x \right] \operatorname{sech}^2 x + 2 \left(\frac{\tau_{io}}{\tau} \overset{o}{s} + \frac{R_s}{R_o} s \right) \right\} \qquad (2.87)$$

For the symmetric Eccles-Jordan case (not necessarily symmetric trigger):

$$\frac{\tau_i\tau_o}{\tau^2}\overset{oo}{x} + \frac{\tau_i + \tau_{oi} + \tau_o + \tau_{io}R_oG_{t\mu}}{\tau}\overset{o}{x} + (1 + R_sG_\mu)x$$

$$= p\left\{2(B_1 - B_2) + 2(1 - \rho)\tanh x - 2\left[\frac{\tau_{io}}{\tau}\overset{oo}{x} + \left(\frac{(1 - \alpha)}{\alpha}\frac{\tau_{io}}{\tau} + \frac{R_s}{R_o}\right)\overset{o}{x}\right.\right.$$

$$\left.\left. - \frac{\tau_{io}}{\tau}(\overset{o}{x})^2\tanh x\right]\operatorname{sech}^2 x + 2\left(\frac{\tau_{io}}{\tau}\overset{o}{s} + \frac{R_s}{R_o}s\right)\right\} \qquad (2.88)$$

where:

$$x = x_1 - x_2 \qquad (2.89a)$$

$$s = s_1 - s_2 \qquad (2.89b)$$

$$G_\mu = G_{1\mu} = G_{2\mu} \qquad (2.89c)$$

All other coefficients being the same for both values of circuit index k, the index has been dropped. (2.89d)

For the general nonsymmetric Eccles-Jordan flipflop:

$$\frac{\tau_{ik}\tau_{ok}}{\tau^2}\overset{oo}{x_k} + \frac{\tau_{ik} + \tau_{oik} + \tau_{ok} + \tau_{iok}R_{ok}G_{tk\mu}}{\tau}\overset{o}{x_k} + (1 + R_{sk}G_{k\mu})x_k$$

$$= p_k\left\{(1 + 2B_k + \rho_k) - (-1)^k(1 - \rho_k)\tanh x\right.$$

$$+ (-1)^k\left[\frac{\tau_{iok}}{\tau}\overset{oo}{x} + \left(\frac{(1 - \alpha)}{\alpha}\frac{\tau_{iok}}{\tau} + \frac{R_{sk}}{R_{ok}}\right)\overset{o}{x} - \frac{\tau_{iok}}{\tau}(\overset{o}{x})^2\tanh x\right]\cdot\operatorname{sech}^2 x$$

$$\left. + 2\left(\frac{\tau_{iok}}{\tau}\overset{o}{s}_k + \frac{R_{sk}}{R_{ok}}s_k\right)\right\}, \qquad k = 1, 2 \qquad (2.90)$$

2.6 The Approximation Problem

We have thus established the nature of flipflop behavior through equations (2.65), (2.70), (2.74) or their respectively equivalent forms.

It is clear that the chances of success of an attempt to solve such equations exactly are very slim indeed [18].

Therefore, in order to get useful results, we must bow and try to find approximate solutions to these equations.

There are two possible approaches to this problem. One is to find an approximate model to the circuit. This model must be described by solvable equations. We then consider such solutions as approximations to the exact solution of the original problem. The other approch is to approximate the original equations directly, rather than the model. The latter approach would probably allow more accurate results to be obtained, since an error introduced in approximating, say $i_{Ck}(v)$ would not necessarily propagate through $\overset{o}{i}_{Ck}(v)$ to $i_{Bk}(v)$, and then to $\overset{o}{i}_{Bk}(v)$. That is to say that each function would be calculated exactly for our original model and then each one of them would be approximated as well as possible.

However, as we will show, this question does not necessarily affect the nature or even the complexity of the equation or system of equations we must analyze. For in fact, since an exact solution is not to be found but instead we must be content with an approximation, we might as well linearize the problem. This would involve dividing the x-axis into regions where the function of x appearing on the right-hand side of the equation can be approximated by a linear function of x. Let N be the number of such regions. Then we would reduce our problem to that of solving N linear second degree differential equations valid in their respective regions and match the solutions

at the border between every pair of adjacent regions. On both the phase plane and time domain, these regions are N strips separated by (N - 1) lines of x = constant.

One of the great advantages of this type of approximation is the relative simplicity of its applications, whether in the problem of analyzing the properties of the circuits involves, or in the actual computation of transition times and waveforms.

If this direction is chosen, then we have decided to pay a price in exactness for the advantages of simplicity and usefulness. Then it is a question of inspection to see that the most promising way to arrive at consistent results is to approximate the transistor pair model, i.e., equations (2.56) through (2.59) must be the basis for the definition of a "reasonable" piecewise linear model [26].

Of course the problem centers on how to linearize tanh x. There is a good degree of arbitrariness here, but we will select the following three region approximation (see Fig. 8).

$$\tanh x \approx \varphi(x) \tag{2.91}$$

$$\varphi(x) = \left\{ \begin{array}{ll} -1, & x \leq -\frac{1}{\gamma} \\ \gamma x, & -\frac{1}{\gamma} \leq x \leq +\frac{1}{\gamma} \\ +1, & +\frac{1}{\gamma} \leq x \end{array} \right\} \tag{2.92}$$

where γ is a factor which depends on the criterion for the approximation. In general γ will be somewhere between 0.5 and 1.0, especially if a minimum integral error is sought. In this case, we would have:

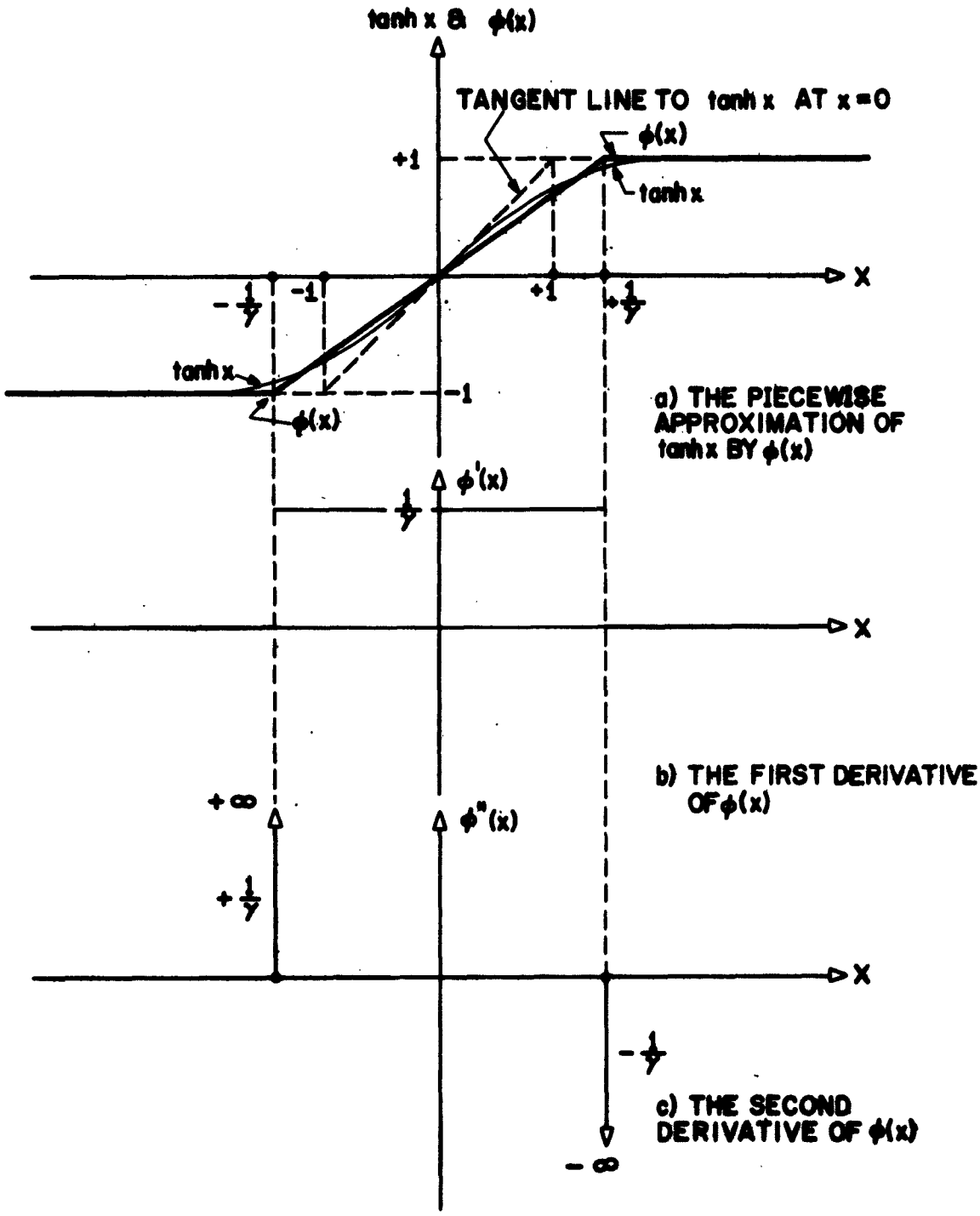

FIGURE 8: THE APPROXIMATION OF tanh x BY $\phi(x)$

$$\lim_{\xi\to\infty}\left\{\int_0^{\frac{1}{\gamma}}(\tanh x - \gamma x)dx + \int_{\frac{1}{\gamma}}^{\xi}(\tanh x - 1)dx\right\} = 0$$

$$\lim_{\xi\to\infty}\left\{\ln\cosh\xi - \frac{1}{2\gamma} - \xi + \frac{1}{\gamma}\right\} = \frac{1}{2\gamma} - \ln = 0$$

i.e.,

$$\gamma = \frac{1}{2\ln 2} \implies \gamma = 0.721$$

This criterion, of course, is quite arbitrary, and there is nothing to prove that it is the best; however, it also reduces the maximum absolute difference between the two functions to about 0.120 at the worst point. This is not a minimum; if γ is selected to minimize this maximum absolute error rather than the integral, then it would be $\gamma \approx 0.714$ and the maximum absolute error would be about 0.115.

So, for simplicity, we could for example, take $\gamma = 0.7$, or alternately (and perhaps better) take $\gamma = \frac{5}{7}$.

Whatever the criterion may be, the intention of using such a factor γ is to reduce somewhat the error by which the solution to the differential equation is affected due to the piecewise linearization process. This would be the ideal criterion if it were not impractical.

A five region approximation could also be used with perhaps better accuracy, but increased labor involved both in computation and analysis. In general the accuracy can be improved by increasing the number of regions, which results also in increased labor.

Since the technique does not change in essence, we shall use the three region approximation in this dissertation.

Equations (2.56) through (2.59) become:

$$w_k = \frac{1}{2}\left\{1 + (-1)^k \varphi(x)\right\} \tag{2.93}$$

$$z_k = \frac{1}{2}\left\{\frac{1-\alpha}{\alpha}\left[1 + (-1)^k \varphi(x)\right] + (-1)^k \overset{o}{x}\varphi'(x)\right\} \tag{2.94}$$

$$\overset{o}{z}_k = (-1)^k \frac{1}{2}\left\{\left[\frac{1-\alpha}{\alpha}\overset{o}{x} + \overset{oo}{x}\right]\varphi'(x) + (\overset{o}{x})^2\varphi''(x)\right\} \tag{2.95}$$

with k = 1, 2. The prime indicates differentiation with respect to x. Also,

$$z_0 = \frac{1}{2}\overset{o}{x}\varphi'(x) \tag{2.96}$$

And obviously,

$$\varphi'(x) = \left\{\begin{array}{ll} 0, & x < -\frac{1}{\gamma} \\ \gamma, & -\frac{1}{\gamma} < x < +\frac{1}{\gamma} \\ 0, & +\frac{1}{\gamma} < x \end{array}\right\} \tag{2.97}$$

Differentiation of $\varphi'(x)$ will clearly consist of two impulse functions, since $\varphi'(x)$ is constant everywhere except for two discontinuities. We get:

$$\varphi''(x) = \gamma\left\{\delta(x + \tfrac{1}{\gamma}) - \delta(x - \tfrac{1}{\gamma})\right\} \tag{2.98}$$

where $\gamma\delta(x)$ is an impulse function of strength γ occurring at x = 0.

The flipflop equations (2.87), (2.88) and (2.90) will be approximated by the following equations, respectively:

For the asymmetric case, (2.87) is approximated by:

$$\frac{\tau_i\tau_o}{\tau^2}\overset{oo}{x} + \frac{\tau_i + \tau_{oi} + \tau_o + \tau_{io}R_oG_\mu}{\tau}\overset{o}{x} + (1 + R_sG_\mu)x$$

$$= p\left\{(1 + 2B + \rho) + (1 - \rho)\varphi(x) - \left[\frac{\tau_{io}}{\tau}\overset{oo}{x} + \left(\frac{1 - \alpha}{\alpha}\frac{\tau_{io}}{\tau} + \frac{R_s}{R_o}\right)\overset{o}{x}\right]\varphi'(x)\right.$$

$$\left. - \frac{\tau_{io}}{\tau}(\overset{o}{x})^2\varphi''(x) + 2\left(\frac{\tau_{io}}{\tau}\overset{o}{s} + \frac{R_s}{R_o}s\right)\right\} \qquad (2.99)$$

For the symmetric Eccles-Jordan case (also not necessarily symmetric trigger), (2.88) is approximated by:

$$\frac{\tau_i\tau_o}{\tau^2}\overset{oo}{x} + \frac{\tau_i + \tau_{oi} + \tau_o + \tau_{io}R_oG_\mu}{\tau}\overset{o}{x} + (1 + R_sG_\mu)x$$

$$= p\left\{2(B_1 - B_2) + 2(1 - \rho)\varphi(x) - 2\left[\frac{\tau_{io}}{\tau}\overset{oo}{x} + \left(\frac{1 - \alpha}{\alpha}\frac{\tau_{io}}{\tau} + \frac{R_s}{R_o}\right)\overset{o}{x}\right]\varphi'(x)\right.$$

$$\left. - 2\frac{\tau_{io}}{\tau}(\overset{o}{x})^2\varphi''(x) + 2\left(\frac{\tau_{io}}{\tau}\overset{o}{s} + \frac{R_s}{R_o}s\right)\right\} \qquad (2.100)$$

with

$$x = x_1 - x_2 \qquad (2.101a)$$

$$s = s_1 - s_2 \qquad (2.101b)$$

$$G_\mu = G_{1\mu} = G_{2\mu} \qquad (2.101c)$$

All other coefficients being the same for both values of circuit index k, the index has been dropped. (2.101d)

For the general nonsymmetric Eccles-Jordan flipflop, (2.90) is approximated by:

$$\frac{\tau_{ik}\tau_{ok}}{\tau^2}\overset{oo}{x}_k + \frac{\tau_{ik} + \tau_{oik} + \tau_{ok} + \tau_{iok}R_{ok}G_{tk\mu}}{\tau}\overset{o}{x}_k + (1 + R_{sk}G_{tk\mu})x_k$$

$$= p_k\left\{(1 + 2B_k + \rho_k) - (-1)^k(1 - \rho_k)\varphi(x)\right.$$

$$+ (-1)^k\left[\frac{\tau_{iok}}{\tau}\overset{oo}{x} + \frac{1-\alpha}{\alpha}\frac{\tau_{iok}}{\tau} + \frac{R_{sk}}{R_{ok}}\overset{o}{x}\right]\varphi'(x) \qquad (2.102)$$

$$\left. + (-1)^k\frac{\tau_{iok}}{\tau}(\overset{o}{x})^2\varphi''(x) + 2\frac{\tau_{iok}}{\tau}\overset{o}{s}_k + \frac{R_{sk}}{R_{ok}}s_k\right\}, \quad k = 1, 2$$

Therefore, equations (2.65) and (2.77) will be approximated by an equation of the type:

$$a_\nu\overset{oo}{x} + b_{\nu\mu}\overset{o}{x} + c_{\nu\mu}x = d_\nu + f(\overset{o}{x})[\delta(x + \tfrac{1}{\gamma}) - \delta(x - \tfrac{1}{\gamma})] + m_\nu\overset{o}{s} + ns \qquad (2.103)$$

where

$\nu = 1, 2, \ldots, N$, is the region index, and

$\mu = 0, 1$ is the trigger index.

The system of equations (2.70) can be similarly approximated:

$$a_{k\nu}\overset{oo}{x}_k + b_{k\nu\mu}\overset{o}{x}_k + c_{k\nu\mu}x_k = a'_{k\nu}\overset{oo}{x} + b'_{k\nu}\overset{o}{x} + c'_{k\nu}x + d_{k\nu} + f_k(\overset{o}{x})[\delta(x + \tfrac{1}{\gamma}) - \delta(x - \tfrac{1}{\gamma})]$$

$$+ m_{k\nu}\overset{o}{s}_k + n_k s_k \qquad (2.104)$$

where

$$\begin{cases} x = x_1 - x_2, & k = 1, 2, \\ \nu \text{ and } \mu \text{ as for (2.103) above} \end{cases}$$

Obs.: Notice that C_i and C_0 may vary with the state of the transistors. We will recognize the possibility of one value in each region, and so, strictly speaking, τ_i, τ_{i0}, τ_{0i} and τ_0 depend on ν, the region index. When necessary we shall indicate this dependence explicitly, but not otherwise.

Tables I.1 and I.2 contain the values of all the parameters of equations (2.103) and (2.104) for the case where the number of regions is three.

Therefore, a detailed study of such equations is useful; it informs us about flipflop characteristics and also serves as a basis for analysis and design procedures, optimization of trigger, and study of interaction with adjacent circuits.

2.7 Summary

In this chapter we have analyzed a general transistor flipflop circuit and discussed its equilibrium equations.

a) The characteristic equations for the transistor pair with both emitters connected to a common constant current source is obtained.

b) Analysis of the asymmetric flipflop leads to a second order nonlinear differential equation.

c) Analysis of the general Eccles-Jordan flipflop leads to a system of two second order nonlinear differential equations. It is shown that both the asymmetric flipflop and the symmetric Eccles-Jordan flipflop can be represented by a single differential equation. In the first case, because one of the equations does not arise since its corresponding would-be

TABLE I.1. COEFFICIENTS OF (2.103) (SEE FIG. 9)

Definitions	Asymmetric Flipflop	$H = 1;\quad \varphi = (1 + 2B + \rho);\qquad B = \dfrac{I_B R_s + E_C}{\frac{1}{2}\alpha I_E R_o};\qquad \rho = \dfrac{1-\alpha}{\alpha}\dfrac{R_s}{R_o}$
	Symmetric Flipflop	$H = 2;\quad \varphi = 2(B_1 - B_2) = \varphi_1 - \varphi_2;\quad \varphi_k = (1 + 2B_k + \rho_k);\quad B_k = \dfrac{I_{Bk} R_{sk} + E_{Ck}}{\frac{1}{2}\alpha I_E R_{ok}};\quad \rho_k = \dfrac{1-\alpha}{\alpha}\dfrac{R_{sk}}{R_{ok}}$

Coefficients	Values	
a_ν	$\dfrac{\tau_i \tau_o}{\tau^2} + Hp\gamma \dfrac{\tau_{io}}{\tau}\begin{bmatrix}0\\1\\0\end{bmatrix}$	
$b_{\nu\mu}$	$\dfrac{\tau_i + \tau_{oi} + \tau_o + \tau_{io} R_o G_\mu}{\tau} + Hp\gamma\left[\dfrac{1-\alpha}{\alpha}\dfrac{\tau_{io}}{\tau} + \dfrac{R_s}{R_o}\right]\begin{bmatrix}0\\1\\0\end{bmatrix}$	
$c_{\nu\mu}$	$1 - Hp\gamma\left[1 - \dfrac{1-\alpha}{\alpha}\dfrac{R_s}{R_o}\right]\begin{bmatrix}0\\1\\0\end{bmatrix} + R_s G_\mu$	Definition: $\begin{bmatrix}a\\b\\c\end{bmatrix} = \begin{cases} a, & \text{if } x < -\frac{1}{\gamma} \\ b, & \text{if } -\frac{1}{\gamma} < x < +\frac{1}{\gamma} \\ c, & \text{if } +\frac{1}{\gamma} < x \end{cases}$ i.e., it is a function of x which takes on values a, b, c, if x is respectively in regions I, II, III.
d_ν	$p\left\{\varphi + \left[1 - \dfrac{1-\alpha}{\alpha}\dfrac{R_s}{R_o}\right]\begin{bmatrix}-1\\0\\+1\end{bmatrix}\right\}$	
m_ν	$2p\dfrac{\tau_{io}}{\tau}$	
$n = pn'$	$2p\dfrac{R_s}{R_o}$	
$f(\overset{o}{x})$	$-Hp\gamma\dfrac{\tau_{ioII}}{\tau}y^2 = -\dfrac{Hm_{II}^{\gamma}}{2}y^2;\quad y = \overset{o}{x}$	$\ell = \dfrac{Hm_{II}}{2a_{II}}$

Obs.: τ_i, τ_{io}, τ_{oi}, τ_o may depend on ν, since C_i and C_o may depend on ν.

TABLE I.2. COEFFICIENTS OF (2.104) (SEE FIG. 9)

Coefficients	Values	
$a_{k\nu}$	$\dfrac{\tau_{ik}\tau_{ok}}{\tau^2}$	
$b_{k\nu\mu}$	$\dfrac{\tau_{ik} + \tau_{oik} + \tau_{ok} + \tau_{iok}R_{ok}G_{k\mu}}{\tau}$	
$c_{k\nu\mu}$	$1 + R_{sk}G_{k\mu}$	
$a'_{k\nu}$	$(-1)^k p_k \gamma \begin{bmatrix} 0 \\ 1 \\ 0 \end{bmatrix}$	
$b'_{k\nu}$	$(-1)^k p_k \gamma \left[\dfrac{1-\alpha}{\alpha}\dfrac{\tau_{ok}}{\tau} + \dfrac{R_{sk}}{R_{ok}}\right]\begin{bmatrix} 0 \\ 1 \\ 0 \end{bmatrix}$	
$c'_{k\nu}$	$-(-1)^k p_k \gamma \left(1 - \dfrac{1-\alpha}{\alpha}\dfrac{R_{sk}}{R_{ok}}\right)\begin{bmatrix} 0 \\ 1 \\ 0 \end{bmatrix}$	Obs.: The symbol $\begin{bmatrix} 0 \\ 1 \\ 0 \end{bmatrix}$ is defined in Table I.1.
$d_{k\nu}$	$p_k\left(1 + 2B_k + \dfrac{1-\alpha}{\alpha}\dfrac{R_{sk}}{R_{ok}}\right)$	
$m_{k\nu}$	$2p_k \dfrac{\tau_{iok}}{\tau}$	
n_k	$2p_k \dfrac{R_{sk}}{R_{ok}}$	
$f_k(\overset{o}{x})$	$(-1)^k p_k \gamma \dfrac{\tau_{iok}}{\tau} y^2;\quad y = \overset{o}{x}$	

Obs.: The coefficients $a_{k\nu}$, $b_{k\nu\mu}$, $c_{k\nu\mu}$ depend on ν because the capacitances themselves may change slightly from one region to another.

variable is forced to be zero at all times. In the second case, because the difference between the two original equations is taken leading to another equation of the same type. Therefore the formal equivalence between symmetric and asymmetric flipflops is established.

d) Triggering is discussed and the representation of triggers in the flipflop equations is presented.

e) Finally, the approximation problem is discussed and a course of action is decided upon, which, although somewhat arbitrary, seems to minimize the unavoidable error.

3. STUDY OF THE FLIPFLOP EQUATION FOR THE CASE OF A RECTANGULAR TRIGGER

3.1 Introduction

We have, so far, broken down the problem of flipflop analysis and design into the analysis of two possible cases a) and b) below:

a) Problem of the fourth degree: the general nonsymmetric Eccles-Jordan flipflop, described by a system of two second order nonlinear differential equations.

b) Problem of the second degree: the asymmetric flipflop and symmetric Eccles-Jordan flipflop, which can both be described by the same single second order nonlinear differential equation. This will be called "the basic flipflop equation," because its analysis, besides its greater practical importance, turns out to be fundamental for the analysis of the general case, since the two equations describing the latter are closely related (formally) to the single equation describing the former. It is also basic (in a sense) in obtaining the equation for the following special case.

c) Problem of the first degree (internally restricted flipflop): We are considering only the second case where the transistors are identical. In this case, if the circuit capacitances are negligible, no matter what the symmetry of the flipflop may be, it can always be described by a single first order nonlinear equation which can have its exact solution presented as a quadrature formula.

In this chapter the problem of the second order (case b)) under a rectangular trigger will be analyzed mainly from a phase plane point of view, but the time domain will be used whenever convenient, to complement such analysis.

In Chapter 5 we will extend the theory to treat a general Eccles-Jordan flipflop (case a)) and also the internally restricted flipflop (case c)) which will be treated as a problem in its own right.

The possibility of different kinds of trigger will also be discussed in Chapter 5, and the methods available for the treatment of such problems will be examined.

Our main concern is the phase plane analysis of the second order flipflop under a rectangular trigger, but, nevertheless, we shall try to approach the most general problem as much as possible.

3.2 Phase Plane Analysis of the Basic Flipflop Equation

3.2.1 General Remarks

Before discussing our specific problem, we should briefly describe the various possible types of singularities on the phase plane for a system of equations such as (3.1), where P and Q are polynomials with no common factor.

$$\left.\begin{aligned} \dot{x} &= P(x,y) \\ \dot{y} &= Q(x,y) \end{aligned}\right\} \qquad (3.1)$$

The plane (x,y) is called the phase plane (by extension, even when $y \neq \dot{x}$); on the phase plane the points (x_0, y_0) such that $\dot{y} = \dot{x} = 0$ are called "singular points" or "singularities" of the system (points of "velocity" zero, "equilibrium points," or "states" of the system) [1, 4, 17, 22].

The singularities are essentially "point paths" in the phase plane, and therefore, as a consequence of the existence and uniqueness theorem a path may tend to a singularity, but will never reach it.

The nature of a singularity P_0 is given by the behavior of the system in an arbitrarily small neighborhood of P_0. This behavior is the same as that of the "system of the first approximation about P_0."

If P_0 has coordinates (x_0, y_0), the system of the first approximation about P_0 is the linear system obtained by:

a) making a transformation of variable

$$\left.\begin{aligned} \bar{x} &= x - x_0 \\ \bar{y} &= y - y_0 \end{aligned}\right\} \quad \text{so} \quad \left.\begin{aligned} P(x,y) &= \bar{P}(x,y) \\ Q(x,y) &= \bar{Q}(x,y) \end{aligned}\right\} \tag{3.2}$$

b) taking

$$\left.\begin{aligned} \dot{\bar{x}} &= A_{11}x + A_{12}y \\ \dot{\bar{y}} &= A_{21}x + A_{22}y \end{aligned}\right\} \tag{3.3}$$

where the A_{ij} are the coefficients of the terms of first order of $\bar{P}$ and $\bar{Q}$, in the order indicated.

The solution of (3.3) in parametric form with parameter t will contain exponentials of $\lambda_\alpha t$ and $\lambda_\beta t$, where λ_α and λ_β are the two characteristic frequencies of the system, i.e., the two eigenvalues of the matrix (A_{ij}), given by the solutions of

$$\begin{vmatrix} A_{11} - \lambda & A_{12} \\ A_{21} & A_{22} - \lambda \end{vmatrix} = 0 \tag{3.4}$$

By definition, the singularity $P_0(x_0,y_0)$ of the original system is called:

(i) Stable node if λ_α and λ_β are real and negative, i.e., x(t) and y(t) contain only damped exponentials.

(ii) Unstable node if λ_α and λ_β are real and positive, i.e., x(t) and y(t) contain only growing exponentials.

(iii) Saddle point if λ_α and λ_β are real and have opposite signs, i.e., both x(t) and y(t) include one growing exponential.

(iv) Stable focus if λ_α and λ_β are complex with negative real part, i.e., x(t) and y(t) undergo damped oscillatory motions.

(v) Unstable focus if λ_α and λ_β are complex with positive real part, i.e., x(t) and y(t) undergo growing oscillatory motions.

The study of singularities is important mostly because if a system maintains the same qualitative properties in a relatively large neighborhood of a singularity, then the nature of the singularity will give us considerable information about its behavior in this neighborhood.

3.2.2 Existence of Singularities

Taking into account equations (2.91) and the group (2.93) through (2.96), equation (2.103) was obtained from (2.65) and (2.77), with parameters as described in Table I; for convenience, we repeat (2.103):

$$a_\nu \overset{oo}{x} + b_{\nu\mu} \overset{o}{x} + c_{\nu\mu} x = d_\nu + f(\overset{o}{x})[\delta(x + \tfrac{1}{\gamma}) - \delta(x - \tfrac{1}{\gamma})] + m_\nu \overset{o}{s} + ns \qquad (2.103)$$

where ν = I, II, III, is the region index.

We define a new variable $y = \overset{o}{x}$, and express (2.103) as a system of two first order equations:

$$\left.\begin{aligned} \overset{o}{x} &= y \\ \overset{o}{y} &= \frac{D}{a_\nu} - \frac{c_{\nu\mu}}{a_\nu} x - \frac{b_{\nu\mu}}{a_\nu} y \end{aligned}\right\} \qquad (3.5)$$

where

$$D = d_\nu + f(\overset{o}{x})[\delta(x + \tfrac{1}{\gamma}) - \delta(x - \tfrac{1}{\gamma})] + m_\nu \overset{o}{s} + ns$$

Notice that d_ν is a constant in each region, and that the impulses occur in the borders between regions I and II and between regions II and III (this is a direct consequence of the way $\varphi(x)$ is defined).

Let us assume that s is a rectangular function and that therefore $\overset{\circ}{s}$ is a pair of impulses:

$$s = \left\{ \begin{array}{ll} 0, & t < t_\theta \\ W, & t_\theta < t < t_\theta + T_\theta \\ 0, & t_\theta + T_\theta < t \end{array} \right\} \tag{3.6}$$

$$s = W\{\delta(t - t_\theta) - \delta(t - t_2 - T_\theta)\} \tag{3.7}$$

Convention on Impulse Amplitude: The impulse contained in $\overset{\circ}{z}$ has its strength proportional to y^2/a, but occurs at a point where both "y" and "a" are discontinuous. In that case we will take those values of "y" and "a" adjacent to the discontinuities but inside region II.†

It is easy to see that any impulse of amplitude A contained in D will correspond to a discontinuity $\Delta\overset{\circ}{x}$ in $\overset{\circ}{x}$:

In the time domain:

$$A\delta(t - t_\alpha) \rightarrow \Delta\overset{\circ}{x} = \lim_{\epsilon \to 0}\{\overset{\circ}{x}(t_\alpha + \epsilon) - \overset{\circ}{x}(t_\alpha - \epsilon)\} = \frac{A}{a_\nu} \tag{3.8}$$

In the phase-plane:

† This is not so arbitrary as it may seem. In fact, we are trying to analyze a nonlinear differential equation by means of a piecewise linear approximation. It is very easy to show that any other choice for "y" and "a" between the respective extremes of their discontinuities will lead to the existence of crossed paths in the phase plane, which certainly will not be a portrait of any physical system.

$$A\delta(x - x_\alpha) \rightarrow \Delta\overset{\circ}{x} = \lim_{\eta \to 0}\{\overset{\circ}{x}(x_\alpha + \eta) - \overset{\circ}{x}(x_\alpha - \eta)\} = \frac{A}{a_\nu} \qquad (3.9)$$

Therefore, whenever an impulse occurs, it can be taken into account by assuming new initial conditions after the impulse with the discontinuity in $\overset{\circ}{x}$ described by (3.8) or (3.9) and x(t) being continuous.

With this device we completely eliminate the impulse functions from our equation, absorbing them into suitable discontinuities of $\overset{\circ}{x}$.

Now we can express (2.104) as two separate cases:

$$\left.\begin{aligned} \overset{\circ}{x} &= y \\ \overset{\circ}{y} &= \frac{d_{\nu\mu}}{a_\nu} - \frac{c_{\nu\mu}}{a_\nu}x - \frac{b_{\nu\mu}}{a_\nu}y \end{aligned}\right\} \qquad (3.10)$$

Therefore, the phase-plane equation is:

$$\frac{dy}{dx} = \frac{d_{\nu\mu} - c_{\nu\mu}x}{a_\nu y} - \frac{b_{\nu\mu}}{a_\nu} \qquad (3.11)$$

where:

$$d_{\nu\mu} = d_\nu + \nu nW, \text{ where } \begin{cases} \text{if trigger is OFF, } \mu = 0 \\ \text{if trigger is ON, } \mu = 1 \end{cases}$$

Obs.: Notice that the definition of $d_{\nu\mu}$ has a meaning only in the case of a rectangular trigger.

The singularities $x_{\nu\mu}$ of (3.11) have the coordinates $(x_{\nu\mu}, y_{\nu\mu})$, where the $x_{\nu\mu}$ are the roots of

$$d_{\nu\mu} - c_{\nu\mu}x = 0 \qquad (3.12)$$

We get

$$x_{\nu\mu} = \frac{d_{\nu\mu}}{c_{\nu\mu}} \quad \text{and} \quad y_{\nu\mu} = 0 \tag{3.13}$$

where

$x_{\nu\mu} = (x_{\nu\mu}, 0)$ is in region ν, and μ is the trigger index.

If $x_{\nu\mu}$ is not in region ν for a particular value of $\nu\mu$, then we refer to this point as a "virtual singularity," since it has an effect on a representative point P only if P is in region ν, but ceases to have any effect over P if P leaves region ν. Since $x_{\nu\mu}$ itself is outside region ν, there is a neighborhood of $x_{\nu\mu}$ in which P is not affected at all by $x_{\nu\mu}$.

Table II lists all possible values of $x_{\nu\mu}$, and also the effect of the trigger; the important special case of state-symmetry and trigger OFF is presented in Table III.

It is not superfluous to point out some of the important results presented in these tables. Let us consider Tables II.1 and II.2 and III. Notice that if $I_\mu < p\gamma\Psi$ holds, then:

a) $x_{I\mu} = -\frac{1}{\gamma}$, then $x_{II\mu} = x_{I\mu}$.

b) $x_{II\mu} = 0$, then $x_{I\mu} = -x_{III\mu}$.

c) $x_{III\mu} = +\frac{1}{\gamma}$, then $x_{II\mu} = x_{III\mu}$.

d) $\varphi + \mu n'W$ is such that $x_{I\mu}$ is virtual, then $x_{II\mu}$ is also virtual, but $x_{III\mu}$ is real.

e) $\varphi + \mu n'W$ is such that $x_{II\mu}$ is real, then $x_{I\mu}$ and $x_{III\mu}$ are also real.

f) $\varphi + \mu n'W$ is such that $x_{III\mu}$ is virtual, then $x_{II\mu}$ is also virtual, but $x_{I\mu}$ is real.

TABLE II. SINGULARITIES (SEE FIG. 9)

TABLE II.1

Singularity	Value	Necessary and Sufficient Condition to be Real
$x_{I\mu} = \frac{d_{I\mu}}{c_{I\mu}}$	$p\,\frac{\mu n'W - H\Psi + \varphi}{I_\mu}$	$I_\mu < p\gamma(H\Psi - \varphi - \mu n'W)$
$x_{II\mu} = \frac{d_{II\mu}}{c_{II\mu}}$	$p\,\frac{\mu n'W + \varphi}{I_\mu - Hp\gamma\Psi}$	$p\gamma\lvert\varphi + \mu n'W\rvert < \lvert I_\mu - Hp\gamma\Psi\rvert$
$x_{III\mu} = \frac{d_{III\mu}}{c_{III\mu}}$	$p\,\frac{\mu n'W + H\Psi + \varphi}{I_\mu}$	$I_\mu < p\gamma(H\Psi + \varphi + \mu n'W)$

TABLE II.2

<table>
<tr><td>Condition</td><td colspan="3"><u>Assumption</u>: Rectangular trigger: $s_k = \mu W$
Asymmetric flipflop: $s = \mu W$
Symmetric flipflop: $s = s_1 - s_2 = \mu(W_1 - W_2) = \mu W$</td></tr>
<tr><td rowspan="3">Definitions</td><td colspan="2">$d_{\nu\mu} = p(\mu n'W + \Psi \begin{bmatrix} -1 \\ 0 \\ +1 \end{bmatrix} + \varphi)$</td><td>$x_{\nu\mu} = \frac{d_{\nu\mu}}{c_{\nu\mu}}$</td></tr>
<tr><td colspan="2">$c_{\nu\mu} = I_\mu - Hp\gamma\Psi \begin{bmatrix} 0 \\ 1 \\ 0 \end{bmatrix}$</td><td>$I_\mu = 1 + R_s G_\mu$</td></tr>
<tr><td>$\rho = \frac{1 - \alpha}{\alpha}\frac{R_s}{R_o}$</td><td>$\Psi = 1 - \frac{1 - \alpha}{\alpha}\frac{R_s}{R_o}$</td><td>$\varphi$ as defined in Table I</td></tr>
</table>

TABLE III. SINGULARITIES (SEE FIG. 9)

Singularity	Value	Necessary and Sufficient Condition to be Real
x_{IO}	$-Hp\frac{\Psi}{I_O}$	$I_O < Hp\gamma\Psi$
x_{IIO}	0	always real
x_{IIIO}	$+Hp\frac{\Psi}{I_O}$	$I_O < Hp\gamma\Psi$

Obs.: This is a special case of Table II for the case of $\varphi = 0$ and $\mu = 0$, i.e., assuming an untriggered, state symmetric flipflop.

g) Therefore, the possibilities are:

i) either three real singularities

ii) or one of the extremes ($x_{I\mu}$ or $x_{III\mu}$) are real, the other extreme ($x_{III\mu}$ or $x_{I\mu}$) and the median ($x_{II\mu}$) are virtual.

However, if $I_\mu > p\gamma\Psi$,

h) Only one (any of the three) singularities is real, the other two being virtual.

Figure 9 illustrates these conclusions.

We will now prove that whenever:

i) three singularities are real (case g-i), the extremes are stable, the median is unstable;

ii) only one singularity is real (cases g-ii or h), it is stable.

3.2.3 The Nature of the Singularities

We have discussed the existence of singular points, and established the importance of several relationships among parameters upon the position of

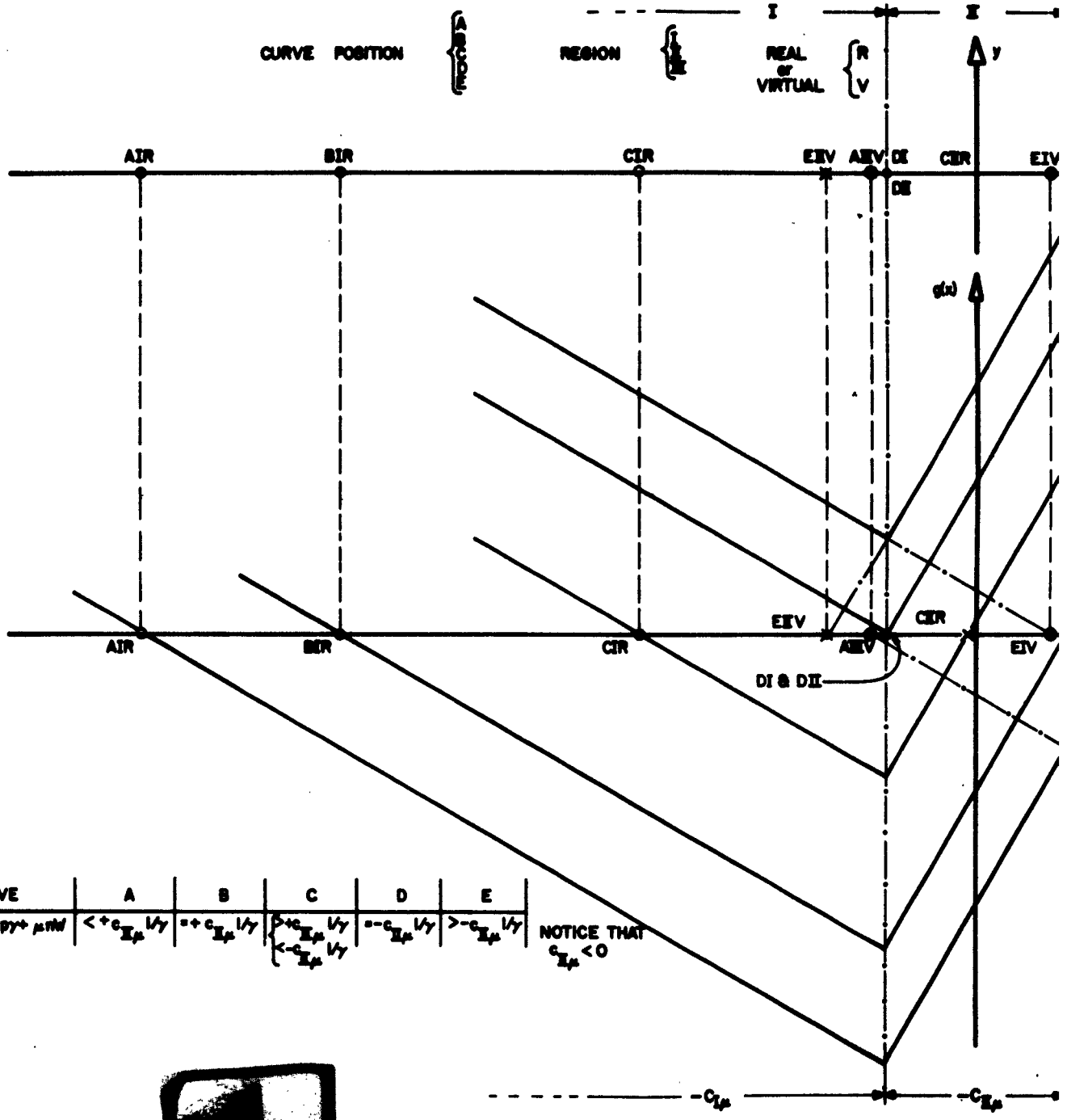

CURVE	A	B	C	D	E
$d_{II\mu} = py + \mu rM$	$< +c_{II\mu}\, l/y$	$= +c_{II\mu}\, l/y$	$> +c_{II\mu}\, l/y$ and $< -c_{II\mu}\, l/y$	$= -c_{II\mu}\, l/y$	$> -c_{II\mu}\, l/y$

NOTICE THAT $c_{II\mu} < 0$

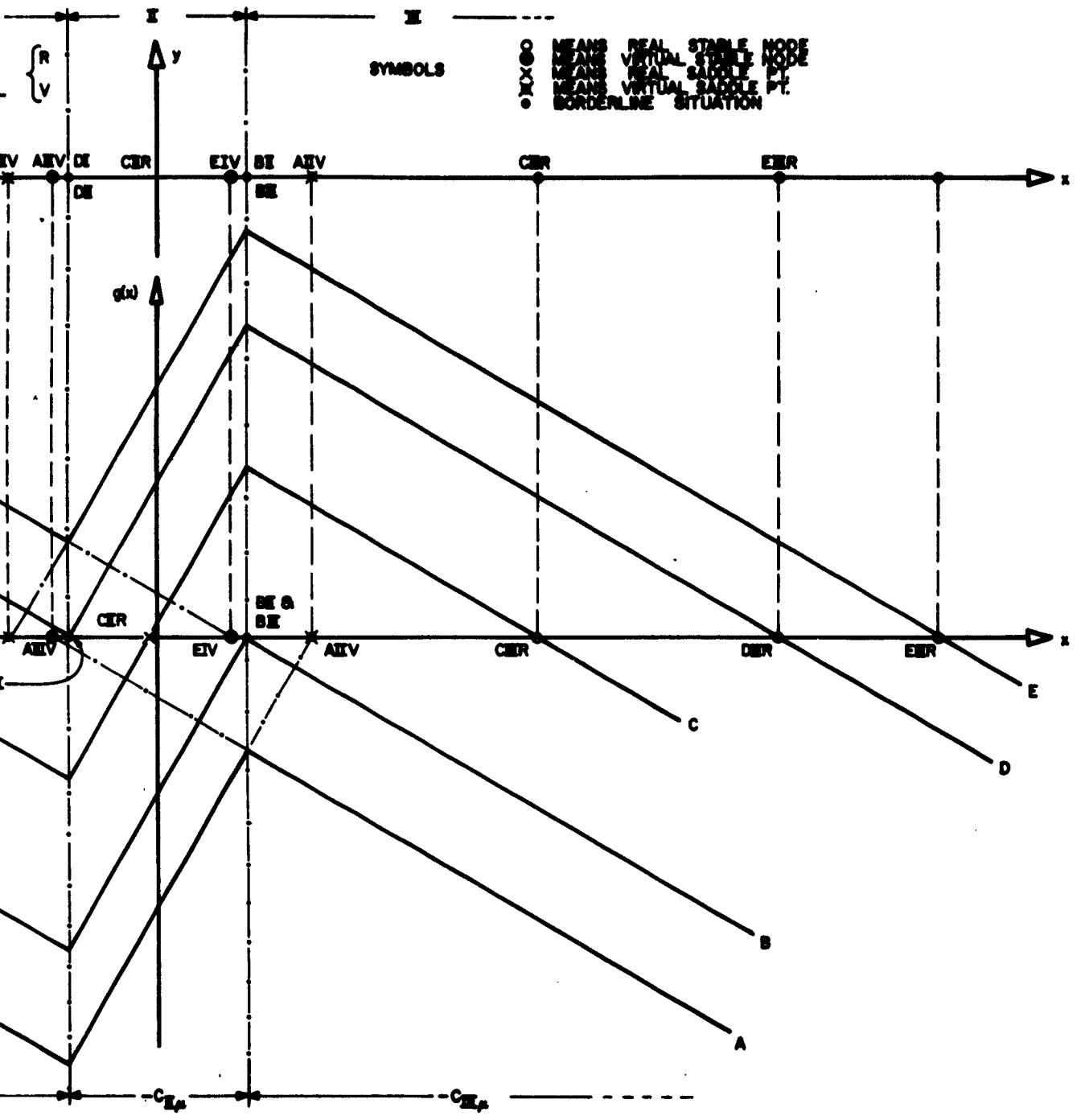

FIGURE 9: EFFECT OF VARIATIONS $d_{\Sigma\mu}$, OF $g(x) = d_{\Sigma\mu} - c_{\Sigma\mu} x$, ON THE POSITION (AND EXISTENCE !) OF SINGULARITIES. SEE TABLES II, III, IV.

singular points, and therefore upon their real or virtual nature. Now we should like to study the nature of these singularities. The system of equations (3.10) can be written in the form of (3.1):

$$\left.\begin{aligned} \overset{o}{x} &= P(x,y) \\ \overset{o}{y} &= Q(x,y) \end{aligned}\right\} \tag{3.14}$$

The "system of the first approximation about the singular point $(x_{\nu\mu}, y_{\nu\mu})$" has been defined as being the system formed by replacing P and Q by their respective first terms of corresponding Taylor series expansions about $(x_{\nu\mu}, y_{\nu\mu}) = (\frac{d_{\nu\mu}}{c_{\nu\mu}}, 0)$.

Let us define the new variables:

$$X = x - x_{\nu\mu}; \quad Y = y - y_{\nu\mu} \tag{3.15}$$

The system of equations (3.14) becomes:

$$\left.\begin{aligned} \overset{o}{X} &= P_x(x_{\nu\mu}, y_{\nu\mu})X + P_y(x_{\nu\mu}, y_{\nu\mu})Y \\ \overset{o}{Y} &= Q_x(x_{\nu\mu}, y_{\nu\mu})X + Q_y(x_{\nu\mu}, y_{\nu\mu})Y \end{aligned}\right\} \tag{3.16}$$

Comparison of (3.14) with (3.10) shows that:

$$\left.\begin{aligned} P(x,y) &= y \\ Q(x,y) &= \frac{d_{\nu\mu}}{a_\nu} - \frac{c_{\nu\mu}}{a_\nu} x - \frac{b_{\nu\mu}}{a_\nu} y \end{aligned}\right\} \tag{3.17}$$

Therefore

$$\left.\begin{aligned} P_x(x_{\nu\mu}, y_{\nu\mu}) &= 0; \qquad P_y(x_{\nu\mu}, y_{\nu\mu}) = 1 \\ Q_x(x_{\nu\mu}, y_{\nu\mu}) &= -\frac{c_{\nu\mu}}{a_\nu}; \quad Q_y(x_{\nu\mu}, y_{\nu\mu}) = -\frac{b_{\nu\mu}}{a_\nu} \end{aligned}\right\} \tag{3.18}$$

Let

$$D = -\frac{c_{\nu\mu}}{a_\nu} \quad \text{and} \quad E = -\frac{b_{\nu\mu}}{a_\nu} \tag{3.19}$$

Then (3.16) becomes

$$\left.\begin{aligned} \overset{\circ}{X} &= 0 \cdot X + 1 \cdot Y \\ \overset{\circ}{Y} &= D \cdot X + E \cdot Y \end{aligned}\right\} \tag{3.20}$$

The characteristic equation of this system is:

$$\begin{vmatrix} -\lambda & 1 \\ D & E - \lambda \end{vmatrix} = 0, \quad \text{i.e.,} \quad \lambda^2 - E\lambda - D = 0 \tag{3.21}$$

So

$$\lambda_{\alpha,\beta} = \frac{1}{2}\left\{E \pm \sqrt{E^2 + 4D}\right\} \tag{3.22}$$

i.e.,

$$\left.\begin{aligned} \lambda_\alpha &= \frac{1}{2}\left\{E - \sqrt{E^2 + 4D}\right\} \\ \lambda_\beta &= \frac{1}{2}\left\{E + \sqrt{E^2 + 4D}\right\} \end{aligned}\right\} \tag{3.23}$$

and we have the following rules:

(i) λ_α and λ_β real and negative $\Rightarrow$ stable node.

(ii) λ_α and λ_β real and positive $\Rightarrow$ unstable node.

(iii) λ_α and λ_β real and opposite signs $\Rightarrow$ saddle point.

(iv) λ_α and λ_β complex conjugates with negative real part $\Rightarrow$ stable focus.

(v) λ_α and λ_β complex conjugates with positive real part $\Rightarrow$ unstable focus.

Application of these rules to equation (3.22) or (3.23) is straightforward; replacement of D and E by their expressions in terms of parameters (through equations (3.19) and Table I) will produce the results summarized in Table IV, as can be shown by the following analysis:

Theorem 1. If $x_{I\mu}$ or $x_{III\mu}$ exist they are stable nodes.

Proof: From definitions of E and D, and from Table I for regions I and III we have:

$$E = -\left.\frac{b_{\nu\mu}}{a_\nu}\right|_{\nu=I,III} = -\frac{\tau_i+\tau_{oi}+\tau_o+\tau_{io}R_oG_\mu}{(\tau_i\tau_o/\tau)} < 0 \qquad (3.24)$$

$$D = -\left.\frac{c_{\nu\mu}}{a_\nu}\right|_{\nu=I,III} = -\frac{1+R_sG_\mu}{\tau_i\tau_o/\tau^2} < 0 \qquad (3.25)$$

Therefore, $|\sqrt{E^2+4D}|$ cannot be greater than $|E|$; we will show next that $E^2+4D>0$: in fact, from the expressions above for E and D, we have

$$E^2+4D = \frac{(\tau_i+\tau_{oi}+\tau_o+\tau_{io}R_oG_\mu)^2 - 4(1+R_sG_\mu)\tau_i\tau_o}{(\tau_i\tau_o/\tau)^2} \qquad (3.26)$$

Consider the numerator M of the fraction above:

TABLE IV. A SUMMARY OF THE NATURE OF THE SINGULARITIES IN ALL POSSIBLE SITUATIONS (SEE FIG. 9)

Possible Situations				Parameter Condition
	Exists	Does Not Exist	Nature	
$x_{I\mu}$	√		Stable Node	$c_{II\mu} > 0$ and $\frac{d_{II\mu}}{c_{II\mu}} < -\frac{1}{\gamma}$
$x_{II\mu}$		√		or
$x_{III\mu}$		√		$c_{II\mu} < 0$ and $\frac{d_{II\mu}}{c_{II\mu}} > +\frac{1}{\gamma}$
$x_{I\mu}$		√		$c_{II\mu} > 0$
$x_{II\mu}$	√		Stable Node	and
$x_{III\mu}$		√		$\left\|\frac{d_{II\mu}}{c_{II\mu}}\right\| < \frac{1}{\gamma}$
$x_{I\mu}$		√		$c_{II\mu} > 0$ and $\frac{d_{II\mu}}{c_{II\mu}} > +\frac{1}{\gamma}$
$x_{II\mu}$		√		or
$x_{III\mu}$	√		Stable Node	$c_{II\mu} < 0$ and $\frac{d_{II\mu}}{c_{II\mu}} < -\frac{1}{\gamma}$
$x_{I\mu}$	√		Stable Node	$c_{II\mu} < 0$
$x_{II\mu}$	√		Saddle Point	and
$x_{III\mu}$	√		Stable Node	$\left\|\frac{d_{II\mu}}{c_{II\mu}}\right\| < \frac{1}{\gamma}$

$$M = (\tau_i + \tau_{oi} + \tau_o + \tau_{io}R_oG_\mu)^2 - 4(1 + R_sG_\mu)\tau_i\tau_o$$

$$= \tau_i^2 + 2\tau_i\tau_o + \tau_o^2 + 2(\tau_i + \tau_o)\tau_{oi} + \tau_{oi}^2 + 2(\tau_i + \tau_{oi} + \tau_o)\tau_oR_iG_\mu$$

$$+ \tau_o^2R_i^2G_\mu^2 - 4\tau_i\tau_o - 4\tau_i\tau_oR_sG_\mu$$

$$= \tau_i^2 - 2\tau_i\tau_o + \tau_o^2 + 2(\tau_i - \tau_o)\tau_{oi} + \tau_{oi}^2 + 4\tau_o\tau_{oi} - 2(\tau_i + \tau_{oi} - \tau_o)\tau_oR_iG_\mu$$

$$+ \tau_o^2R_i^2G_\mu^2$$

$$= (\tau_{oi} + \tau_i - \tau_o)^2 - 2R_iG_\mu\tau_o(\tau_{oi} + \tau_i - \tau_o) + \tau_o^2R_i^2G_\mu + \tau_{oi}^2 + 4\tau_o\tau_{oi}$$

So

$$M = [\tau_{oi} + \tau_i - \tau_o(1 + \tau_oR_iG_\mu)]^2 + \tau_{oi}[\tau_{oi} + 4\,\tau_o] > 0 \qquad (3.27)$$

This implies that $E^2 + 4D > 0$, and so λ_α and λ_β are real and negative in both regions I and III, which means that $x_{I\mu}$ and $x_{III\mu}$, if they exist, are stable nodes, which was to be shown.

Notice that even if one of them (or both) is virtual, its action upon its corresponding region will be that of a stable node. This follows from the proof of Theorem 1 and from the nature of the coefficients of equation (2.103)

Theorem 2. If $p\gamma\Psi > I_\mu$ † and if $x_{II\mu}$ exists, then it is a saddle point.

† Parameters as defined in Table II; this is a necessary condition for bistable behavior (but not sufficient), for otherwise, either $x_{I\mu}$ or $x_{III\mu}$ will exist, but not both! This is stated in an equivalent way in conclusion h, page 48.

Proof: From definitions of E and D, and from Table I for region II we have:

$$E = -\frac{b_{II\mu}}{a_{II}} = -\frac{\tau_i + \tau_{oi} + \tau_o + \tau_{io}R_oG_\mu + p\gamma\tau\left[\frac{1-\alpha}{\alpha}\cdot\frac{\tau_{io}}{\tau} + \frac{R_s}{R_o}\right]}{\frac{\tau_i\tau_o}{\tau} + p\gamma\tau_{io}} < 0 \tag{3.28}$$

$$D = -\frac{c_{II\mu}}{a_{II}} = -\frac{\tau(I_\mu - p\gamma\Psi)}{\frac{\tau_i\tau_o}{\tau} + p\gamma\tau_{io}} > 0 \tag{3.29}$$

Therefore $|\sqrt{E^2 + 4D}| > |E|$; λ_α and λ_β are then real with opposite signs, and consequently $x_{II\mu}$ is a saddle point as was to be shown.

Theorem 3. If $p\gamma\Psi < I_\mu$,† then the existing $x_{V\mu}$ will be a stable node.

Proof: Using the calculations made for the proof of Theorems 1 and 2 we get, if region II is considered:

$$E^2 + 4D = \frac{\tau N}{\left(\frac{\tau_i\tau_o}{\tau} + p\gamma\tau_{io}\right)^2} \tag{3.30}$$

where

$$N = M + 2(\tau_i + \tau_{oi} + \tau_o + \tau_{io}R_oG_\mu)p\gamma\left[\frac{1-\alpha}{\alpha}\frac{\tau_{io}}{\tau} + \frac{R_s}{R_o}\right] \tag{3.31}$$

$$+ \left\{p\gamma\left[\frac{1-\alpha}{\alpha}\frac{\tau_{io}}{\tau} + \frac{R_s}{R_o}\right]\right\}^2 - I_\mu p\gamma\tau_{io} + p\gamma\Psi\left(\frac{\tau_i\tau_o}{\tau} + p\gamma\tau_{io}\right) > N'$$

$$N' = M' - I_\mu p\gamma\tau_{io} + I_\mu\left(\frac{\tau_i\tau_o}{\tau} + p\gamma\tau_{io}\right) \tag{3.32}$$

† No bistable behavior is possible!

where M' stands for the sum of the first three terms of N, and $p\gamma\Psi < I_\mu$ was used. Then

$$N' = M' + I_\mu \frac{\tau_i \tau_o}{\tau} \tag{3.33}$$

since $M > 0$, $M' > 0$ and $N' > 0$. Therefore $N > 0$; as a consequence, λ_α and λ_β are real and negative and if $x_{II\mu}$ exists it is a stable node. Of course the proof of Theorem 1 is independent of $\frac{p\gamma\Psi}{I_\mu}$, and therefore it is valid under the present hypothesis of $p\gamma\Psi < I_\mu$. Thus the proof of this Theorem 3 is complete.

3.2.4 Diagonalization of the Characteristic Matrix of the System

The eigenvalues and corresponding eigenvectors of the characteristic matrix are given by:

$$\Gamma = \begin{pmatrix} 0 & 1 \\ D & E \end{pmatrix} \begin{pmatrix} k_i \\ \ell_i \end{pmatrix} = \lambda_i \begin{pmatrix} k_i \\ \ell_i \end{pmatrix} \tag{3.34}$$

Therefore, $\ell_i = \lambda_i k_i$; $i = \alpha, \beta$.

Let $k_i = 1$ arbitrarily, and $\ell_i = \lambda_i$.

Column i can be normalized by multiplying it by a factor $\frac{1}{\sqrt{\lambda_i^2 + 1}}$, but it is more convenient not to normalize it.

The polar matrix of Γ is

$$\Gamma_p = \begin{pmatrix} 1 & 1 \\ \lambda_\alpha & \lambda_\beta \end{pmatrix} \tag{3.35}$$

Its inverse is:

$$\Gamma_p^{-1} = \frac{1}{\lambda_\beta - \lambda_\alpha} \begin{pmatrix} \lambda_\beta & -1 \\ -\lambda_\alpha & +1 \end{pmatrix} \tag{3.36}$$

The diagonal matrix of Γ is

$$\Gamma_d = \begin{pmatrix} \lambda_\alpha & 0 \\ 0 & \lambda_\beta \end{pmatrix} \tag{3.37}$$

and the diagonal form of Γ is [28]:

$$\Gamma = \Gamma_p \cdot \Gamma_d \cdot \Gamma_p^{-1} \tag{3.38}$$

Therefore:

$$\begin{pmatrix} 0 & 1 \\ D & E \end{pmatrix} = \begin{pmatrix} 1 & 1 \\ \lambda_\alpha & \lambda_\beta \end{pmatrix} \begin{pmatrix} \lambda_\alpha & 0 \\ 0 & \lambda_\beta \end{pmatrix} \begin{pmatrix} \lambda_\beta & -1 \\ -\lambda_\alpha & +1 \end{pmatrix} \frac{1}{\lambda_\beta - \lambda_\alpha} \tag{3.39}$$

The system of equations (3.20) can be expressed in matrix form

$$\begin{pmatrix} \dot{X} \\ \dot{Y} \end{pmatrix} = \begin{pmatrix} 0 & 1 \\ D & E \end{pmatrix} \begin{pmatrix} X \\ Y \end{pmatrix} \tag{3.40}$$

whose solution is:

$$\begin{pmatrix} X \\ Y \end{pmatrix} = e^{\begin{pmatrix} 0 & 1 \\ D & E \end{pmatrix} T} \cdot \begin{pmatrix} X_0 \\ Y_0 \end{pmatrix}, \quad \text{with} \begin{cases} T = t - t_0 \\ X_0 = X(0) \\ Y_0 = Y(0) \end{cases} \tag{3.41}$$

where, by definition, given a diagonalizable matrix A, with polar matrix A_p and corresponding diagonal matrix A_d,

$$e^{A} = A_p \cdot e^{A_d} \cdot A_p^{-1} \tag{3.42}$$

and for any diagonal matrix Q

$$e^{Q} = \begin{pmatrix} e^{q_1} & 0 & \cdots \\ 0 & e^{q_2} & \\ \vdots & & \ddots \end{pmatrix} \quad \text{if} \quad Q = \begin{pmatrix} q_1 & 0 & \cdots \\ 0 & q_2 & \\ \vdots & & \ddots \end{pmatrix} \tag{3.43}$$

Therefore, from (3.39), (3.41), (3.42), (3.43), we get:

$$\begin{pmatrix} X \\ Y \end{pmatrix} = \begin{pmatrix} 1 & 1 \\ \lambda_\alpha & \lambda_\beta \end{pmatrix} \begin{pmatrix} e^{\lambda_\alpha T} & 0 \\ 0 & e^{\lambda_\beta T} \end{pmatrix} \begin{pmatrix} \lambda_\beta & -1 \\ -\lambda_\alpha & +1 \end{pmatrix} \frac{1}{\lambda_\beta - \lambda_\alpha} \begin{pmatrix} X_0 \\ Y_0 \end{pmatrix} \tag{3.44}$$

and this turns out to be:

$$\begin{pmatrix} X \\ Y \end{pmatrix} = \frac{1}{\lambda_\beta - \lambda_\alpha} \begin{pmatrix} X_0 \left[\lambda_\beta e^{\lambda_\alpha T} - \lambda_\alpha e^{\lambda_\beta T}\right] + Y_0 \left[-e^{\lambda_\alpha T} + e^{\lambda_\beta T}\right] \\ X_0 \lambda_\alpha \lambda_\beta \left[e^{\lambda_\alpha T} - e^{\lambda_\beta T}\right] + Y_0 \left[-\lambda_\alpha e^{\lambda_\alpha T} + \lambda_\beta e^{\lambda_\beta T}\right] \end{pmatrix} \tag{3.45}$$

In another form

$$\left.\begin{aligned} X &= \frac{X_0\lambda_\beta - Y_0}{\lambda_\beta - \lambda_\alpha} e^{\lambda_\alpha T} + \frac{-X_0\lambda_\alpha + Y_0}{\lambda_\beta - \lambda_\alpha} e^{\lambda_\beta T} \\ Y &= \frac{X_0\lambda_\beta - Y_0}{\lambda_\beta - \lambda_\alpha} \lambda_\alpha e^{\lambda_\alpha T} + \frac{-X_0\lambda_\alpha + Y_0}{\lambda_\beta - \lambda_\alpha} \lambda_\beta e^{\lambda_\beta T} \end{aligned}\right\} \qquad (3.46)$$

and we recall the definitions of X and Y:

$$X = x - x_{\nu\mu};\quad Y = y - y_{\nu\mu} = y, \quad \text{since } y_{\nu\mu} = 0 \qquad (3.15)$$

Equations (3.46) furnish the integration constants A and B of the differential equation as functions of natural frequencies and initial values.

Substitution of (3.15) into (3.46) yields the general equation for the flipflop transition, if we keep in mind that:

(i) Changing from one region into another changes all parameters; therefore one must be careful in calculating new initial conditions, new singularity position (which can be virtual!) and new natural frequencies.

(ii) The same thing occurs if there is a change in trigger level, in particular when it is turned ON or OFF.

(iii) Impulses produce discontinuities in y (and therefore in Y), but everything else remains unchanged. Remember that the effects of such impulses depend on a_ν, which changes from one region to another; the impulses due to effects of base current occur when a_ν is changing from a_I to a_{II} and also when it is changing from a_{II} to a_{III}; in each case we will take the average of the two adjacent values of a_ν.

The results are presented in equation (3.56), section 3.3.

However equation (3.46) is also a very practical form; discontinuities of X and Y can be calculated from equations (3.15) whenever they occur.

Some more information can be obtained from the "canonical system of the first approximation"; this is defined as:

$$\begin{pmatrix} \overset{\circ}{\Phi} \\ \overset{\circ}{\chi} \end{pmatrix} = \begin{pmatrix} \lambda_\alpha & 0 \\ 0 & \lambda_\beta \end{pmatrix} \begin{pmatrix} \Phi \\ \chi \end{pmatrix} \tag{3.47}$$

where

$$\begin{pmatrix} \Phi \\ \chi \end{pmatrix} = \frac{1}{\lambda_\beta - \lambda_\alpha} \begin{pmatrix} \lambda_\beta & -1 \\ -\lambda_\alpha & +1 \end{pmatrix} \begin{pmatrix} X \\ Y \end{pmatrix} \tag{3.48}$$

Of course, system (3.47) is equivalent to system (3.40) under the transformation of variables (3.48). Such a system clearly has a unique singularity at the origin. Solution of (3.47) is:

$$\begin{pmatrix} \Phi \\ \chi \end{pmatrix} = \begin{pmatrix} e^{\lambda_\alpha T} & 0 \\ 0 & e^{\lambda_\beta T} \end{pmatrix} \begin{pmatrix} \Phi_0 \\ \chi_0 \end{pmatrix} \tag{3.49}$$

i.e.,

$$\left.\begin{aligned} \Phi &= \Phi_0 e^{\lambda_\alpha T} \\ \chi &= \chi_0 e^{\lambda_\beta T} \end{aligned}\right\} \tag{3.50}$$

from which we find

$$t - t_0 = \frac{1}{\lambda_\alpha} \ln \frac{\Phi}{\Phi_0} = \frac{1}{\lambda_\beta} \ln \frac{\chi}{\chi_0} \tag{3.51}$$

and therefore,

$$\boxed{\left(\frac{\Phi}{\Phi_0}\right)^{\lambda_\beta} = \left(\frac{\chi}{\chi_0}\right)^{\lambda_\alpha}} \tag{3.52}$$

which is the equation for the phase plane trajectory in this canonic system.

If the singularity is a stable node, then $\lambda_\alpha < 0$ and $\lambda_\beta < 0$, and we assume either $|\lambda_\alpha| < |\lambda_\beta|$ or $|\lambda_\alpha| > |\lambda_\beta|$ (which is irrelevant, since the ordering of λ_α and λ_β is arbitrary!).

From (3.52) we get:

$$\chi = \frac{\chi_0}{\Phi_0^{(\lambda_\beta/\lambda_\alpha)}} \cdot \Phi^{(\lambda_\beta/\lambda_\alpha)} \tag{3.53}$$

and, by differentiation,

$$\frac{d\chi}{d\Phi} = \frac{\lambda_\beta}{\lambda_\alpha} \cdot \frac{\chi_0}{\Phi_0^{(\lambda_\beta/\lambda_\alpha)}} \cdot \Phi^{(\lambda_\beta/\lambda_\alpha)-1} \tag{3.54}$$

Therefore, (3.53) defines a family of curves of the parabolic type in the plane (Φ,χ), for $\chi = f(\Phi)$ [1].

From (3.51) it is seen that the direction of movement of a representative point P over any of these trajectories is clearly towards the origin. Figures 10 show the two types of parabolic curve according to whether

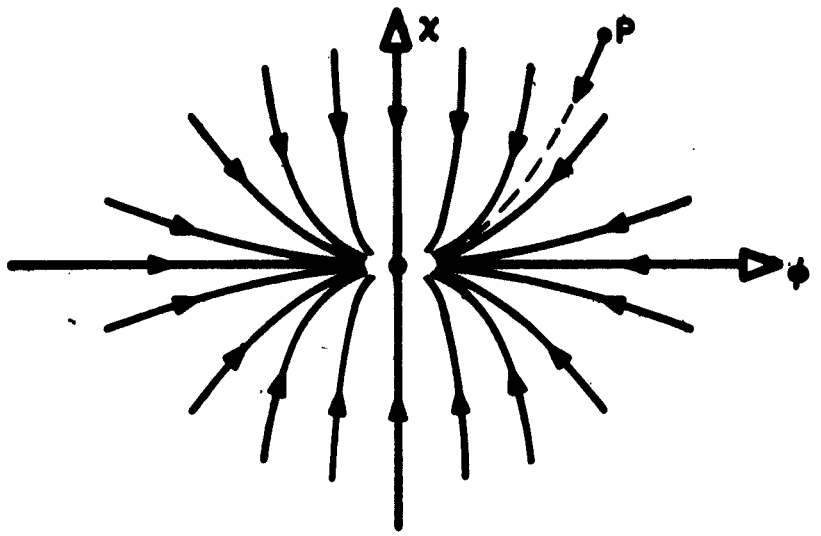

(a) $|\lambda_\alpha| < |\lambda_\beta|$,

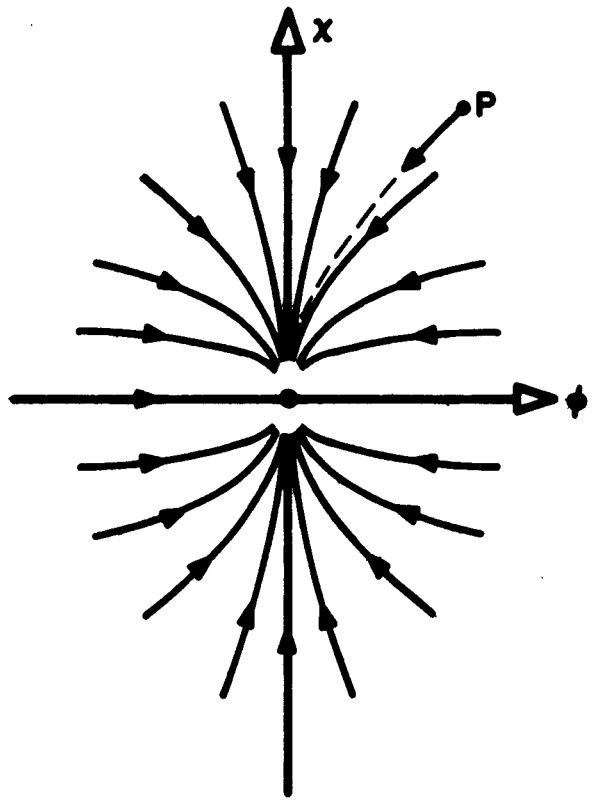

(b) $|\lambda_\alpha| > |\lambda_\beta|$

FIGURE 10: CANONIC SYSTEM TRAJECTORIES WHEN THE SINGULARITY IS A NODE. IF IT IS A STABLE NODE, i.e., IF λ_α & λ_β ARE NEGATIVE, THEN THE REPRESENTATIVE POINT P MOVES TOWARDS THE ORIGIN (SINGULARITY) WITH INCREASING TIME.

$|\lambda_\alpha| < |\lambda_\beta|$ or $|\lambda_\alpha| > |\lambda_\beta|$. If the singularity is a saddle point, then we take $\lambda_\alpha < 0 < \lambda_\beta$ (again no loss of generality) and inspection of (3.53) and (3.54) shows that (3.53) represents a family of hyperbolic curves with the coordinate axes as asymptotes [1].

From (3.51) it is seen that the direction of movement of the representative point P along any of these trajectories is found to be towards smaller values of $|\Phi|$ and larger values of $|\chi|$. See Figs. 11.

We wish to know how these curves transform into the (X,Y) plane, i.e., the system of the first approximation, which, although not canonic, also has a unique singularity at the origin.

The best way to see this is to find the lines in the (X,Y) plane that correspond to the Φ and χ axes. From (3.48) (definition of Φ and χ) we get:

$$\left.\begin{array}{lll} \Phi \text{ axis: } \chi = 0 & \Rightarrow & Y = \lambda_\alpha X \\ \chi \text{ axis: } \Phi = 0 & \Rightarrow & Y = \lambda_\beta X \end{array}\right\} \qquad (3.55)$$

We realize that in the case of a node with $|\lambda_\alpha| > |\lambda_\beta|$, i.e., with $\lambda_\alpha < \lambda_\beta < 0$, the trajectories have the Φ axis as the direction of their axes of symmetry, and that they are tangent to the χ axis at the singularity point (origin), as shown in Fig. 9b. In the case of a saddle point, the curves are asymptotic to both axes.

The linear transformation conserve all these properties, and also the direction of motion of the trajectories with increasing times.

Therefore we can get a fairly good picture of the family of trajectories in the (X,Y) plane if we know them in the (Φ,χ) plane. The results are qualitatively illustrated in Figs. 12 and 13.

Figure 14 qualitatively shows some portraits of the original system (x,y) from what we have found so far [1, 22].

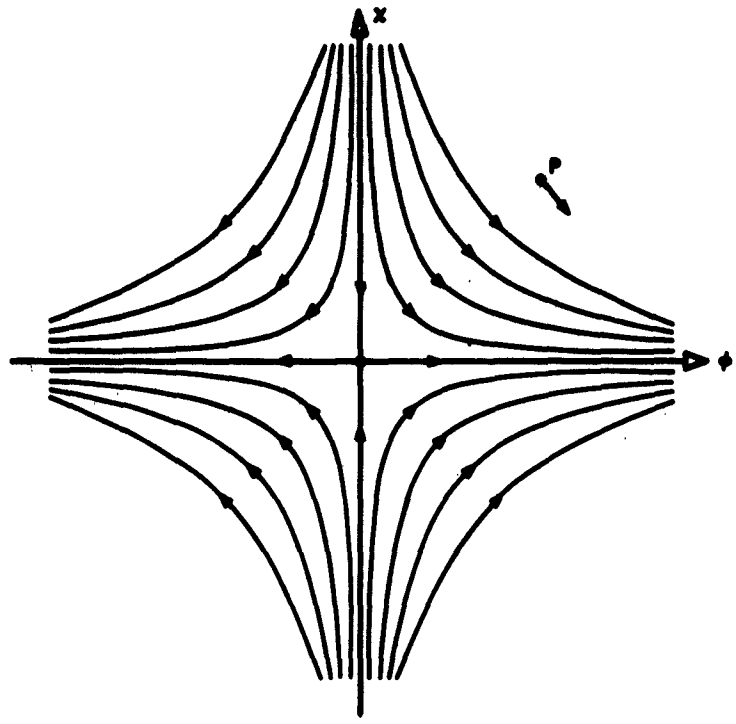

(a) $\lambda_\alpha > 0$, $\lambda_\beta < 0$

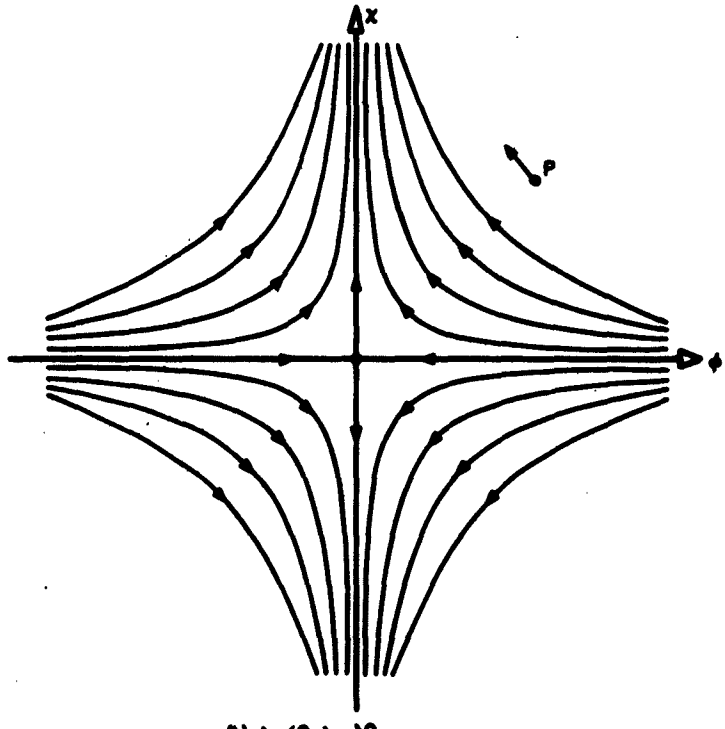

(b) $\lambda_\alpha < 0$, $\lambda_\beta > 0$

COMMENT: THE REPRESENTATIVE POINT P MOVES IN THE DIRECTION OF HEAVY ARROWS WITH INCREASING TIME.

FIGURE 11: CANONIC SYSTEM TRAJECTORIES WHEN THE SINGULARITY IS A SADDLE POINT.

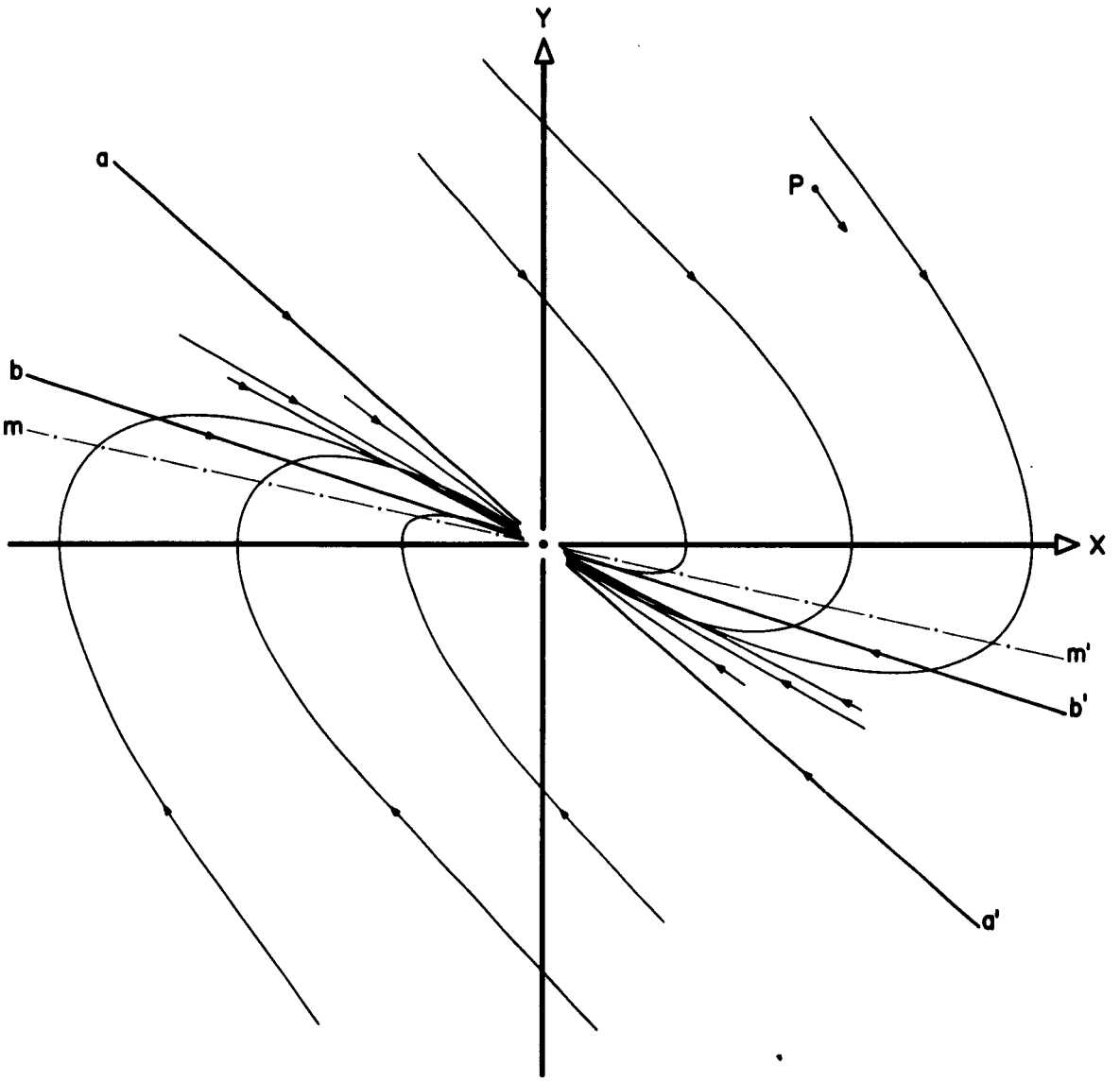

COMMENT: SLOPE OF $aa' = \lambda_\alpha$
SLOPE OF $bb' = \lambda_\beta$
SLOPE OF $mm' = \frac{\lambda_\alpha \lambda_\beta}{\lambda_\alpha + \lambda_\beta}$

FIGURE 12: TRAJECTORIES IN THE SYSTEM OF THE FIRST APPROXIMATION, CASE OF A STABLE NODE WITH $|\lambda_\alpha| > |\lambda_\beta|$ – (CORRESPONDS TO FIGURE 10b).

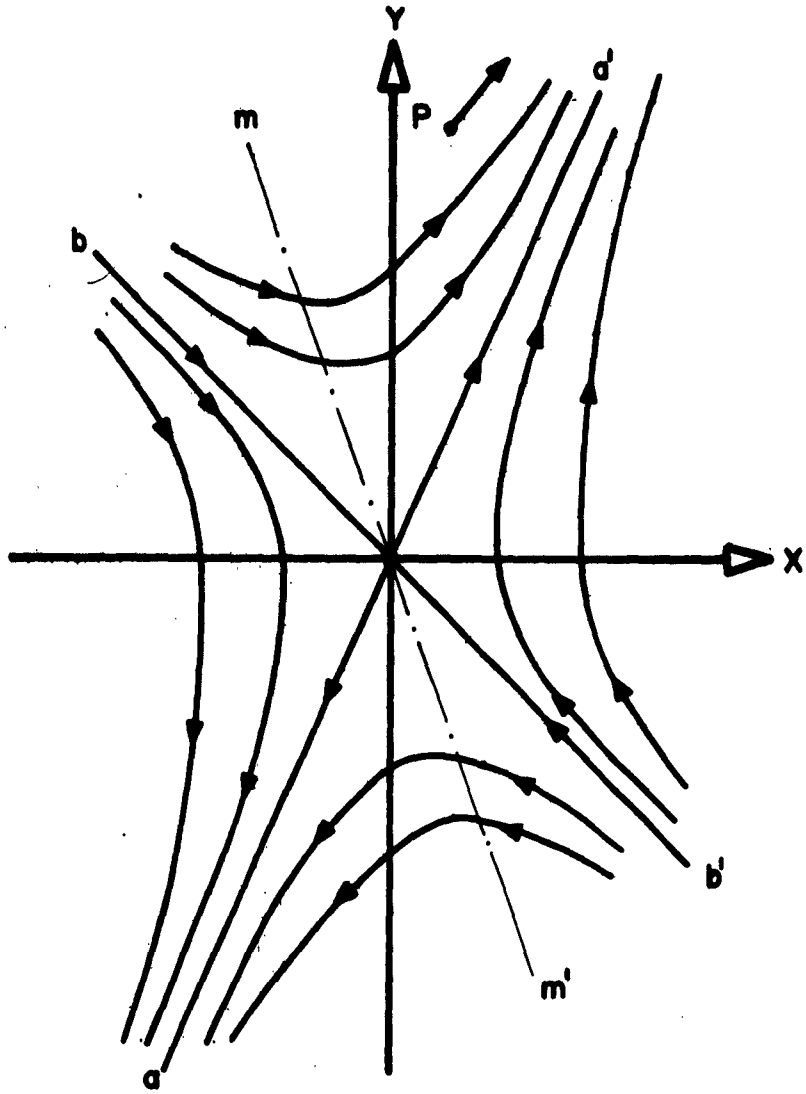

COMMENTS: SLOPE OF $aa' = \lambda_\alpha$

SLOPE OF $bb' = \lambda_\beta$

SLOPE OF $mm' = \dfrac{\lambda_\alpha \lambda_\beta}{\lambda_\alpha + \lambda_\beta}$

THE CURVES ARE HYPERBOLIC, ALL ASYMPTOTIC TO LINES aa' & bb', WITH MAXIMA AND MINIMA ON LINE mm'; ALL CURVES CROSS THE X-AXIS PERPENDICULARLY. HEAVY ARROWS INDICATE DIRECTION OF MOVEMENT OF P WITH INCREASING TIME.

FIGURE 13: TRAJECTORIES IN THE SYSTEM OF THE FIRST APPROXIMATION, CASE OF A SADDLE POINT, WITH $\begin{cases} \lambda_\alpha > 0 \\ \lambda_\beta < 0 \end{cases}$

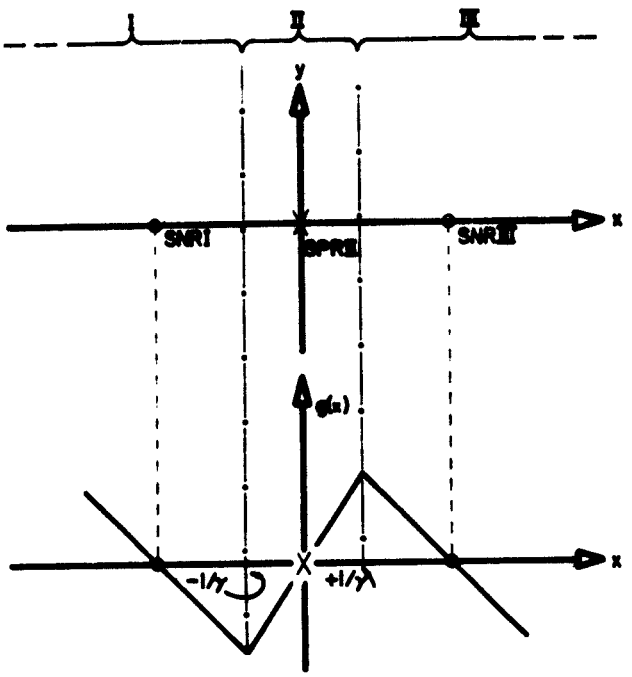

(a) BALLANCED g(x): $d_{II_\mu}=0$; but $c_{II_\mu}<0$

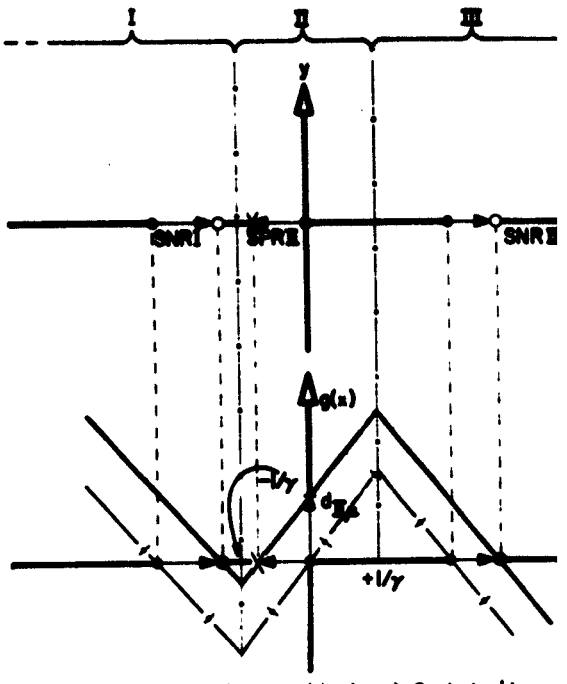

(b) POSITIVE BIAS ON g(x): $d_{II_\mu}>0$ but $|d_{II_\mu}$ $<1/\gamma$, $c_{II_\mu}<0$

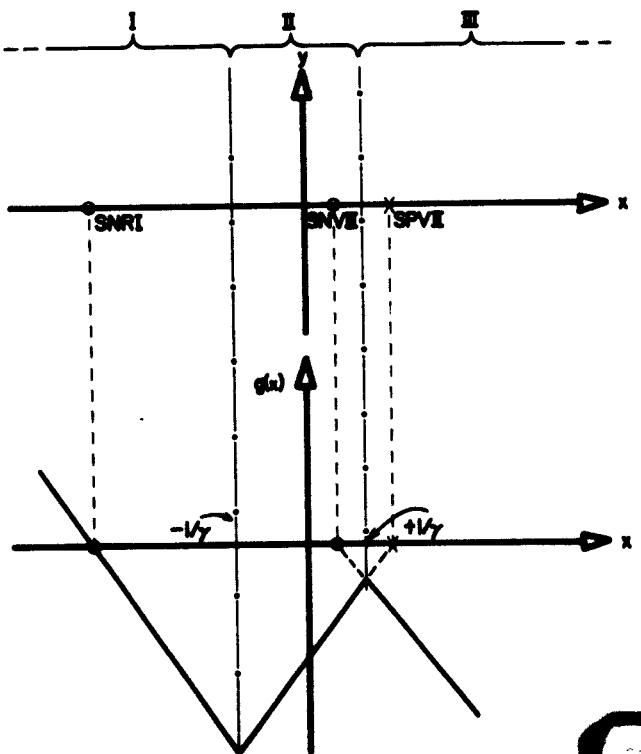

(c) MONOSTABLE SYSTEM IN I: $d_{II_\mu}/c_{II_\mu} > +1/\gamma$

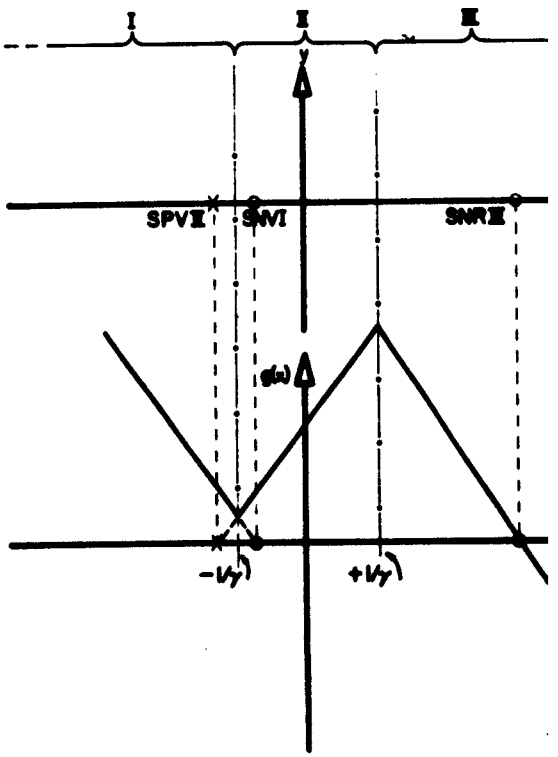

(c) MONOSTABLE SYSTEM IN III: d_{II_μ}/c_{II_μ} <-1

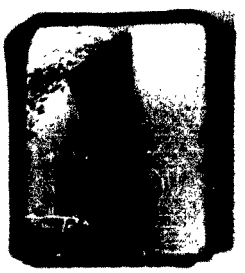

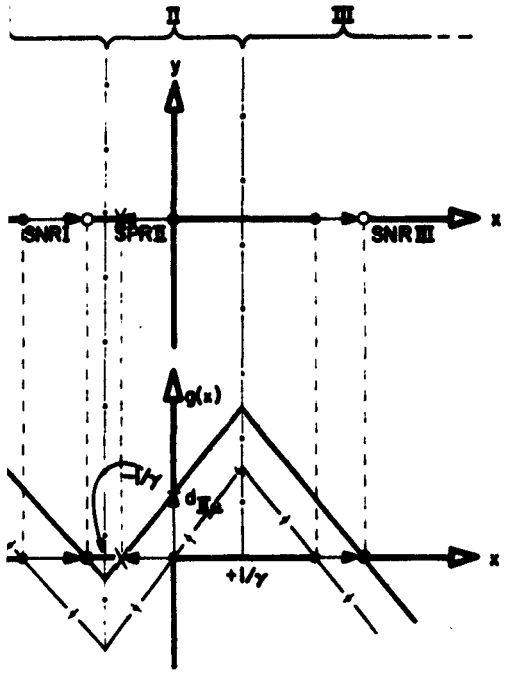

IVE BIAS ON g(x): $d_{II_\mu} > 0$ but $|d_{II_\mu}/c_{II}|$ $c_{II_\mu} < 0$

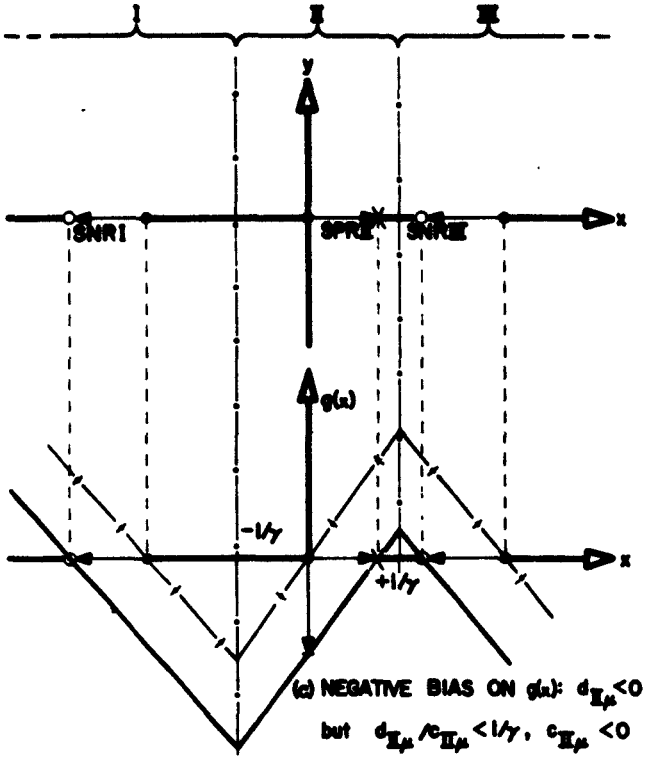

(c) NEGATIVE BIAS ON g(x): $d_{II_\mu} < 0$ but $d_{II_\mu}/c_{II_\mu} < 1/\gamma$, $c_{II_\mu} < 0$

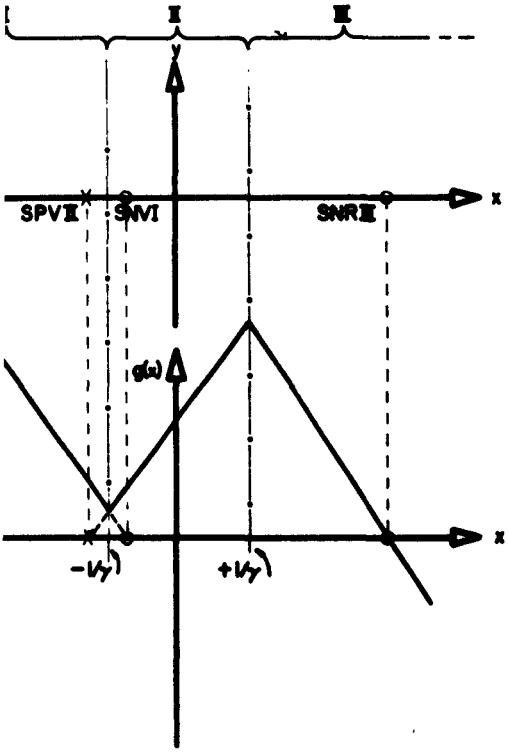

OSTABLE SYSTEM IN II: $d_{II_\mu}/c_{II_\mu} < -1/\gamma$

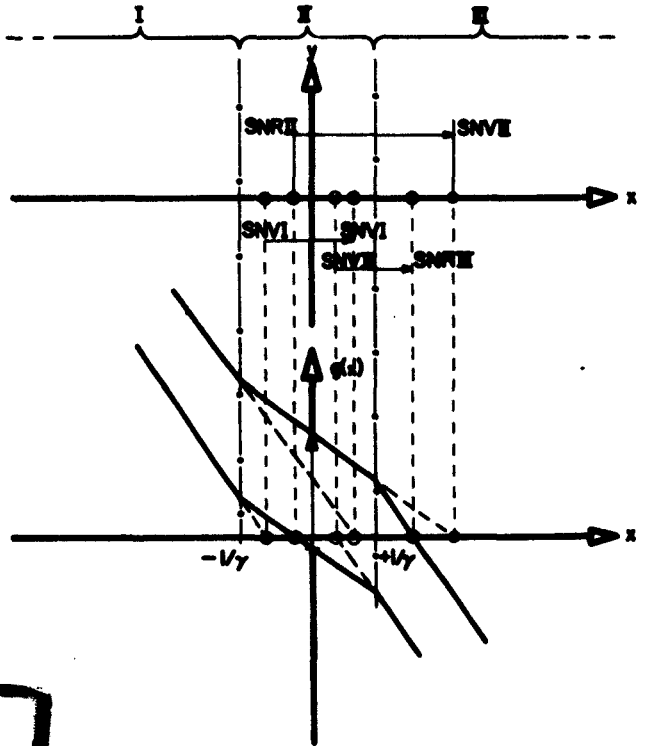

(*) STABLE SYSTEM: c_{II_μ} : >0:

FIGURE 14: $g(x) = d_{sys} - c_{sys}x$; d_{sys} & c_{sys} AS IN TABLE I

2

It is worth reminding that, due to the piecewise linear character of our complete system in (x,y), in each region the solution of the corresponding system of the first approximation is exactly equal to the solution of the original system.

3.2.5 Comments on Figs. 14

a) Balanced g(x): $d_{II\mu} = 0$; this situation would usually correspond to a state symmetric ($d_{II0} = 0$) untriggered ($\mu = 0$) system. However, we could have this same situation if $d_{II0} \neq 0$, $nW = -d_{II0}$, and $\mu = 1$, since $d_{II\mu} = d_{II0} + \mu nW$, in this case $d_{III} = 0$.

b) and c) Nonzero bias on g(x): $d_{II\mu} \neq 0$; this situation would correspond either to a state asymmetric ($d_{II0} = 0$) untriggered ($\mu = 0$) system, or to a partially triggered (no matter what kind of state symmetry) system ($d_{III} = d_{II0} + nW \neq 0$).

d) and e) Monostable systems in either region I or III: $\left|\frac{d_{II\mu}}{c_{II\mu}}\right| > \frac{1}{\gamma}$; either from a large bias in an untriggered system, or from an adequate trigger in any potentially bistable system.†

f) Stable system: $c_{II\mu} > 0$; the system is not a flipflop.

General Comments

1) Notice the relationship between $d_{II\mu}$ (bias or triggering or both, $d_{III} = d_{II0} + nW$) and the position of the singularities; the value of $\frac{dg}{dx}$ at a singular point and its nature:

† Potentially bistable system is any system which would exhibit bistable behavior if adequately biased, i.e., any system for which $c_{II0} < 0$; therefore, the system of Fig. 13f is not potentially bistable.

$\frac{dg}{dx} > 0 \Rightarrow$ stable singularity (in our case, stable node)

$\frac{dg}{dx} < 0 \Rightarrow$ unstable singularity (in our case, saddle point)

Of course, the exact nature of the singularity also depends on a_ν and $b_{\nu\mu}$.

2) The position of the singularity, if it is real, must be inside its corresponding region; otherwise, it is virtual.

3) The singularity nature and position is just a translation of the coefficients of the differential equation; this is one way to interpret the "action" of a singularity over its corresponding region no matter where it happens to be and justifies calling it "virtual" if it happens to be outside its region of influence: it does not really exist, but it would exist if the parameters $c_{\nu\mu}$ and $d_{\nu\mu}$ were the same throughout the phase plane as they are inside the proper region. In this sense, this would-be singularity adequately translates the coefficients of the differential equation inside its proper region.

4) We have used a coded tag to describe the singularities in this figure:

SN = Stable Node	R = Real
SP = Saddle Point	V = Virtual

The last symbol of the tags on the singularities is one of I, II or III, and designates the proper (corresponding) region of the singularity; so, if the position of the singularity agrees with this symbol, it is real; otherwise it is virtual. The symbol R or V is therefore redundant, but has been used for clarity.

3.3 Trajectory Equations

Solution to equation (2.103) is

$$\left.\begin{aligned} x_{\nu\mu} &= A_{\alpha\nu\mu} e^{\lambda_{\alpha\nu\mu}(t-t_{\nu\mu})} + A_{\beta\nu\mu} e^{\lambda_{\beta\nu\mu}(t-t_{\nu\mu})} + c_{\nu\mu} \\ y_{\nu\mu} &= \overset{\circ}{x}_{\nu\mu} \end{aligned}\right| \qquad (3.56)$$

where

a) ν refers to the region: ν = I, II, III

μ refers to the trigger: μ = 0, 1 => 0 trigger OFF, ON

b) $A_{\alpha\nu\mu}$, $A_{\beta\nu\mu}$, $c_{\nu\mu}$ are parameters corresponding to a given value of the pair $\nu\mu$.†

c) $\lambda_{\alpha\nu\mu}$, $\lambda_{\beta\nu\mu}$ are the natural frequencies corresponding to a value of the pair $\nu\mu$.

d) $t_{\nu\mu}$ is the instant of time when the pair of indices assumes a new value.

e) The most common sequence of index pair values is $\nu\mu$ = I0, I1, II1, III1, III0.

f) Let us use, in general, a prime to mean:

a', b', c', d',	differential equation parameter values in the previous $\nu\mu$ condition
A'_α, A'_β, C'	solution parameter values in the previous $\nu\mu$ condition
λ'_α, λ'_β	natural frequencies in the previous $\nu\mu$ condition
t', x', y'	values of t, x, y at the end of previous $\nu\mu$ condition

† Actually $c_{\nu\mu} = x_{\nu\mu}$ is the abscissa of singular point $X_{\nu\mu}$ --and here $X_{\nu\mu}$ has nothing to do with $X = x - x_{\nu\mu}$ used in the previous section.

Unprimed symbols will refer to parameters and variables throughout the present $\nu\mu$ conditions, which, whenever necessary, will be indicated.

g)
$$t_0 = t'$$

$$x_0 = x'$$

$$y_0 = y + \frac{U}{a}$$

with

U = magnitude of any impulse occurring during the transition from the previous value of $\nu\mu$ to the present value; it is zero if no impulse occurs at this point. It may be a function of y_0 or y', as in Table V.

t_0, x_0, y_0 = values of t, x, y at the beginning of present $\nu\mu$ condition.

h)
$$A_\alpha = + \frac{(x_0 - x^*)\lambda_\beta - y_0}{\lambda_\beta - \lambda_\alpha}$$

$$A_\beta = - \frac{(x_0 - x^*)\lambda_\alpha - y_0}{\lambda_\beta - \lambda_\alpha}$$

$$C = \frac{d}{c} = x^*$$

where

$(x^*,0) = (\frac{d}{c},0)$ = location of singularity corresponding to present $\nu\mu$ conditions.

TABLE V. IMPULSE VALUES FOR CHANGES IN $\nu\mu$

	$\nu\mu$ Condition Change		Magnitude of Impulse U	Comments
	From	To		
I to III Transition	IO	Il	$+2p \frac{\tau_{io}}{\tau} \lvert W \rvert$	$W > 0$
	Il	III	$-Hp\gamma \frac{\tau_{io}}{\tau} y_0^2$	y_0 is initial value of y in region II
	III	IIII	$+Hp\gamma \frac{\tau_{io}}{\tau} y'^2$	y' is final value of y in region II
	IIII	IIIO	$-2p \frac{\tau_{io}}{\tau} \lvert W \rvert$	$W > 0$
III to I Transition	IIIO	IIII	$-2p \frac{\tau_{io}}{\tau} \lvert W \rvert$	$W < 0$
	IIII	III	$+Hp\gamma \frac{\tau_{io}}{\tau} y_0^2$	y_0 is the initial value of y in region II
	III	Il	$-Hp\gamma \frac{\tau_{io}}{\tau} y'^2$	y' is the final value of y in region II
	Il	IO	$+2p \frac{\tau_{io}}{\tau} \lvert W \rvert$	$W < 0$

H is the symmetry factor: $H = \begin{cases} 1 \text{ for asymmetric flipflop.} \\ 2 \text{ for symmetric flipflop.} \end{cases}$

i)
$$\lambda_\alpha = \frac{1}{2a}\left\{-b + \sqrt{b^2 - 4c}\right\}$$

$$\lambda_\beta = \frac{1}{2a}\left\{-b - \sqrt{b^2 - 4c}\right\}$$

j) And for completeness we repeat equation (2.103) in the new notation:

$$a\overset{oo}{x} + b\overset{o}{x} + cx = d, \quad \text{for a given } \nu\mu$$

Now equation (3.56) becomes

$$\left.\begin{aligned} x &= A_\alpha e^{\lambda_\alpha(t-t_0)} + A_\beta e^{\lambda_\beta(t-t_0)} + X \\ y &= A_\alpha\lambda_\alpha e^{\lambda_\alpha(t-t_0)} + A_\beta\lambda_\beta e^{\lambda_\beta(t-t_0)} \end{aligned}\right\} \qquad (3.57)$$

In the phase plane, from (k) and (h),

$$t - t_0 = \frac{1}{\lambda_\beta}\,\ell n\,\frac{(x - x^*)\lambda_\alpha - y}{(x_0 - x^*)\lambda_\alpha - y_0} = \frac{1}{\lambda_\alpha}\,\ell n\,\frac{(x - x^*)\lambda_\beta - y}{(x_0 - x^*)\lambda_\beta - y_0} \qquad (3.58)$$

or, in another form:

$$e^{\lambda_\alpha\lambda_\beta(t-t_0)} = \left\{\frac{(x - x^*)\lambda_\alpha - y}{(x_0 - x^*)\lambda_\alpha - y_0}\right\}^{\lambda_\alpha} = \left\{\frac{(x - x^*)\lambda_\beta - y}{(x_0 - x^*)\lambda_\beta - y_0}\right\}^{\lambda_\beta} \qquad (3.59)$$

Notice that t and λ are normalized and have no dimensions!

Obs.: Equations (3.58) and (3.59) are phase plane trajectory equations, and the calculation of transition time is based on them. Also based on them is the phase plane graphical construction which simplifies not only transition time calculations but also the analysis of waveforms and design optimization of both circuit and trigger.

In this analysis the trigger is assumed rectangular, so the term $ns = \mu nW$ is imbedded into d; the impulse terms $m\overset{o}{s} = \mu mW[\delta(t - t_\theta) - \delta(t - t_\theta - T_\theta)]$ and also $f(\overset{o}{x})[\delta(x + \frac{1}{\gamma}) - \delta(x - \frac{1}{\gamma})]$ are both considered in g), with their magnitudes represented by U. This is summarized in Table V.

Therefore, expansion of g) yields for this special case:

Discontinuity	Transition	Through Line	
$y_0 = y' - \ell y_0^2$	I → II	$x = -\frac{1}{\gamma}$	(3.60a)
$y_0 = y' + \ell y'^2$	II → III	$x = +\frac{1}{\gamma}$	(3.60b)
$y_0 = y' + \ell y_0^2$	III → II	$x = +\frac{1}{\gamma}$	(3.60c)
$y_0 = y' - \ell y'^2$	II → I	$x = -\frac{1}{\gamma}$	(3.60d)

where

a) $\ell = \frac{Hm_{II}\gamma}{2a_{II}}$

b) m_{II} and a_{II} as in Table I

c) H is called the "symmetry factor":

$$H = \begin{cases} 1 \text{ for the asymmetric flipflop} \\ 2 \text{ for the symmetric flipflop} \end{cases}$$

We can write equations (3.60) in more explicit forms, and also obtain the inverse functions:

Discontinuity	Transition	Through Lines	
(i) $y_0 = \frac{1}{2\ell}\left\{+\sqrt{1 + 4\ell y'} - 1\right\}$ (ii) $y' = (1 + \ell y_0)y_0$	I → II	$x = -\frac{1}{\gamma}$	(3.61a)
(i) $y_0 = (1 + \ell y')y'$ (ii) $y' = \frac{1}{2\ell}\left\{+\sqrt{1 + 4\ell y_0} - 1\right\}$	II → III	$x = +\frac{1}{\gamma}$	(3.61b)
(i) $y_0 = \frac{1}{2\ell}\left\{-\sqrt{1 - 4'y'} + 1\right\}$ (ii) $y' = (1 - \ell y_0)y_0$	III → II	$x = +\frac{1}{\gamma}$	(3.61c)
(i) $y_0 = (1 - \ell y')y'$ (ii) $y' = \frac{1}{2\ell}\left\{-\sqrt{1 - 4\ell y_0} + 1\right\}$	II → I	$x = -\frac{1}{\gamma}$	(3.61d)

Notice that in cases (a) and (b) we have the I to III transition, i.e., $y > 0$ through the transition, whereas in cases (c) and (d) we have the III to I transition, i.e., $y < 0$ through the transition. The signs of the square roots are selected from this physical consideration.

3.4 Separatrices

We are using the word separatrix in a somewhat looser sense than its strictly mathematical meaning [17]. We shall call a "separatrix" any phase plane trajectory which divides the phase plane portrait of the system into qualitatively distinct families of trajectories.

The concept of "qualitatively distinct" is purposely vague; this means that a separatrix will be so with respect to some stated qualitative distinction

between the two families of trajectories in which it divides the phase plane portrait of the system.

In order to define a separatrix, all we need to do is to find one of its points Q, let $Q = (x_Q, y_Q)$, and enter x_Q and y_Q instead of x_0 and y_0 into equation (3.58) or (3.59). Also x* must be known (x* as defined in (3.56h)).

We have a special interest in defining two types of separatrix over the whole portrait:

(i) "Transition Separatrix" which divides the portrait into two families of trajectories: those that cross through region II and those that do not. This separatrix, as illustrated in Figs. 15 and 16, is composed of four branches: A, B; C, D; $\bar{A}$, $\bar{B}$; $\bar{C}$, $\bar{D}$.

These lines will be given special names:

a) ABCD: (I to III) transition separatrix.

b) $\bar{A}\bar{B}\bar{C}\bar{D}$: (III to I) transition separatrix.

c) $AB\bar{B}\bar{A}$: end-point separatrix.

d) $DC\bar{C}\bar{D}$: initial-point separatrix.

Since

a) ABCD separates the lines which are trajectories from region I to region III from the lines which are not so.

b) $\bar{A}\bar{B}\bar{C}\bar{D}$ separates the lines which are trajectories from region III to region I from the lines which are not so.

c) $AB\bar{B}\bar{A}$ divides the portrait into two sets of trajectories: those that terminate in $x_{I\mu}$ and those that terminate in $x_{III\mu}$.

d) $DC\bar{C}\bar{D}$ divides the portrait into two sets of trajectories: those that originate in region I and those that originate in region III.

(ii) "Critical Separatrix," whose importance will be later explained, divides the portrait into two families of trajectories: those that lie partly

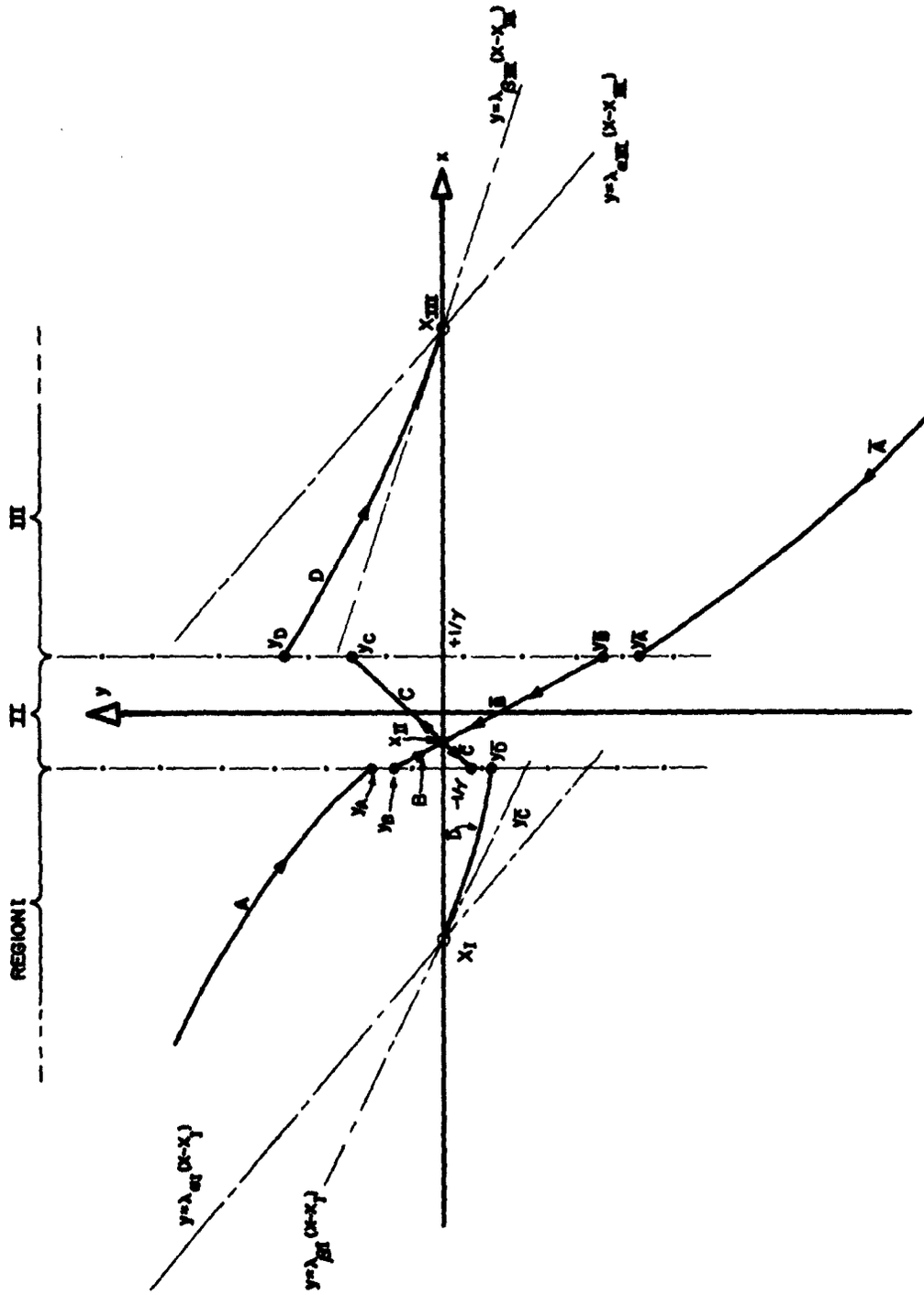

FIGURE 15: SEPARATRIX FOR A SYSTEM WHERE $d_{II\mu} > 0$, $c_{II\mu} < 0$, AND $|d_{II\mu}/c_{II\mu}| < 1/\gamma$

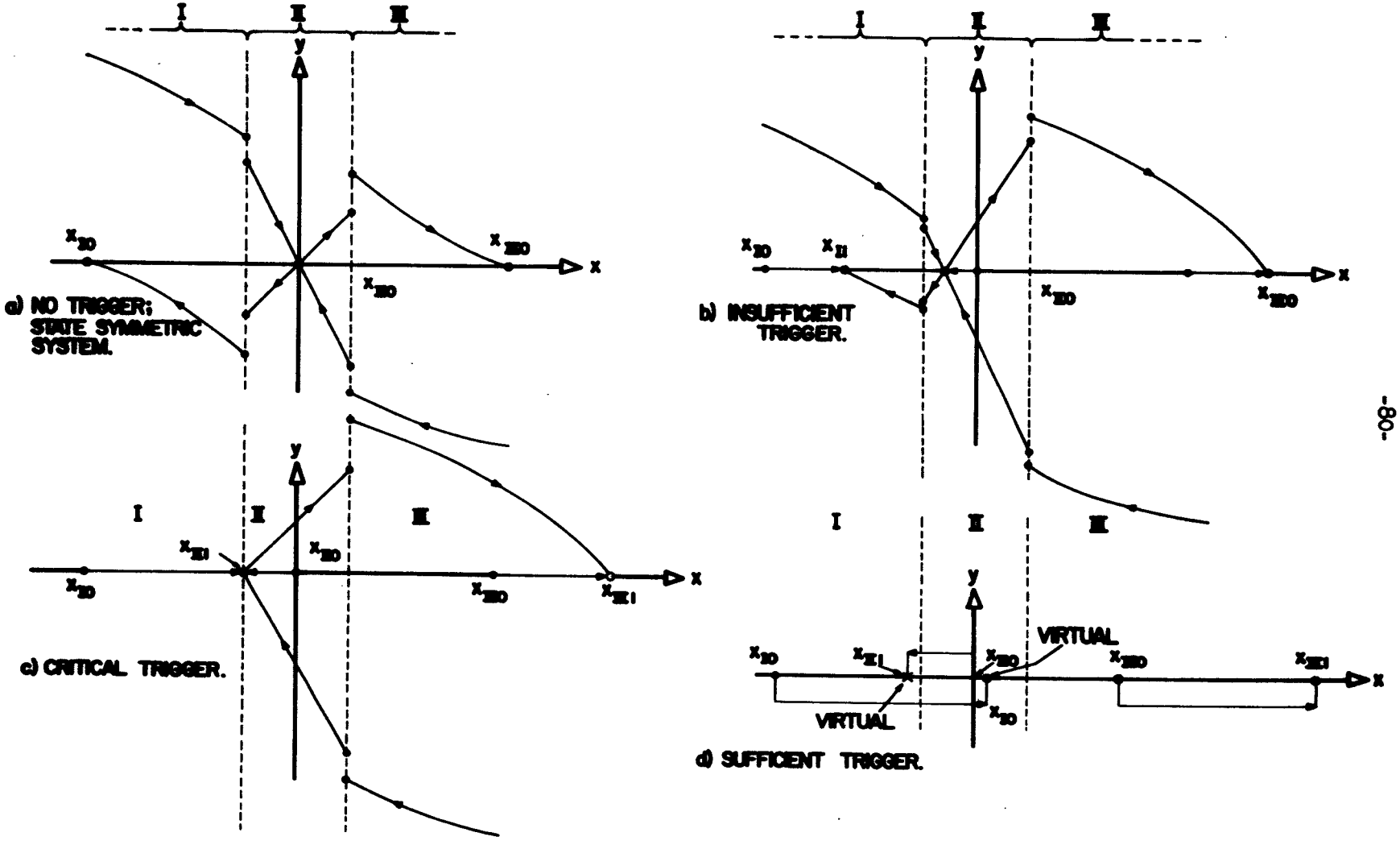

FIGURE 16: EFFECT OF TRIGGER ON PHASE PLANE PORTRAIT.

in region II and those that lie exclusively in region I or III. Fig. 15 illustrates the separatrices and the notation used in this section. Notice the following:

a) <u>The Transition Separatrix Determining Points</u>: Obviously, in region II, the separatrix itself consists of the two asymptotes whose equations are (see Fig. 14):

$$\left.\begin{aligned} y_\alpha &= \lambda_\alpha \cdot (x - x^*); \quad \text{let} \quad y_B = y_\alpha(-\tfrac{1}{\gamma}), \quad y_{\overline{B}} = y_\alpha(+\tfrac{1}{\gamma}) \\ y_\beta &= \lambda_\beta \cdot (x - x^*); \quad \text{let} \quad y_C = y_\beta(+\tfrac{1}{\gamma}), \quad y_{\overline{C}} = y_\beta(-\tfrac{1}{\gamma}) \end{aligned}\right\} \quad (3.62)$$

where

x is in region II

$(x^*,0)$ is the singularity corresponding to region II

λ_1 and λ_2 are the natural frequencies inside region II

We find

$$y_A, \qquad y_D, \qquad y_{\overline{A}}, \qquad y_{\overline{D}}$$

respectively from

$$y_B, \qquad y_C, \qquad y_{\overline{B}}, \qquad y_{\overline{C}}$$

through equation (3.59):

$$(a,ii), \quad (b,i), \quad (c,ii), \quad (d,i),$$

after the replacements:

$$\left\{\begin{aligned} &y_A \to y', \quad y_D \to y_0, \quad y_{\overline{A}} \to y', \quad y_{\overline{D}} \to y_0 \\ &y_B \to y_0, \quad y_C \to y', \quad y_{\overline{B}} \to y_0, \quad y_{\overline{C}} \to y \end{aligned}\right.$$

We get the following equations:

$$y_A = (1 + \ell y_B)y_B \tag{3.63a}$$

$$y_D = (1 + \ell y_C)y_C \tag{3.63b}$$

$$y_{\bar{A}} = (1 + \ell y_{\bar{B}})y_{\bar{B}} \tag{3.63c}$$

$$y_{\bar{D}} = (1 + \ell y_{\bar{C}})y_{\bar{C}} \tag{3.63d}$$

b) The Critical Separatrix Determining Points: Of course those trajectories which cross the x axis at points $x = -\frac{1}{\gamma}$ and $x = \frac{1}{\gamma}$ are the two branches of the critical separatrix.

c) The Separatrices: The two separatrices, as illustrated in Fig. 15, are given by the general trajectory equation (3.58) or (3.59) (they are entirely equivalent). Since here we are more concerned with geometrical properties, we prefer the latter, which we repeat here as equation (3.64), leaving out the exponential of time, and replacing (x_0,y_0) by (x_Q,y_Q). So the separatrices are given by:

$$\left\{\frac{(x - x^*)\lambda_\alpha - y}{(x_Q - x^*)\lambda_\alpha - y_Q}\right\}^{\lambda_\alpha} = \left\{\frac{(x - x^*)\lambda_\beta - y}{(x_Q - x^*)\lambda_\beta - y_Q}\right\}^{\lambda_\beta} \tag{3.64}$$

and Tables VI and VII furnish the values of the parameters.

Besides the separatrices, three more lines at each stable node are important in the qualitative study of trajectories in the phase plane. These lines are: (by definition) assuming $\lambda_\alpha < \lambda_\beta$ (see Fig. 12):

a) The "tangent line": $y = \lambda_\beta(x - x^*)$, which is a tangent to all trajectories at point $(x^*,0)$.

TABLE VI. PARAMETERS OF THE SEPARATRIX EQUATION (3.64)

	Calculate by	--	Equation (3.63)	Table II	Equation (3.56i) and Table I
	Parameter	x_Q	y_Q (depend on μ)	x^*	λ_i $i = \alpha, \beta$
	Branch	Value			
Transition Separatrix	Branch A	$-\frac{1}{\gamma}$	y_A	$x_{I\mu}$	$\lambda_{iI\mu}$
	Branch D	$+\frac{1}{\gamma}$	y_D	$x_{III\mu}$	$\lambda_{iIII\mu}$
	Branch $\bar{A}$	$-\frac{1}{\gamma}$	$y_{\bar{A}}$	$x_{III\mu}$	$\lambda_{iIII\mu}$
	Branch $\bar{D}$	$-\frac{1}{\gamma}$	$y_{\bar{D}}$	$x_{I\mu}$	$\lambda_{iI\mu}$
Critical Separatrix	Branch E	$-\frac{1}{\gamma}$	0	$x_{I\mu}$	$\lambda_{iI\mu}$
	Branch $\bar{E}$	$+\frac{1}{\gamma}$	0	$x_{III\mu}$	$\lambda_{iIII\mu}$

Notice that the index μ merely indicates if the trigger is ON or OFF; the actual direction and effects of the trigger (if ON) must be computed through Tables I and II.

TABLE VII. RESULTS OF EQUATIONS (3.62) FOR THE BRANCHES OF THE TRANSITION SEPARATRIX INSIDE REGION II

	Branch	Equations (3.62)	Furnish	
Transition Separatrix	Branch B, $\bar{B}$	$y_\alpha = \lambda_\alpha \cdot (x - x_{II})$	$y_B = y_\alpha(-\frac{1}{\gamma})$	$y_{\bar{B}} = y_\alpha(+\frac{1}{\gamma})$
	Branch C, $\bar{C}$	$y_\beta = \lambda_\beta \cdot (x - x_{II})$	$y_C = y_\beta(+\frac{1}{\gamma})$	$y_{\bar{C}} = y_\beta(-\frac{1}{\gamma})$

Notice that both y_i's and λ_i's, $i = \alpha, \beta$, depend on μ, so all y's depend on μ.

b) The "direction line": $y = \lambda_\alpha(x - x^*)$, which does not cross any trajectory except at point $(x^*,0)$, where it crosses all trajectories.

c) The "max-min line": $y = \frac{\lambda_\alpha\lambda_\beta}{\lambda_\alpha + \lambda_\beta}(x - x^*)$ which crosses all trajectories at $(x^*,0)$ and also every trajectory at its point of maximum or minimum value of $y(x)$.

d) The line described in (b) also applies to the case of saddle points, except that, at the singularity $(x^*,0)$ it crosses only the asymptotes, since the other trajectories do not pass through the singularity.

3.5 Trajectories and the Action of the Trigger

The simplest trigger is the rectangular current trigger. In fact the action of a trigger of a different waveform will, in general, differ in detail, but not in principle from the action of the rectangular trigger. For this reason we have considered it important enough to be the basis of this work, and, in this section, we will discuss its action in a qualitative manner.

3.5.1 Turning the Trigger ON and Possibility of "Under-Triggering"

Figures 16 show various possibilities of trigger action upon the phase plane portrait--singularities and separatrices--and also the corresponding initial value of y.

Let us assume that the flipflop is in stable state I, i.e., the representative point P is at stable node I, when a rectangular trigger of amplitude W is applied (a positive trigger).

The immediate effect of the trigger upon the phase plane portrait is to shift the stable nodes to points respectively Δx_I and Δx_{III} to the right, and to shift the saddle point by Δx_{II} to the left, where $\Delta x_\nu = x_{\nu 1} - x_{\nu 0}$, as given by Table II.

At the same time P is shifted upwards to a point at (x_{IO}, y_O), i.e., the x coordinate does not change, but y goes to an initial value

$$y_O = \frac{m_I}{a_I} W \tag{3.65}$$

Suppose that the singularities have not been shifted out of their proper regions (Fig. 16b). The transition separatrix in region I approaches the critical separatrix (whose shape changes!), thus reducing the minimum initial value y_{Omin} of y necessary for a complete transition to occur.

Let $X_{\nu\mu}$ denote the singularity $(x_{\nu\mu}, 0)$, and let y_{Omin} be the least initial ordinate at x_{IO}, for which a I to III transition occurs.

There will be two possibilities:

a) $y_O < y_{Omin}$, then P will follow some parabolic trajectory and tend towards X_{II}. Here there are yet three possibilities.

   1. $y_O < \lambda_\alpha \Delta x_I$: P will not cross the x axis, moving towards X_{II}, in an overdamped manner.
   2. $y_O = \lambda_\alpha \Delta x_I$: P will not cross the x axis, following a straight path towards X_{II}, approaching it in a critically damped way.
   3. $y_O > \lambda_\alpha \Delta x_I$: P will cross the x axis, moving towards X_{II} in an underdamped way.

In case 3 we might still distinguish the two possibilities of P going through region II (entering it under point y_a) or not.

b) $y_O > y_{Omin}$, then P will also follow a parabolic path towards $X_{I\mu}$ in the underdamped way, as in (a.3) above, but it enters region II <u>above</u> point y_a before reaching the x axis. Then a transition occurs. This effect will be called "under-triggering" (Fig. 19).

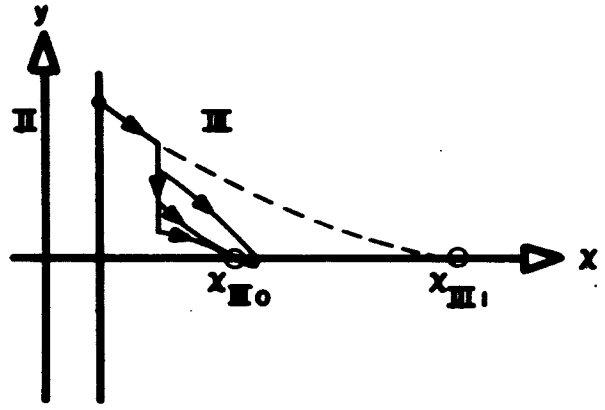

a) $x(T) < x_{III_0}$; $y(T+) > 0$

THREE DIFFERENT WAYS TO APPROACH x_{III_0}, DEPENDING ON THE VALUE OF $y(T+)$

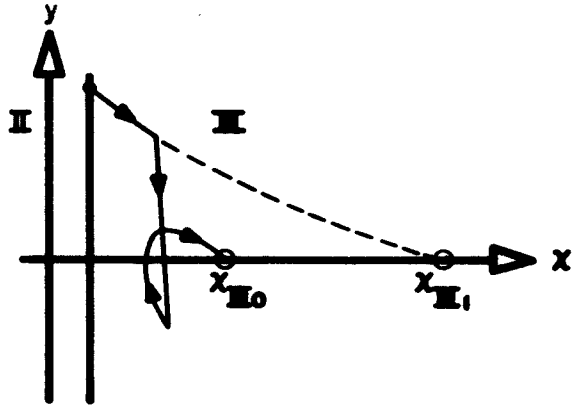

b) $x(T)$ x_{III_0} ; $y(T+)$ 0

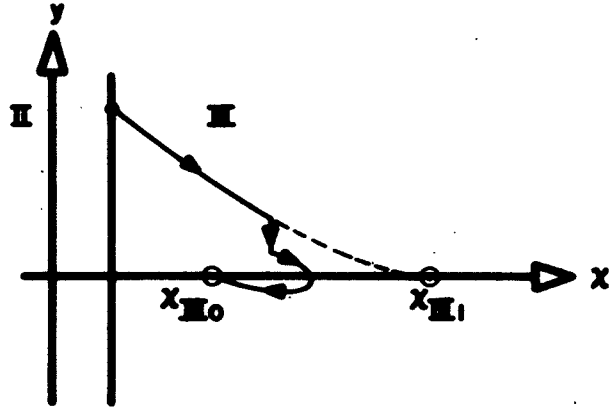

c) $x(T) > x_{III_0}$; $y(T+) > 0$

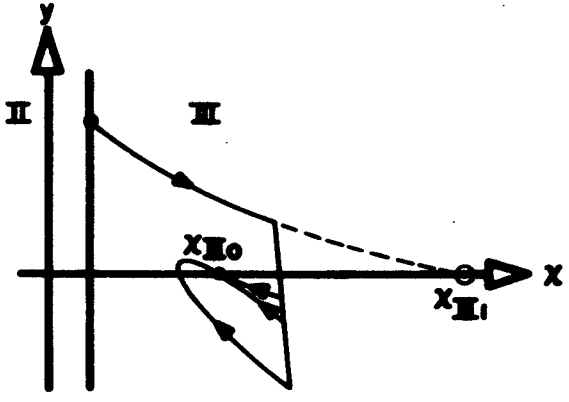

d) $x(T) > x_{III_0}$; $y(T+) < 0$;

THREE WAYS TO APPROACH x_{III_0}, DEPENDING ON THE VALUE OF $y(T+)$

FIGURE 17: TRAJECTORIES AFTER TRIGGER TURN-OFF.

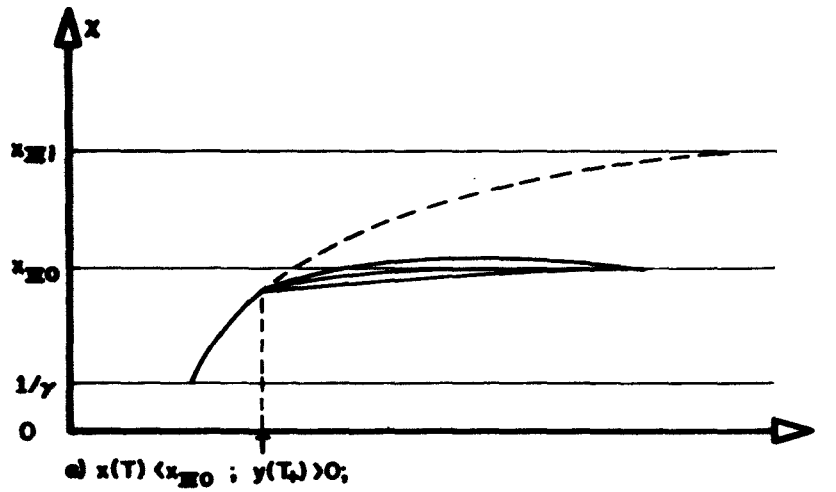

a) $x(T) < x_{EQ0}$; $y(T_+) > 0$;

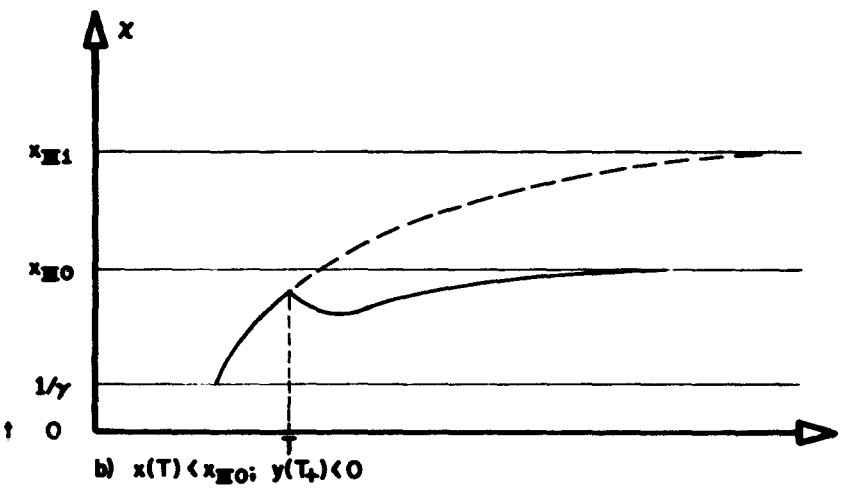

b) $x(T) < x_{EQ0}$; $y(T_+) < 0$

THREE DIFFERENT WAYS TO APPROACH x_{EQ0}, DEPENDING ON $y(T_+)$.

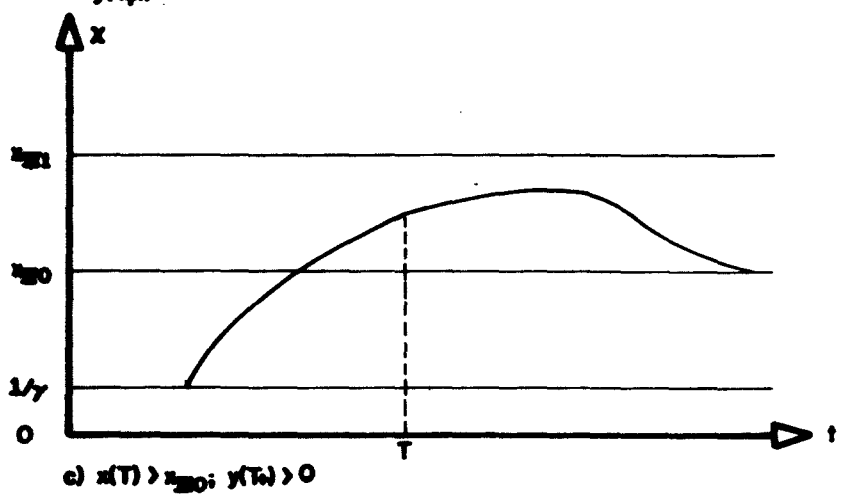

c) $x(T) > x_{EQ0}$; $y(T_+) > 0$

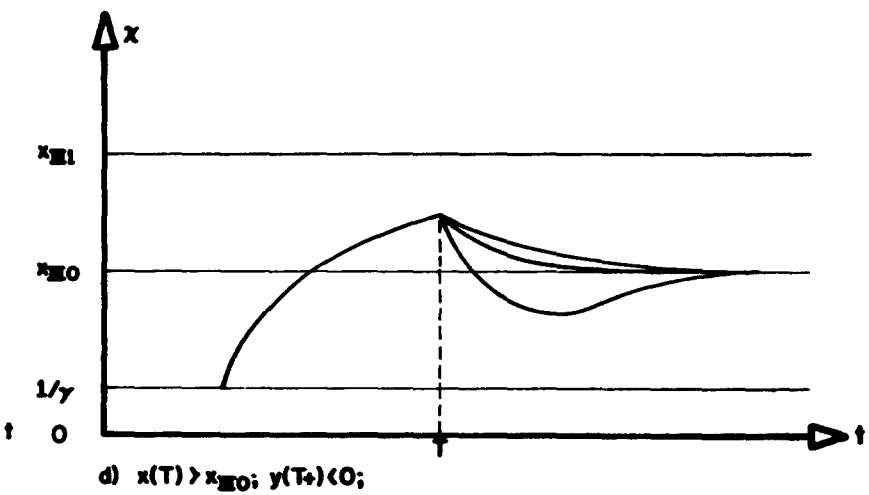

d) $x(T) > x_{EQ0}$; $y(T_+) < 0$;

THREE WAYS TO APPROACH x_{EQ0}, DEPENDING ON $y(T_+)$.

FIGURE 18: TRAJECTORIES AFTER TRIGGER TURN-OFF IN TIME DOMAIN, CORRESPONDING TO CASES ILLUSTRATED IN FIGURE 17

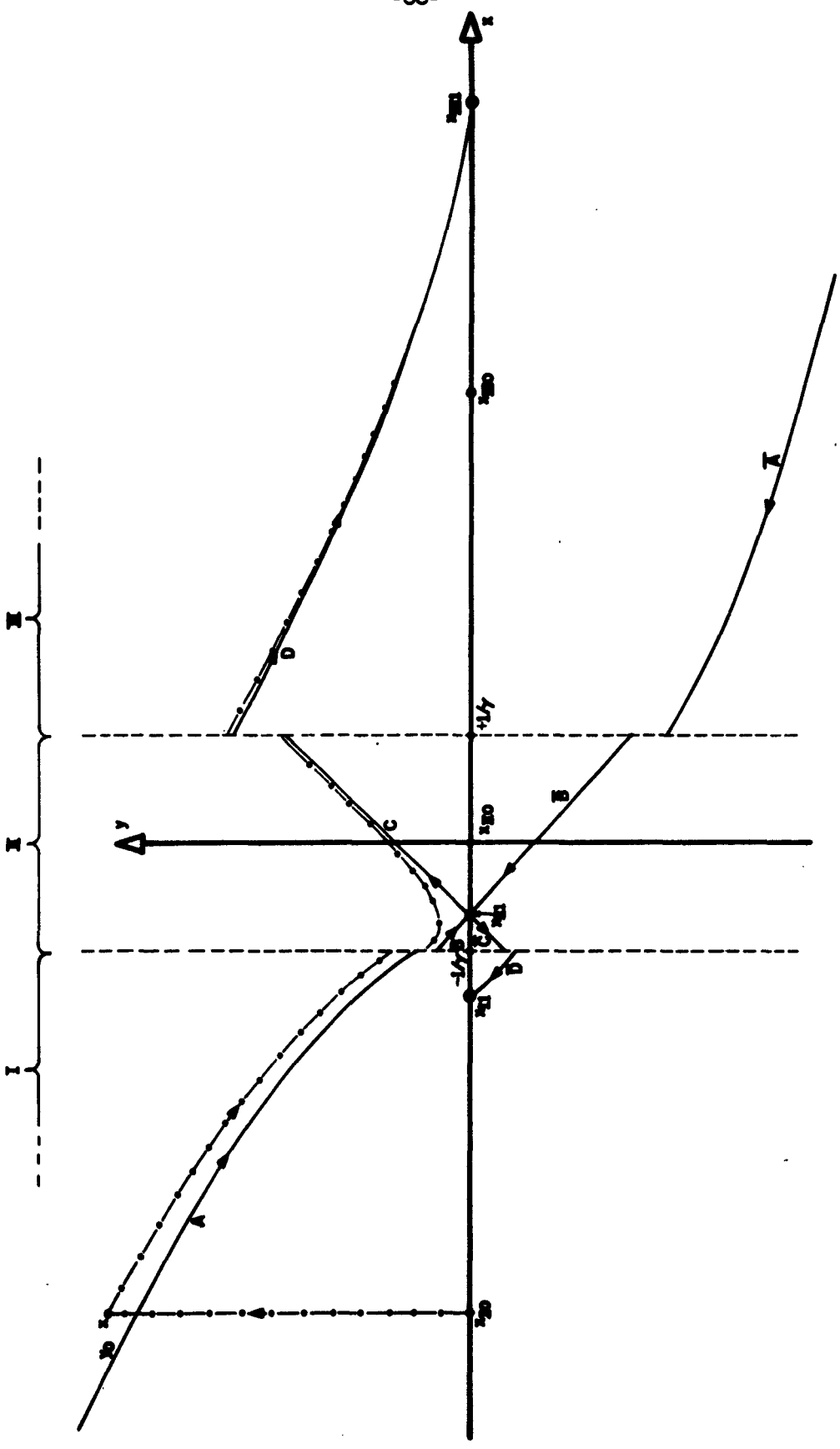

FIGURE 19- UNDER-TRIGGERING; HEAVY LINES ARE THE SEPARATRIX BRANCHES WITH TRIGGER ON, BROKEN DOTTED LINES IN THE TRAJECTORY OF P IN CASE OF UNDER-TRIGGERING.

One might then expect that the minimum value W_{min} of W necessary to cause a transition would be slightly less than the value W_{crit} of W necessary to shift $X_{I\mu}$ and $X_{II\mu}$ out of their proper regions (and into virtual existence!). But this is usually not so, as it will be proved at the end of this section that, under certain (usual) conditions, of all possibilities mentioned above only (a.1) occurs, all others being impossible for the type of circuit under consideration. Therefore, under-triggering usually does not occur for this type of circuit. However, it is a possibility, especially in a general equation, whose coefficients were related in some other manner. We will later study this effect in some detail.

3.5.2 Virtual Singularities and the Trajectory

We establish that $W_{min} \equiv W_{crit} \equiv W_0$; suppose that $W > W_0$; then the portrait becomes as in Fig. 16d. There is only one real singularity, and this is the stable node X_{III1}; the end-point separatrix vanishes (since all lines must now terminate at X_{III1}); the critical separatrix and part of the initial-point separatrix also vanish, and the remaining part of the initial-point separatrix loses its meaning.

From its initial position at (x_{I0}, y_0), P "sees" only the virtual stable node X_{I1} (somewhere in region II or III) and starts to move on a parabolic path towards it. However, before reaching x_{I1}, P crosses the line $x = -\frac{1}{\gamma}$ where y suffers a discontinuity $(-\Delta_b y)$,† and enters region II where now it "sees" only the virtual saddle point X_{III} (somewhere in region I) and changes its trajectory into a hyperbolic path asymptotic to the line $y = \lambda_{III} \cdot (x - x_{III})$ (a remaining part of the initial-point separatrix, and here we see why it is meaningless);

† See footnote on page 90.

finally, P crosses the line $x = +\frac{1}{\gamma}$, where y suffers a discontinuity $(+\Delta_c y)$,† and enters region III.

Once in region III, P will "see" only the real stable node x_{III1}, towards which it will start to move in a parabolic path (in an overdamped manner, as will be shown).

3.5.3 Turning the Trigger OFF

The next event with the trajectory of P is the turning OFF of the trigger.

Rigorously, the trigger may be turned OFF as soon as P has progressed far enough into region II, i.e., to a point where, after the negative jump of y caused by the trigger turning OFF, P finds itself at side III of the end-point separatrix (of the $\mu = 0$ system, of course).

On the other extreme, we could leave the trigger ON for an indefinite amount of time.

We are interested in establishing a criterion with which to judge the adequacy of the trigger duration.

3.5.4 Discussing Trigger Duration

Assuming the trigger is sufficiently long to produce a transition, we recognize five possibilities for the trigger (see Figs. 17 and 18):

(i) Too short: if it is turned OFF while P is still in region II.

(ii) Short: if it is turned OFF long before P reaches the line $x = x_{III0}$, but after P is in region III (Figs. 17a, b and 18a, b).

† Discontinuities caused by impulses $\mp \ell y^2 \frac{d^2\varphi(x)}{dx^2}$ respectively.

(iii) Fair: if it is turned OFF approximately as P crosses the line $x = x_{III0}$.

(iv) Long: if it is turned OFF long after P crosses the line $x = x_{III0}$, but before it approaches X_{III1} (Figs. 17c, d and 18c, d).

(v) Too long: if it is turned OFF after P is already close to X_{III1}.

Of course, these definitions can be formalized and made exact: so, a sufficient rectangular trigger starting at $t_0 = 0$ and having duration T is said to be:

(i) Too short: if $x(T) < -\frac{1}{\gamma}$

(ii) Short: if $+\frac{1}{\gamma} < x(T) < x_{III0} - \epsilon_{0-}$

(iii) Fair: if $x_{III0} - \epsilon_{0-} < x(T) < x_{III0} + \epsilon_{0+}$

(iv) Long: if $x_{III0} + \epsilon_{0+} < x(T) < x_{III1} - \epsilon_1$

(v) Too long: if $x_{III1} - \epsilon_1 < x(T)$

where ϵ_{0-}, ϵ_{0+}, ϵ_1 are positive numbers such that all the inequalities above can be satisfied.

No matter which case occurs, y will suffer a discontinuity equal to $(-y_0)$; from the point $(x(T), y(T))$, P will jump to $(x(T), y(T) - y_0)$, and then it will move towards X_{III0} by some parabolic path, thus completing the transition.

NOTE: Of course, P never reaches X_{III0}, but given an arbitrary neighborhood ϵ_{III0} of X_{III0}, there is a time $T_{III0}(\epsilon_{III0})$ such that for any $t > T_{III0}(\epsilon_{III0})$, P is in ϵ_{III0}. We can therefore, arbitrarily select a neighborhood N_{III0} of X_{III0}, and, by definition, say that a transition is complete after P enters N_{III0} for the last time.

3.5.5 The Concept of "Optimum Trigger Duration"

Call:

$$\left.\begin{array}{l} P_{T-} \text{ the point } (x(T),\ y(T)) \\ \text{and} \\ P_{T+} \text{ the point } (x(T),\ y(T) - y_0) \end{array}\right\} \qquad (3.66)$$

and let $\vec{P}_{T-}$, $\vec{P}_{T+}$, $\vec{X}_{IIIO}$, etc., be vectors with the same coordinates as the points designated by the symbols under the arrows.

By definition, let

$$R_{IIIO}(W,T) = |\vec{P}_{T+} - \vec{X}_{IIIO}| \qquad (3.67)$$

Given a rectangular trigger of amplitude W, we define "optimum duration T*" as that value of T for which $R_{IIIO}(T)$ is a minimum. That is:

$$R_{IIIO}(W,T^*) = \min_{T} R_{IIIO}(W,T) \qquad (3.68)$$

Since for each value of W there is a corresponding value T*, we conclude that, for a given circuit, T* is a function of W:

$$T^* = \Theta(W) \qquad (3.69)$$

This function $\Theta(W)$ is a characteristic of the complete circuit, i.e., flipflop and triggering circuit together.

Notice however that the definition of T* is somewhat arbitrary, and probably there is no ideal criterion on which to base a definition of optimum duration. It certainly depends under what criterion we would like to have the transition optimized.

A more practical definition is as follows: given a rectangular trigger of amplitude W, we define "optimum duration T*" as the value of T for which $x(T) = x_{III0}$. That is

$$x(T^*) = x_{III0} \tag{3.70}$$

The discussion presented in this subsection can be applied to a III to I transition, if we make the necessary (and obvious) changes.

The criterion for the definition of T* expressed by equation (3.70) is the most useful, and will be used throughout this report. So, unless otherwise specified, the expression of "optimum duration" or the symbol T* will imply "as defined by equation (3.70)."

3.5.6 Possibility of "Back-Triggering"

We have said that after the trigger is turned OFF, if it is sufficiently long, P (whose y coordinate has suffered a negative discontinuity equal to $(-y_0)$) "sees" only X_{III0} towards which it moves by some parabolic path.

However, we must ask ourselves if this is always true. There seems to be nothing in the nature of the equation to warrant this assumption. The objection is: "The position $(x(T-), y(T-))$ of P at the moment of turning the trigger OFF might be such that the new position of P, $(x(T+), y(T+))$ (where $y(t+) = y(T-) - y_0$) would be under the branch $\bar{A}$ of the transition separatrix, and therefore P would return to X_{I0}, rather than going to X_{III0}!" This effect will be called "back-triggering."

In fact, the possibility of back-triggering is small, unless the coefficients of the differential equation were not related by the circuit parameters (representing some other analogous type of bistable device).

We will prove that, under certain (usual) conditions, back-triggering is not possible for the circuits under consideration.† The conditions that make back-triggering impossible are the same that make under-triggering impossible.

Actually, these two characteristics are closely related. We will presently discuss these effects in some detail, explain their interrelation, and find the conditions that make them impossible to occur.

3.5.7 Trajectory After the Trigger is Turned OFF

Let us assume the trigger duration is sufficient and that no back-triggering occurs. Figures 17 and 18 illustrate the four cases as considered below:

(i) $x(T) < x_{III0}$, $y(T+) > 0$

(ii) $x(T) < x_{III0}$, $y(T+) < 0$

(iii) $x(T) > x_{III0}$, $y(T+) > 0$

(iv) $x(T) < x_{III0}$, $y(T+) < 0$

Figure 19 illustrates the three possibilities in the case of optimum triggering: $x(T) = x_{III0}$.

(i) $y(T+) > 0$

(ii) $y(T+) = 0$

(iii) $y(T+) < 0$

We should point out that $x(T)$ is quite arbitrary, since we have absolute control of the trigger duration T; but, for a given circuit, $y(T+)$ is

---

† We point out again that back-triggering refers only to the case of sufficient trigger, i.e., there must be an interval of time $T_{min} < T < T_{max}$ for which a normal transition would occur. $T < T_{min}$ means insufficient trigger duration; T_{max} would be imposed by back-triggering.

a function of $x(T)$ given by the phase plane portraits of the differential equations (with trigger ON and OFF). This means that, for a given differential equation, selection of $T = T^*$ will lead to a certain value of $y(T^*+)$ for which $y(T^*+) \gtrless 0$; the equation and also the trigger amplitude W will determine which relationship holds.

It would be interesting to know how the coefficients of the equation and the circuit parameters, as well as the trigger amplitude affect the curve $y(T)$ versus $x(T)$. It would also be useful to know how T^* and $y(T^*+)$ depend on W for a given equation.

In the following chapters these questions will be considered.

3.6 Under-Triggering and Back-Triggering

Let us analyze the possibilities of under-triggering and back-triggering for

(i) a given differential equation of type (2.103) with coefficients defined in the three regions

(ii) ignoring, in this section, the relationships established in Table I, but still assuming

(iii) a rectangular trigger (i.e., (3.6) and (3.7) hold) and that, as before

(iv) the function $f(\overset{o}{x}) \equiv f(y)$, the magnitude of the impulses occurring at $x = \mp \frac{1}{\gamma}$, are:

$$f(y) = \begin{cases} \lim_{\epsilon \to 0} \left[-\ell_{II} y^2 \right] \Big|_{|x| = \frac{1}{\gamma} - \epsilon} , & \text{at } x = \mp \frac{1}{\gamma} \\ \\ \text{undefined for any } x \neq \mp \frac{1}{\gamma} \; \dagger \end{cases} \tag{3.71}$$

with

$$\ell_{II} = \frac{m_{II}}{2a_{II}} \text{ or } \frac{m_{II}}{a_{II}} \text{ , according to whether the flipflop is asymmetric or symmetric.}$$

3.6.1 Under-Triggering

Suppose a trigger of amplitude $W < W_0$ is applied to the system; assume P was at $X_{I0} = (x_{I0}, 0)$ before the trigger was turned ON.

P jumps to a point $P_0 = (x_{I0}, y_0)$; if P is above branch A of the transition separatrix of the triggered system, then a transition will occur, with P going to X_{III}, rather than to X_{II} (under-triggering). Fig. 19 illustrates this effect. Therefore a transition will occur if and only if

$$y_0 > y_{al0}$$

where y_{al0} is the ordinate of branch A of the transition separatrix of the triggered system ($\mu = 1$) at $x = x_{I0}$.

The problem is to find the value W_{min} of W that, for a given system, will cause the point (x_{I0}, y_0) to be on branch A of the transition separatrix of the triggered system (i.e., $\mu = 1$).

---

† We could keep the expression $f(y) = -\ell y^2$ at any other point $x \neq \mp \frac{1}{\gamma}$, taking $\ell = \ell_{\nu\mu}$, $\nu\mu$ indicating region and state of trigger; but this would be irrelevant, since the function is multiplied by zero at these points anyway!

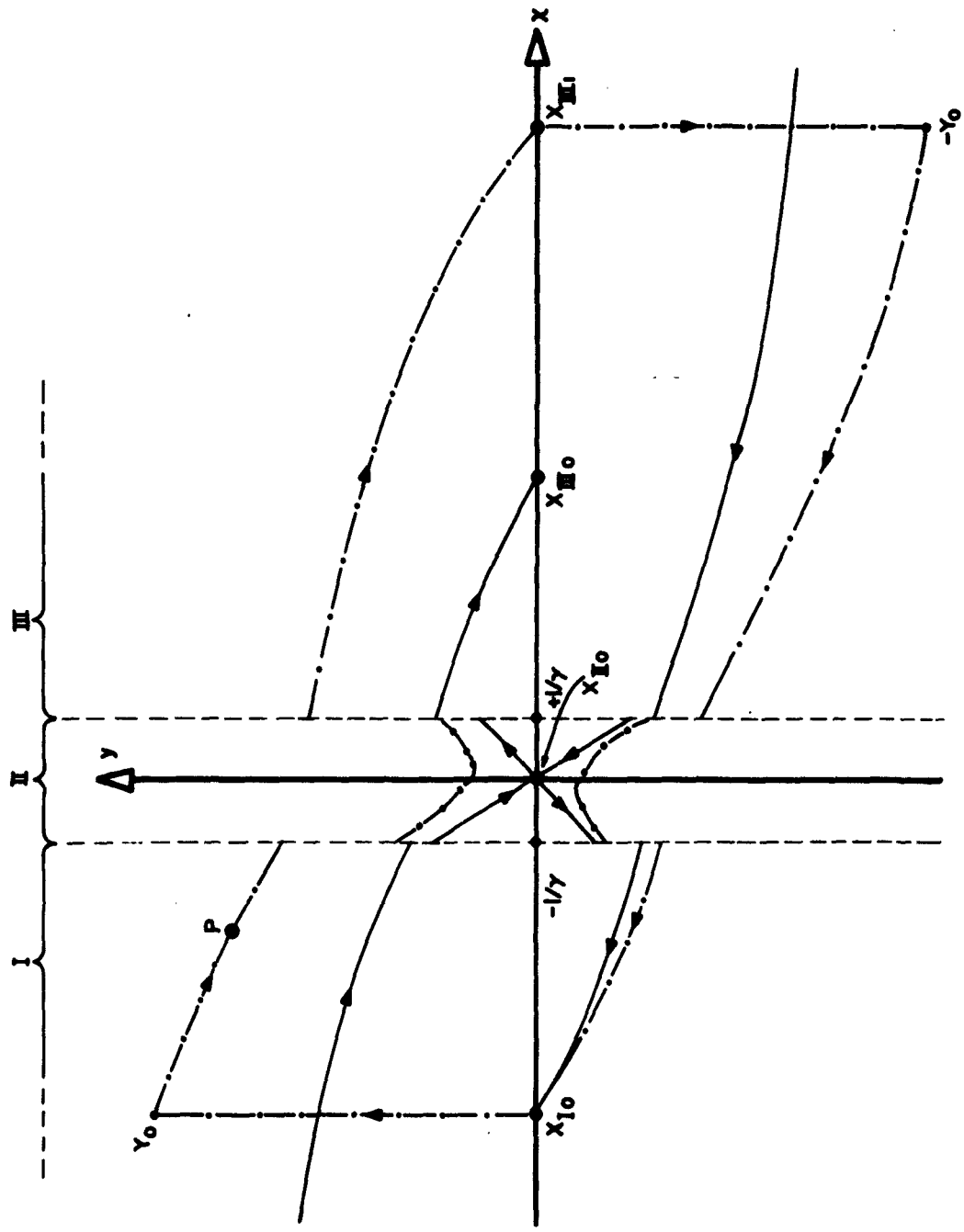

FIGURE 20: BACK-TRIGGERING; HEAVY LINES ARE SEPARATING BRANCHES WITH TRIGGER OFF; BROKEN DOTTED LINE IS THE TRAJECTORY OF P IN CASE OF UNDER-TRIGGERING. I TO III TRAJECTORY IS IRRELEVANT HERE.

As could be expected, we will see that it is not possible to solve this problem analytically, but only by a graphical or iterative numerical procedure. In fact, we have a set of formulae, repeated here for convenience, that can be used to solve this problem:

From (3.13) and the Obs. at the end of section 3.2.2,

$$x_{\nu\mu} = \frac{d_{\nu\mu}}{c_{\nu\mu}} = \frac{d_{\nu}}{c_{\nu\mu}} + \mu \frac{n}{c_{\nu\mu}} W \tag{3.72}$$

from which we get:

$$\left.\begin{aligned} x_{I0} &= \frac{d_I}{c_{I0}} & x_{II0} &= \frac{d_{II}}{c_{II0}} \\ x_{I1} &= \frac{d_I}{c_{I1}} + \frac{n}{c_{I1}} W & x_{II1} &= \frac{d_{II}}{c_{II1}} + \frac{n}{c_{II1}} W \\ 0 < W < W_0 \Rightarrow x_{I0} < x_{I1} < -\frac{1}{\gamma} & & 0 < W < W_0 \Rightarrow 0 > x_{II1} > -\frac{1}{\gamma} & \end{aligned}\right\} \tag{3.73}$$

From (3.62), using the notation $\lambda_{\alpha\nu\mu}$ and $\lambda_{\beta\nu\mu}$ as before:

$$y_{B1} = -\lambda_{\alpha II1} \cdot (\tfrac{1}{\gamma} + x_{II1}), \qquad W < W_0 \Rightarrow y_{B1} > 0 \tag{3.74}$$

$$y_{A1} = y_{B1} \cdot (1 + \ell y_{B1}), \qquad \text{clearly} \quad y_{A1} > y_{B1} \tag{3.75}$$

with

$$\ell = \frac{H}{2} \frac{m_{II}}{a_{II}}, \qquad H = \begin{cases} 1 \text{ for the asymmetric flipflop} \\ 2 \text{ for the symmetric flipflop} \end{cases}$$

Also, from equation (2.103) itself (see section 3.5.1):

$$y_0 = \frac{m_I}{a_I} W \tag{3.76}$$

And finally, the general trajectory equation, expressed by (3.59) can be rewritten as:

$$\left\{\frac{(x_i - x^*)\lambda_\alpha - y_i}{(x_j - x^*)\lambda_\alpha - y_j}\right\}^{\lambda_\alpha} = \left\{\frac{(x_i - x^*)\lambda_\beta - y_i}{(x_j - x^*)\lambda_\beta - y_j}\right\}^{\lambda_\beta} \tag{3.77}$$

where (x_i, y_i) and (x_j, y_j) are any two points over the same trajectory, in the same region, and x^* is the abcissa of the singularity and λ_α and λ_β are the natural frequencies corresponding to that region; so, in (3.77) let:

$$\left.\begin{aligned} &(x_i, y_i) = (x_{IO}, y_O); \qquad x^* = x_{I1} \\ &(x_j, y_j) = (-\tfrac{1}{\gamma}, y_A); \qquad \lambda_\alpha \text{ and } \lambda_\beta = \lambda_{\alpha I1} \text{ and } \lambda_{\beta I1} \end{aligned}\right\} \tag{3.78}$$

Considering (3.73), (3.74), (3.75), (3.76) and (3.78), (3.77) yields:

$$\left\{\frac{\frac{m_I}{a_I} W + \lambda_{\alpha I1}\left(\frac{d_I + nW}{c_{I1}} - \frac{d_I}{c_{IO}}\right)}{\lambda_{\alpha III}\left(\frac{1}{\gamma} + \frac{d_{II} + nW}{c_{III}}\right)\left[\ell\lambda_{\alpha III}\left(\frac{1}{\gamma} + \frac{d_{II} + nW}{c_{III}}\right) - 1\right] + \lambda_{\alpha I1}\left(\frac{1}{\gamma} + \frac{d_I + nW}{c_{I1}}\right)}\right\}^{\lambda_{\alpha I1}}$$

$$= \left\{\frac{\frac{m_I}{a_I} W + \lambda_{\beta I1}\left(\frac{d_I + nW}{c_{I1}} - \frac{d_I}{c_{IO}}\right)}{\lambda_{\alpha III}\left(\frac{1}{\gamma} + \frac{d_{II} + nW}{c_{III}}\right)\left[\ell\lambda_{\alpha III}\left(\frac{1}{\gamma} + \frac{d_{II} + nW}{c_{III}}\right) - 1\right] + \lambda\beta_{I1}\left(\frac{1}{\gamma} + \frac{d_I + nW}{c_{I1}}\right)}\right\}^{\lambda_{\beta I1}} . \tag{3.79}$$

which can be numerically solved for W.

If a real and positive root W_{rI} can be found for (3.79), such that $W_{rI} < W_0$, then we have under-triggering whenever the trigger duration W satisfies

$$W_{rI} < W < W_0 \tag{3.80}$$

In this case,

$$W_{min} = W_{rI} \tag{3.81}$$

If no such W_{rI} exists, then no under-triggering can occur, and we have:

$$W_{min} = W_0 \tag{3.82}$$

Expansion of the numerator and denominator in the fractions appearing in (3.79) furnish:

$$\left\{\frac{K_{\alpha I}(W + M_{\alpha I})}{(W^2 + P_{\alpha I}W + Q_{\alpha I})}\right\}^{\lambda_{\alpha II}} = \left\{\frac{K_{\beta I}(W + M_{\beta I})}{(W^2 + P_{\beta I}W + Q_{\beta I})}\right\}^{\lambda_{\beta II}} \tag{3.83}$$

with $K_{\alpha I}$, $M_{\alpha I}$, $P_{\alpha I}$, $Q_{\alpha I}$, $K_{\beta I}$, $M_{\beta I}$, $P_{\beta I}$, $Q_{\beta I}$ as in Table VIII.1.

An entirely analogous analysis could be made for the case of a III to I transition: reverse the signs of all coordinates and trigger, and change subscripts I to III, A to $\bar{A}$, B to $\bar{B}$.

3.6.2 Back-Triggering

We will consider only the possibility of back-triggering in the case of too-long trigger, i.e., P is assumed to be at $X_{IIII} = (x_{IIII}, 0)$ when the trigger is turned OFF.

TABLE VIII.1. PARAMETERS OF (3.83) AS FUNCTIONS OF THE PARAMETERS OF (3.79)

$K_{\alpha I}$	$\dfrac{\left(\dfrac{m_I}{a_I} + \lambda_{\alpha I1}\dfrac{n}{c_{I1}}\right)}{\ell\left(\lambda_{\alpha III}\dfrac{n}{c_{III}}\right)^2}$
$M_{\alpha I}$	$\dfrac{\lambda_{\alpha I1}\left(\dfrac{d_I}{c_{I1}} - \dfrac{d_I}{c_{I0}}\right)}{\left(\dfrac{m_I}{a_I} + \lambda_{\alpha I1}\dfrac{n}{c_{I1}}\right)}$
$P_{\alpha I}$	$\dfrac{c_{III}}{n\ell\lambda_{\alpha III}}\left\{2\ell\lambda_{\alpha III}\left(\dfrac{1}{\gamma} + \dfrac{d_{II}}{c_{III}}\right) + \dfrac{\lambda_{\alpha I1}c_{III}}{\lambda_{\alpha III}c_{I1}} - 1\right\}$
$Q_{\alpha I}$	$\dfrac{c_{III}^2}{n^2\ell\lambda_{\alpha III}}\left\{\left(\dfrac{1}{\gamma} + \dfrac{d_{II}}{c_{III}}\right)\left[\ell\lambda_{\alpha III}\left(\dfrac{1}{\gamma} + \dfrac{d_{II}}{c_{III}}\right) - 1\right] + \lambda_{\alpha I1}\left(\dfrac{1}{\gamma} + \dfrac{d_I}{c_{I1}}\right)\right\}$
$K_{\beta I}$	$\dfrac{\left(\dfrac{m_I}{a_I} + \lambda_{\beta I1}\dfrac{n}{c_{I1}}\right)}{\ell\left(\lambda_{\alpha III}\dfrac{n}{c_{III}}\right)^2}$
$M_{\beta I}$	$\dfrac{\lambda_{\beta I1}\left(\dfrac{d_I}{c_{I1}} - \dfrac{d_I}{c_{I0}}\right)}{\left(\dfrac{m_I}{a_I} + \lambda_{\beta I1}\dfrac{n}{c_{I1}}\right)}$
$P_{\beta I}$	$\dfrac{c_{III}}{n\ell\lambda_{\alpha III}}\left\{2\ell\lambda_{\alpha III}\left(\dfrac{1}{\gamma} + \dfrac{d_{II}}{c_{III}}\right) + \dfrac{\lambda_{\beta I1}c_{III}}{\lambda_{\alpha III}c_{I1}} - 1\right\}$
$Q_{\beta I}$	$\dfrac{c_{III}^2}{n^2\ell\lambda_{\alpha III}}\left\{\left(\dfrac{1}{\gamma} + \dfrac{d_{II}}{c_{III}}\right)\left[\ell\lambda_{\alpha III}\left(\dfrac{1}{\gamma} + \dfrac{d_{II}}{c_{III}}\right) - 1\right] + \lambda_{\beta I1}\left(\dfrac{1}{\gamma} + \dfrac{d_I}{c_{I1}}\right)\right\}$

P jumps to a point $P_0 = (x_{III1}, -y_0)$; if P_0 is under branch $\bar{A}$ of the transition separatrix of the untriggered system ($\mu = 0$), a transition will occur, with P returning to X_{I0}, rather than going to X_{III0} (back-triggering). Figure 20 illustrates this effect. Therefore, a transition will occur if and only if:

$$-y_0 < y_{\bar{a}01} \quad \text{or} \quad y_0 > |y_{\bar{a}01}| \tag{3.84}$$

where $y_{\bar{a}01}$ is the ordinate of branch $\bar{A}$ of the transition separatrix of the untriggered system ($\mu = 0$) at $x = x_{III1}$.

The problem is to find the value W_{max} of W that, for a given system, will cause the point $(x_{III1}, -y_0)$ to be on branch $\bar{A}$ of the transition separatrix of the untriggered system (i.e., $\mu = 0$).

As for the case of under-triggering, we will see that this problem cannot be solved analytically either, but only by a graphical or numerical iterative procedure.

A set of formulas similar to the one used in the case of under-triggering can be used to solve this problem.

We had obtained (3.72) which we repeat here for convenience:

$$x_{\nu\mu} = \frac{d_{\nu\mu}}{c_{\nu\mu}} = \frac{d_\nu}{c_{\nu\mu}} + \mu \frac{n}{c_{\nu\mu}} W \tag{3.72}$$

We get:

$$\left.\begin{aligned} x_{II0} &= \frac{d_{II}}{c_{II0}} & x_{III0} &= \frac{d_{III}}{c_{III0}} \\ x_{II1} &= \frac{d_{II}}{c_{II1}} + \frac{n}{c_{II1}} W & x_{III1} &= \frac{d_{III}}{c_{III1}} + \frac{n}{c_{III1}} W \\ 0 < W < W_0 &\Rightarrow 0 > x_{II1} > -\frac{1}{\gamma} & 0 < W < W_0 &\Rightarrow x_{III0} < x_{III1} \\ & & &< (2 - \tfrac{1}{\gamma}) x_{III0} \end{aligned}\right\} \quad (3.85)$$

Again from (3.62), retaining the notation $\lambda_{\alpha\nu\mu}$ and $\lambda_{\beta\nu\mu}$:

$$y_{\bar{B}0} = \lambda_{\alpha II0} \cdot (\tfrac{1}{\gamma} + x_{II0}) \quad (3.86)$$

$$y_{\bar{A}0} = y_{\bar{B}0} \cdot (1 - \ell y_{\bar{B}0}) \quad (3.87)$$

From equation (2.103) itself:

$$-y_0 = -\frac{m_{III}}{a_{III}} W \quad (3.88)$$

(we have implicitly taken $a_{III} = a_I$ and $m_{III} = m_I$, but they may be not strictly true).

And, for convenience, we repeat the general trajectory equation (3.59), in the form (3.77):

$$\left\{\frac{(x_i - x^*)\lambda_\alpha - y_i}{(x_j - x^*)\lambda_\alpha - y_j}\right\}^{\lambda_\alpha} = \left\{\frac{(x_i - x^*)\lambda_\beta - y_i}{(x_j - x^*)\lambda_\beta - y_j}\right\}^{\lambda_\beta} \quad (3.77)$$

with (x_i, y_i), (x_j, y_j), x^*, λ_α and λ_β as before.

Now let

$$\left.\begin{aligned} &(x_i, y_i) = (x_{III1}, -y_0); \qquad x^* = x_{III0} \\ &(x_j, y_j) = (+\tfrac{1}{\gamma},\ y_{\overline{A0}}); \qquad \lambda_\alpha \text{ and } \lambda_\beta = \lambda_{\alpha III0} \text{ and } \lambda_{\beta III0} \end{aligned}\right\} \tag{3.89}$$

Considering (3.85), (3.86), (3.87), (3.88) and (3.89), (3.77) yields:

$$\left\{\frac{\frac{m_{III}}{a_{III}} W + \lambda_{\alpha III0}\left(\frac{d_{III} + nW}{c_{III1}} - \frac{d_{III}}{c_{III0}}\right)}{\lambda_{\alpha II0}\left(\frac{1}{\gamma} + \frac{d_{II}}{c_{II0}}\right)\left[\ell\lambda_{\alpha II0}\left(\frac{1}{\gamma} + \frac{d_{II}}{c_{II0}}\right) - 1\right] + \lambda_{\alpha III0}\left(\frac{1}{\gamma} - \frac{d_{III}}{c_{III0}}\right)}\right\}^{\lambda_{\alpha III0}}$$

$$= \left\{\frac{\frac{m_{III}}{a_{III}} W + \lambda_{\beta III0}\left(\frac{d_{III} + nW}{c_{III1}} - \frac{d_{III}}{c_{III0}}\right)}{\lambda_{\alpha II0}\left(\frac{1}{\gamma} + \frac{d_{II}}{c_{II0}}\right)\left[\ell\lambda_{\alpha II0}\left(\frac{1}{\gamma} + \frac{d_{II}}{c_{II0}}\right) - 1\right] + \lambda_{\beta III0}\left(\frac{1}{\gamma} - \frac{d_{III}}{c_{III0}}\right)}\right\}^{\lambda_{\beta III0}} \tag{3.90}$$

which can be numerically solved for W.

If a real and positive root W_{rIII} can be found for (3.90), then we have back-triggering whenever the trigger duration W satisfies

$$W_{rIII} < W \tag{3.91}$$

In this case,

$$W_{max} = W_{rIII} \tag{3.92}$$

and in order to obtain a permanent transition, we must have

$$W < W_{max} \tag{3.93}$$

If no such W_{rIII} exists, then no value of W will cause back-triggering.

Expansion of the numerator and denominator in the fractions appearing in (3.90) furnish:

$$\left\{\frac{K_{\alpha III}(W + M_{\alpha III})}{(W^2 + P_{\alpha III}W + Q_{\alpha III})}\right\}^{\lambda_{\alpha III0}} = \left\{\frac{K_{\beta III}(W + M_{\beta III})}{(W^2 + P_{\beta III}W + Q_{\beta III})}\right\}^{\lambda_{\beta III0}} \qquad (3.94)$$

with $K_{\alpha III}$, $M_{\alpha III}$, $P_{\alpha III}$, $Q_{\alpha III}$, $K_{\beta III}$, $M_{\beta III}$, $P_{\beta III}$, $Q_{\beta III}$ as in Table VIII.2.

An entirely analogous analysis could be made for the case of a III to I transition: reverse the signs of all coordinates and trigger, and change subscripts III to I, $\bar{A}$ to A, $\bar{B}$ to B.

3.6.3 Discussion

It is clear from inspection of either Fig. 20 or equation (3.79) and of either Fig. 21 or equation (3.90) that the necessary and sufficient conditions for the impossibility of occurrence of

under-triggering:

$$|\lambda_{\alpha I1}| \cdot |\Delta_W x_I| > \frac{m_I}{a_I} W, \quad 0 \le W \le W_0 \qquad (3.95)$$

back-triggering:

$$|\lambda_{\alpha III0}| \cdot |\Delta_W x_{III}| > \frac{m_{III}}{a_{III}} W, \quad 0 \le W \le W_0 \qquad (3.96)$$

where

$$\Delta_W x_\nu = x_{\nu 1}(W) - x_{\nu 0} \qquad (3.97)$$

Expansion of (3.97) yields

TABLE VIII.2. PARAMETERS OF (3.94) AS FUNCTIONS OF THE PARAMETERS OF (3.90)

$K_{\alpha III}$	$\dfrac{\left(\dfrac{m_{III}}{a_{III}} + \lambda_{\alpha III0}\dfrac{n}{c_{III1}}\right)}{\ell\left(\lambda_{\alpha II0}\dfrac{n}{c_{II0}}\right)^2}$
$M_{\alpha III}$	$\dfrac{\lambda_{\alpha III0}\left(\dfrac{d_{III}}{c_{III1}} - \dfrac{d_{III}}{c_{III0}}\right)}{\left(\dfrac{m_{III}}{a_{III}} + \lambda_{\alpha III0}\dfrac{n}{c_{III1}}\right)}$
$P_{\alpha III}$	$\dfrac{c_{II0}}{n\ell\lambda_{\alpha II0}}\left\{2\ell\lambda_{\alpha II0}\left(\dfrac{1}{\gamma} + \dfrac{d_{II}}{c_{II0}}\right) - \dfrac{\lambda_{\alpha III0}c_{II0}}{\lambda_{\alpha II0}c_{III0}} - 1\right\}$
$Q_{\alpha III}$	$\dfrac{c_{II0}^2}{n^2\ell\lambda_{\alpha II0}}\left\{\left(\dfrac{1}{\gamma} + \dfrac{d_{II}}{c_{II0}}\right)\left[\ell\lambda_{\alpha II0}\left(\dfrac{1}{\gamma} + \dfrac{d_{II}}{c_{II0}}\right) - 1\right] + \lambda_{\alpha III0}\left(\dfrac{1}{\gamma} - \dfrac{d_{III}}{c_{III0}}\right)\right\}$
$K_{\beta III}$	$\dfrac{\left(\dfrac{m_{III}}{a_{III}} + \lambda_{\beta III0}\dfrac{n}{c_{III1}}\right)}{\ell\left(\lambda_{\alpha II0}\dfrac{n}{c_{II0}}\right)^2}$
$M_{\beta III}$	$\dfrac{\lambda_{\beta III0}\left(\dfrac{d_{III}}{c_{III1}} - \dfrac{d_{III}}{c_{III0}}\right)}{\left(\dfrac{m_{III}}{a_{III}} + \lambda_{\beta III0}\dfrac{n}{c_{III1}}\right)}$
$P_{\beta III}$	$\dfrac{c_{II0}}{n\ell\lambda_{\alpha II0}}\left\{2\ell\lambda_{\alpha II0}\left(\dfrac{1}{\gamma} + \dfrac{d_{II}}{c_{II0}}\right) - \dfrac{\lambda_{\beta III0}c_{II0}}{\lambda_{\alpha II0}c_{III0}} - 1\right\}$
$Q_{\beta III}$	$\dfrac{c_{II0}^2}{n^2\ell\lambda_{\alpha II0}}\left\{\left(\dfrac{1}{\gamma} + \dfrac{d_{II}}{c_{II0}}\right)\left[\ell\lambda_{\alpha II0}\left(\dfrac{1}{\gamma} + \dfrac{d_{II}}{c_{II0}}\right) - 1\right] + \lambda_{\beta III0}\left(\dfrac{1}{\gamma} - \dfrac{d_{III}}{c_{III0}}\right)\right\}$

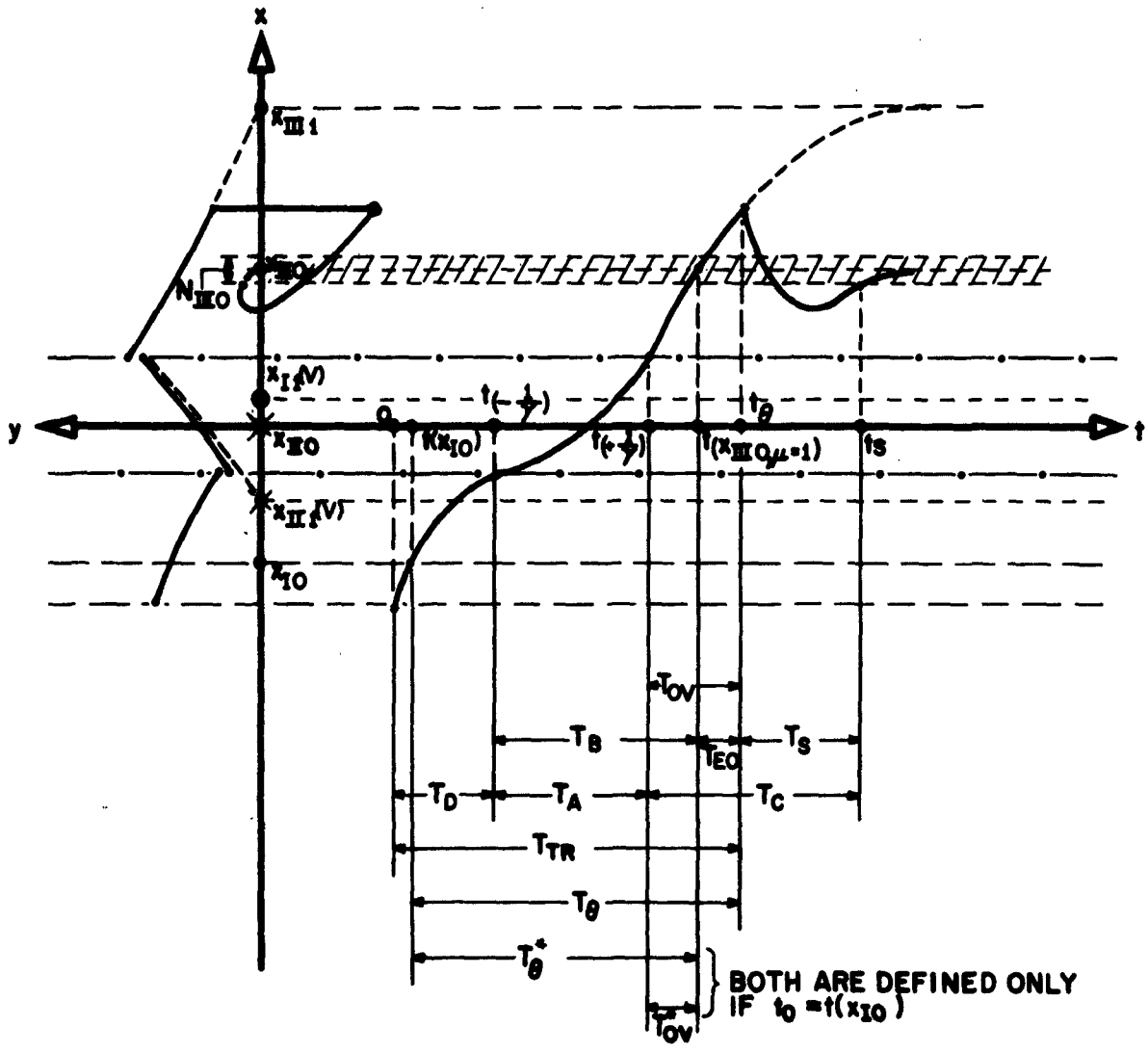

FIGURE 21: DEFINITION OF TIME INTERVALS OVER A TRAJECTORY IN THE TIME DOMAIN, RELATED TO THE PHASE PLANE. (SEE TABLE IX).

$$\Delta_W x_\nu = \frac{n}{c_{\nu 1}} W + \frac{d_\nu}{c_{\nu 1}} - \frac{d_\nu}{c_{\nu 0}} = \frac{n}{c_{\nu 1}} W - d_\nu \frac{c_{\nu 1} - c_{\nu 0}}{c_{\nu 0} c_{\nu 1}} \qquad (3.98)$$

Notice that if either of conditions (3.95) and (3.96) is not met, then there will exist real positive solutions W_{rI} or W_{rIII} to (3.79) and (3.90) respectively.

We clearly see that conditions (3.95) and (3.96) are formally the same.

a) If we make the further assumption that the coefficients of equation (2.103) except d_ν are the same in regions I and III (a realistic assumption!), then the only difference between them is the effect of different values of the coefficients with the index μ (neglecting variation of capacitances).

b) If we make the further assumption that the coefficients of equation (2.103) are invariant with μ (i.e., trigger circuit is fixed!), then the two conditions are identical.

This shows a close relationship between these two effects, i.e., they have the same intrinsic nature and origin from the circuit parameter point of view, and if any distinction exists between them, it is due to the fact that the circuit itself is not the same in each case (unless the two conditions above hold!).

One further assumption leads us to an interesting point: assume that

$$G_\mu = 0, \quad \mu = 0, 1 \qquad (3.99)$$

i.e., consider the case of a trigger circuit that closely approximates a true current source. Then we have the

Theorem 4. If equation (2.103) describes either an asymmetric or a symmetric flipflop (coefficients as in Table I), and if the trigger circuit satisfies (3.99) above, then no under-triggering or back-triggering can occur.

Proof. Conditions a and b can be expressed as a single condition:

$$|\lambda_\alpha| \cdot n > \frac{m}{a} \tag{3.100}$$

since

$$c_{\nu\mu} = 1 \quad \text{for} \quad \nu = \text{I, III}; \ \mu = 0, 1$$

and with

$$\lambda_\alpha = -(b + \sqrt{b^2 - 4a}\,)\,\frac{1}{2a}$$

$$a = \frac{\tau_i \tau_o}{\tau^2}$$

$$b = \frac{\tau_i + \tau_{oi} + \tau_o}{\tau}$$

$$m = 2p\,\frac{\tau_{io}}{\tau}$$

$$n = 2p\,\frac{R_s}{R_o}$$

as in Table I, for regions I and III. Therefore, (3.100) becomes, after expansion and simplification:

$$2\tau_{io} < \left\{(\tau_i + \tau_{oi} + \tau_o) + \sqrt{(\tau_i + \tau_{oi} + \tau_o)^2 - 4\tau_i\tau_o}\right\}\frac{R_s}{R_o} \tag{3.101}$$

This becomes

$$1 < \frac{1}{2}\,(1 + \frac{1}{r})\left\{(c + cr + r) + \sqrt{(c + cr + r)^2 - 4cr}\right\} = f(c,r) \tag{3.102}$$

where

$$c = \frac{C_1}{C_o}, \quad \text{and} \quad r = \frac{R_o}{R_1}$$

Now, let us make a change of variable, as follows:

$$\begin{cases} r = r \\ \\ c = \delta r \end{cases}$$

so that $f(c,r)$ becomes $g(\delta,r)$:

$$g(\delta,r) = \frac{1}{2}\left(1 + \frac{1}{r}\right)\left\{(\delta r + \delta r^2 + r) + \sqrt{(\delta r + \delta r^2 + r)^2 - 4\delta r^2}\right\}$$

or

$$g(\delta,r) = \frac{1}{2}(r + 1)\left\{(1 + \delta + \delta r) + \sqrt{(1 + \delta + \delta r)^2 - 4\delta}\right\} \dagger \qquad (3.103)$$

Condition (3.102) has become:

$$1 < g(\delta,r) \qquad (3.104)$$

Let us find the partial derivative of $g(\delta,r)$ with respect to r:

$$\frac{\partial g(\delta,r)}{\partial r} = \frac{1}{2}\left[(1+\delta+\delta r) + \sqrt{(1+\delta+\delta r)^2 - 4\delta} + (r+1)\delta\left\{1 + \frac{2(1 + \delta + \delta r)}{\sqrt{(1+\delta+\delta r)^2 - 4\delta}}\right\}\right] \qquad (3.105)$$

Then

---

† The discriminant always positive, since $(1 + \delta + \delta r)^2 - 4\delta = (1 - \delta + \delta r)^2 + 4\delta^2 r > 0$ so $g(\delta,r)$ is a real positive number.

$$\frac{\partial g(\delta,r)}{\partial r} > 0, \quad \text{for all} \quad \delta > 0,\ r > 0 \tag{3.106}$$

Therefore

$$\lim_{\substack{r\to 0\\ \delta\to 0}} g(\delta,r) < g(\delta,r)\Big|_{\substack{r>0\\ \delta>0}} \tag{3.107}$$

But

$$\lim_{\substack{r\to 0\\ \delta\to 0}} g(\delta,r) = 1 \tag{3.108}$$

Substitution of (3.108) in (3.107) yields:

$$1 < g(\delta,r)\Big|_{\substack{r>0\\ \delta>0}} \tag{3.109}$$

and therefore condition (3.100) holds, and the theorem is proved.

Comments:

1) Notice that the theorem is very strong, in the sense that condition (3.109) is strong; in fact, 1 is not only a lower bound for $g(\delta,r)$, but it is an infimum of $g(\delta,r)$, i.e., its greatest lower bound! So, anything at all upsetting the assumptions made, may invalidate the theorem, and in this case either under-triggering or back-triggering, or both, at least in principle, could occur!

2) Notice also that (3.106) is weak. In fact,

$$\frac{\partial g(\delta,r)}{\partial r}\Big|_{\substack{r>0\\ \delta>0}} > \lim_{\substack{r\to 0\\ \delta\to 0}} \frac{\partial g(\delta,r)}{\partial r} = 1 \tag{3.110}$$

So, in fairness, we should point out that the possibility of occurrence of under-triggering or back-triggering in practice is not so great, since any "reasonable" value at all of c and r ought to satisfy condition (3.100) with a good margin.

3.7 Summary

In this chapter we have analyzed the phase plane characteristics of the basic flipflop equation in the case of a rectangular trigger.

Conditions related to the existence and nature of singularities were discussed and three theorems were proved with respect to this point.

Some properties of the system were also established by diagonalization of the characteristic matrix of the system (in effect, considering two possibilities, respectively for the two possible types of singularity).

A general trajectory equation was established, and the geometry of the separatrices was discussed, as well as the action of a trigger upon the system phase plane portrait, with special attention to the effects of turning the trigger ON and OFF. Here the possibilities of under-triggering and back-triggering were discussed, and a theorem on the conditions for such a possibility to exist was proved for an important special case.

4. ANALYSIS AND DESIGN TECHNIQUES

4.1 Introduction

At this point we would like to utilize this information we have about the bistable system represented by equation (2.103) to the purpose of developing some analysis and design techniques. Specifically, we would like to find effective† methods to solve the following problem: given a flipflop, its loading and triggering circuits, find the transition wave forms of:

(i) base currents and voltages

(ii) collector currents and voltages

We would then be able to find the optimum trigger duration. Furthermore, knowledge of the base and collector currents and voltages as functions of time would help to improve the design of the overall system [1, 4].

And finally, if the influence of the circuit parameters upon wave form characteristics is known, we would have a means of optimizing the design of the system towards approaching some transition requirements [7].

Lastly, if the transistors are given (τ is given) and also the trigger, but if the circuit (resistors and capacitors) is abritrary, then the lower limit in transition time can be calculated, and a convenient figure of merit for transistors describing their performance in switching circuits can be defined, and would certainly be useful in the selection of transistors for switching applications (see Chapter 5) [10, 20].

4.2 Definitions of Time Intervals

We have divided the range of the variable x into three parts, which were called regions I, II and III. Remember that x is a normalized form of

† By "effective" we mean: "a sensible compromise between accuracy and ease of application."

the base-to-base voltage. Let us consider the variables w_k, which are normalized forms of the collector currents (of transistors 1 and 2 for k = 1, 2, respectively), as given by equation (2.93).

It is clear that, as long as x is in region I, $w_1 = 0$ and $w_2 = 1$; whenever x is in region III, this situation is reversed, with $w_1 = 1$ and $w_2 = 0$; in both these cases one of the transistors is cutt off, and the other is conducting a fixed current, i.e., the transistors are inactive; they are active only when x is in region II.

Def. 4.1. So, in a I to III transition, from the point of view of collector currents, the time during which x is crossing region I, from $x(t_0)$ towards $-\frac{1}{\gamma}$, is really a delay. It will be called "delay time" and designated by T_D.† If the circuit were settled, $x(t_0) = x_{IO}$; otherwise, it may happen that $x(t_0) \neq x_{IO}$.

Def. 4.2. The time interval when x is in region II, going from $-\frac{1}{\gamma}$ to $+\frac{1}{\gamma}$, is characterized by activity of the transistors, and variation of collector currents. It will be called "active time" and designated by T_A.

Def. 4.3. And finally, for the time interval when x is already in region III, from $+\frac{1}{\gamma}$ until final settling in a neighborhood N_{IIIO} of x_{IIIO}, the collector currents are constant (having reached their final values) and the transistors are again inactive. It will be called "complementary time" and designated by T_C.

However, many things can happen while x is in region III.

Def. 4.4. The time interval in which x goes from $+\frac{1}{\gamma}$ to x_{IIIO}, with trigger ON, is called "balanced time" and designated T_B.

Def. 4.5. The time interval between the moment the trigger is turned OFF and the moment x settles inside N_{IIIO} is called "settling time" and designated T_S.

† This time interval is often called "discrimination time."

Def. 4.6. The time interval between the moment x reaches x_{III0} (or would reach x_{III0} if the trigger were kept ON) and the moment the trigger is turned OFF is called "trigger excess overtime" and designated T_{EO}. We will make the convention of using negative values of T_{EO} if the trigger is turned OFF before x reaches x_{III0}, i.e., given the function t(x), then $T_{EO} = T_\theta - t(x_{III0})$ where $t(x_{III0})$ is calculated assuming a sufficiently long trigger (or measured!) and T_θ is the trigger duration.

Def. 4.7. The time interval between the instant x reaches $+\frac{1}{\gamma}$ and the instant the trigger is turned OFF is called "trigger overtime" or simply "overtime," and designated T_{OV}, i.e., $T_{OV} = T_\theta - t(+\frac{1}{\gamma})$.

With our criterion for optimum trigger duration T^*_θ (see equation (3.70)) we will have:

$$T^*_\theta = t(x_{III0}) \tag{4.1a}$$

and if $T_\theta = T^*_\theta$, then from Def. 4.6,

$$T_{EO} = 0 \tag{4.1b}$$

And we define "optimum overtime" T^*_{OV}:

$$T^*_{OV} = T^*_\theta - t(+\frac{1}{\gamma}) = T_R \tag{4.1c}$$

Def. 4.8. In the case of too long a trigger, we define the "long settling time," T_{LS}, as the time interval between the moment x reaches $+\frac{1}{\gamma}$ and the moment it settles inside a given neighborhood N_{III1} of x_{III1}.

Def. 4.9. Finally, we call "I-III transition time," T_{TR}, the total time interval between the moment the trigger is turned ON and the moment x crosses the line x_{III0}.

The following relations are obvious from the definitions:

$$T_{TR} = T_D + T_A + T_B, \quad \text{if} \quad x(t_0) = x_{I0} \tag{4.2a}$$

$$T_C = T_{OV} + T_S \tag{4.2b}$$

$$T_{OV} = T_B + T_{EO} \tag{4.2c}$$

$$T_{EO} = 0 \quad \text{implies} \quad T_{OV} = T^*_{OV} = T_B \tag{4.2d}$$

Naturally, all the above definitions apply equally well to a III-I transition by replacing III by I and I by III everywhere. The symbol $T_{\overline{TR}}$ denotes the "III-I transition time."

Table IX contains these definitions of time intervals, which are also illustrated in Fig. 21.

4.3 Calculation of a Time Interval Over a Trajectory by an Iterative Formula

It is not possible to explicit y in (3.59). Therefore, given an initial point $P_0:(x_0,y_0)$[†] and the abcissa x_f of another point P_f, in order to find the other coordinate y_f of P_f such that P_0 and P_f are on the same trajectory, we must apply an iterative procedure to (3.59); the time intervals can be found from (3.58).

Equation (3.59) can be expressed as

$$\left\{\frac{M_\alpha - y}{Q_\alpha}\right\}^{\lambda_\alpha} = \left\{\frac{M_\beta - y}{Q_\beta}\right\}^{\lambda_\beta} \tag{4.3}$$

[†] Read: P_0 "whose coordinate are" (x_0,y_0).

TABLE IX. DEFINITIONS OF TIME INTERVALS OVER A TRAJECTORY (SEE FIG. 21)

Symbol	Name	Definition	Comments
T_D	Delay Time	$t(-\frac{1}{\gamma}) - t_0$	If circuit was settled at x_{I1} at t_0, $t(x_{I0}) = t_0$; otherwise $t(x_{I0}) \neq t_0$. t_0 is the instant the trigger is turned ON.
T_A	Active Time	$t(+\frac{1}{\gamma}) - t(-\frac{1}{\gamma})$	--
T_C	Complementary Time	$t_s - t(-\frac{1}{\gamma})$	t_s is the instant when P enters N_{III0} for the last time.
T_B	Balance Time	$t(x_{III0}, \mu = 1) - t(-\frac{1}{\gamma})$	$t(x_{III0}, \mu = 1)$ is the instant P crosses $x = x_{III0}$, assuming the trigger stays ON ($\mu = 1$) all the time.
T_S	Settling Time	$t_s - t_\theta$	t_θ is the instant the trigger is turned OFF.
T_{EO}	Trigger Excess Overtime	$t_\theta - t(x_{III0}, \mu = 1)$	--
T_{OV}	Trigger Overtime	$t_\theta - t(+\frac{1}{\gamma})$	--
T_{TR}	Transition Time	$t_s - t_0$	Notice that it is measured since t_0 (not $t(x_{I0})$!) until t_s.
T_θ	Trigger Duration	$t_\theta - t_0$	--
T^*_θ and T^*_{OV}	Optimum Trigger Duration and Overtime respectively	Defined only if $t_0 = t(x_{I0})$, equivalent to letting $t_\theta = t(x_{III0}, \mu = 1)$.	Of course, only approximately realizable.

for region ν and trigger condition μ. Parameters M_α, M_β, Q_α, Q_β are given in Table X.

We obtain either one of two formulae

$$y_{n+1} = M_\alpha - Q_\alpha e^{\frac{\lambda_\beta}{\lambda_\alpha} \ln\left[\frac{M_\beta - y_n}{Q_\beta}\right]} \tag{4.4a}$$

or

$$y_{n+1} = M_\beta - Q_\beta e^{\frac{\lambda_\alpha}{\lambda_\beta} \ln\left[\frac{M_\alpha - y_n}{Q_\alpha}\right]} \tag{4.4b}$$

The only difference between them is a question of convergence.

In fact, given two implicit functions f and g of y, the equation

$$f(y) = g(y) \tag{4.5}$$

can be solved by an iterative procedure by means of a formula such as†

$$f(y_{n+1}) = g(y_n) \tag{4.6}$$

i.e.,

$$y_{n+1} = f^{-1}[g(y_n)] \tag{4.7}$$

Let y_f be the solution of equation (4.5)

The iterative formula (4.6) will converge, i.e., $\lim_{n\to\infty} y_n = y_f$, if and only if there is a number $\epsilon > 0$ such that, if $|y_n - y_f| < \epsilon$, there is a positive number K such that:

---

† No loss of generality, since the symbols f and g can be interchanged.

TABLE X. DEFINITION OF THE PARAMETERS OF EQUATION (4.3)

Parameters of (4.3)	Expressed as Functions of the Parameters of (3.59)
M_α	$(x - x^*)\lambda_\alpha$
Q_α	$(x_0 - x^*)\lambda_\alpha - y_0$
M_β	$(x - x^*)\lambda_\beta$
Q_β	$(x_0 - x^*)\lambda_\beta - y_0$

Comments: a) Region ν, trigger condition μ

b) $x^* = x_{\nu\mu}$

c) $\lambda_\alpha = \lambda_{\alpha\nu\mu}$, $\lambda_\beta = \lambda_{\beta\nu\mu}$

d) (x_0, y_0) = any given point on the branch of trajectory under conditions $\nu\mu$.

e) x = some abcissa such that there is an ordinate y satisfying the condition: "(x,y) is on the same trajectory $\nu\mu$ branch as (x_0, y_0)."

f) y is to be found.

$$\left|\frac{\Delta y_{n+1}}{\Delta y_n}\right| < K, \quad K < 1 \tag{4.8}$$

However, it is clear that

$$\lim_{n\to\infty} \frac{\Delta y_{n+1}}{\Delta y_n} = \frac{g'(y_f)}{f'(y_f)} \tag{4.9}$$

where the prime means "derivative with respect to y_f."

Now (4.8) and (4.9) imply that (4.6) converges if and only if

$$\left|\frac{g'(y_f)}{f'(y_f)}\right| < 1 \tag{4.10}$$

Therefore, one of formulae (4.4a, b) converges and the other diverges. There is no way to know a priori which one will converge, since we would need the solution y_f of (4.3) to answer this question. However, assuming we start from a good initial guess y_1, if we calculate y_2 and y_3 from both formulae (4.4a, b), the initial tendency should be clear.

Another way would be to differentiate both sides of (4.3) with respect to y, and compare the two results for the initial guess y_1, hoping that comparison at y_f would yield the same qualitative result. Call f(y) and g(y), respectively, the sides of (4.3) with the larger and smaller absolute value at point y_1, and take that of formulae (4.4a, b) which conforms to (4.7).

If eventually, the selected formula diverges, then we should try to improve the initial guess y_1 and repeat the procedure outlined in the previous paragraph.

A method of extrapolation usually allows improvement of any trial y_n using the previous results for y_{n-1} and y_{n-2}: from (4.7) we write (4.11) below:

$$\Delta y_n = f^{-1}[g(y_n)] - y_n \tag{4.11}$$

So, to y_{n-2} and y_{n-1} there correspond respectively the variations Δy_{n-2} and Δy_{n-1}; the two points $(y_{n-2}, \Delta y_{n-2})$ and $(y_{n-1}, \Delta y_{n-1})$ define a line $(y_n, \overline{\Delta y_n})$:†

$$\overline{\Delta y_n} = y_n\left(\frac{\Delta y_{n-1}}{\Delta y_{n-2}} - 1\right) + \left(y_{n-1} - y_{n-2}\frac{\Delta y_{n-1}}{\Delta y_{n-2}}\right) \tag{4.12}$$

Let

$$\overline{\Delta y_n} = 0$$

then:

$$y_n = \frac{y_{n-2}\Delta y_{n-1} - y_{n-1}\Delta y_{n-2}}{\Delta y_{n-1} - \Delta y_{n-2}} \tag{4.13}$$

Try substituting y_n into (4.11). Stop when Δy_n is small enough.

This method, even though more involved, would speed up the convergence, it is more tolerant with respect to initial guesses, and stabilizes the method to the point of usually producing a convergent sequence of numbers $y_n \to y_s$ even in a case for which, if directly applied, equation (4.7) would diverge.

If the problem consists in finding time intervals only, and we are not concerned with other characteristics of the trajectory, then the trajectory equations (3.57) in the time domain could be used directly. They can be written as

† $\overline{\Delta y_n}$ is the extrapolated, or expected, value of Δy_n.

$$x_f = A_\alpha e^{\lambda_\alpha T_{0f}} + A_\beta e^{\lambda_\beta T_{0f}} + x^* \tag{4.14a}$$

$$y_f = A_\alpha \lambda_\alpha e^{\lambda_\alpha T_{0f}} + A_\beta \lambda_\beta e^{\lambda_\beta T_{0f}} \tag{4.14b}$$

where $T_{0f} = t_f - t_0$, and x^* is the abcissa of the singular point corresponding to the region; clearly (x_0, y_0) is the initial point. So:

$$x_{n+1} = A_\alpha e^{\lambda_\alpha T_n} + A_\beta e^{\lambda_\beta T_n} + x^* \tag{4.15}$$

and, by the use of a method like the one expressed by equation (4.13),

$$T_{n+1} = \frac{x\Delta T_{n-1} + (x_n T_{n-1} - x_{n-1} T_n)}{x_n - x_{n-1}} \tag{4.16}$$

Now, T_{n+1} would be used in (4.15). The numbers x_{n-1} and x_n are respectively the results of (4.15) when fed with T_{n-1} and T_n. Clearly

$$\Delta T_n = T_n - T_{n-1} \tag{4.17}$$

When ΔT_n is small enough, the process is stopped and T_{0f} corresponding to x_f could be fed into (4.14b) to find the corresponding value of y.

There remains the problem of how to find a fairly good initial value for the iterative procedure. One good way is to assume that, in a crude approximation, in regions I and III, P moves in a straight line towards the singularity (virtual or real), and that in region II it moves parallel to the asymptote of positive slope.

Therefore:

In regions I and III, with x* standing for the corresponding singularity:

$$y_1 = \frac{(x^* - x_f)y_0}{x^* - x_0} \tag{4.18}$$

In region II, with λ_β being the positive natural frequency:

$$y_1 = \lambda_\beta(x_f - x_0) + y_0 \tag{4.19}$$

Both in (4.18) and (4.19), (x_0,y_0) is the initial position, and we wish to find the first approximation y_1 to the ordinate y_f corresponding to the abcissa x_f.

To find a first approximation T_{01} to the time interval for P to go from (x_0,y_0) to (x_f,y_f), consider the first approximation to the trajectory as being a straight line from (x_0,y_0) to (x_f,y_1). We know that, whatever the trajectory y(x) may be,

$$T_{0f} = \int_{x_0}^{x_f} \frac{1}{y(x)}\, dx \tag{4.20}$$

Therefore, if y(x) is a straight line with slope y', going through (x_0,y_0) and (x_f,y_1), then P crosses the line x after a time interval:

$$T_{01} = \frac{1}{y'} \ln \frac{y_1}{y_0} \tag{4.21}$$

and naturally,

$$y' = \frac{y_1 - y_0}{x_f - x_0} \tag{4.22}$$

NOTE: In a general form, if a trajectory is a straight line between points $P_a:(x_a,y_a)$ and $P_b:(x_b,y_b)$, $T_{ab} = t_b - t_a$ is

$$T_{ab} = \frac{1}{y'} \ln \frac{y_b}{y_a} \tag{4.23}$$

and

$$y' = \frac{y_b - y_a}{x_b - x_a} \tag{4.24}$$

Whenever x_0 and x_f are in different regions, we have to proceed by steps. Assume a I to III transition with x_0 in region I and x_f in region III; y_0 is, of course, given, and y_f is to be found. Then (with the notation shown in Fig. 22):

(i) With (x_0,y_0) as initial point on the equation, find y_a, at $x_a = -\frac{1}{\gamma}\Big|_-$, by iteration.

(ii) Use equation (3.61a.i) to find y_b, at $x_b = -\frac{1}{\gamma}\Big|_+$.

(iii) With (x_b,y_b) as initial values on the equations, find y_c, at $x_c = +\frac{1}{\gamma}\Big|_-$, by iteration.

(iv) Use equation (3.61b.i) to find y_d at $x_d = +\frac{1}{\gamma}\Big|_+$.

(v) With (x_d,y_d) as initial values, find the point $\bar{y}_f$, at $x = x_f$, by iteration, assuming that P crosses $x = x_f$ while the trigger is ON.

(vi) Calculate all time intervals by (3.58). Then $T'_{0f} = T_{0a} + T_{bc} + T_{df}$.

(vii) Consider the trigger duration T_W, and suppose that P crosses $x = x_f$ after the trigger is turned OFF, either for the first or second time.

(viii) With (x_d,y_d) as initial values of the coordinates, find $(x_e,\bar{y}_e)$, by iteration, where, after a time interval $T = T_W - (T_{0a} + T_{bc})$, trigger turn-off occurs.

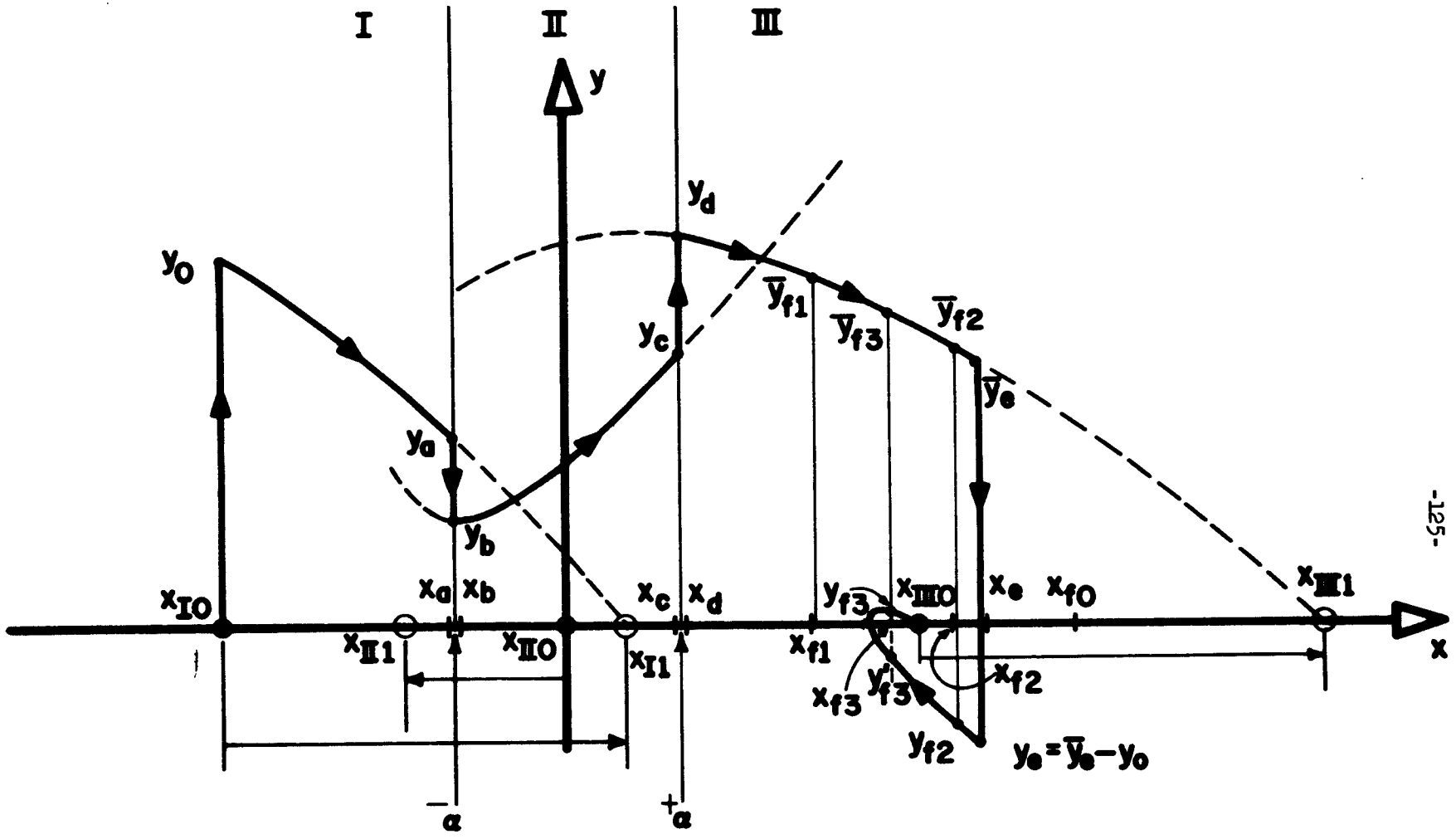

FIGURE 22: NOTATION FOR A TRANSITION CALCULATION. NOTICE THAT, FOR A GIVEN x_f, THERE MAY BE NONE, ONE, TWO, OR THREE DIFFERENT ORDINATES, DEPENDING ON THE RELATIVE POSITIONS OF x_{IIIO}, x_e, AND x_f.

(ix) Find $y_e = \bar{y}_e - y_0$.

(x) With (x_e, y_e) as initial values, find y_f, at $x = x_f$, by iteration; there may be none, one, or two values.

(xi) The time intervals can be calculated by (3.58), and, in this case, where P crosses $x = x_f$ after trigger turn-off,†

$$T_{Of} = T_W + T_{ef}$$

Of course, this algorithm, with slight modifications of detail, can be used to find optimum values for T_W, instead of having T_W as part of the data.

This same algorithm can be applied to a III to I transition, after the obvious interchange of reference to regions I and III.

See illustrative examples in Chapter 6.

4.4 Graphical Constructions

4.4.1 The (Φ, χ) Plane Method

Equations (3.15) and (3.48) define the transformation of variables from (x,y) to (Φ,χ), and can be written equivalently in a single pair of expressions:

$$\left.\begin{aligned} \Phi &= \frac{1}{\lambda_\beta - \lambda_\alpha}\left[+\lambda_\beta \cdot (x - x^*) - y\right] \\ \chi &= \frac{1}{\lambda_\beta - \lambda_\alpha}\left[-\lambda_\alpha \cdot (x - x^*) + y\right] \end{aligned}\right\} \qquad (4.25)$$

NOTE: Considering that $y^* = 0$.

† Of course, if P crosses $x = x_f$ twice after trigger turn-off, we must know up to which passage of P by $x = x_f$ we wish to calculate T_{ef}.

Here equation (3.50) and (3.51) are repeated for convenience, with $(t - t_0)$ replaced by T:

$$\left.\begin{aligned} \Phi &= \Phi_0 e^{\lambda_\alpha T} \\ \chi &= \chi_0 e^{\lambda_\beta T} \end{aligned}\right\} \tag{4.26}$$

$$T = \frac{1}{\lambda_\alpha} \ln \frac{\Phi}{\Phi_0} = \frac{1}{\lambda_\beta} \ln \frac{\chi}{\chi_0} \tag{4.27}$$

We see that it is possible to define a new pair of variables, say $\bar{\Phi}$ and $\bar{\chi}$, as follows:

$$\left.\begin{aligned} \bar{\Phi} &= \ln \frac{\Phi}{\Phi_0} \\ \bar{\chi} &= \ln \frac{\chi}{\chi_0} \end{aligned}\right\} \tag{4.28}$$

where Φ_0 and χ_0 are the initial values of Φ and χ, so that $\bar{\Phi}_0 = \bar{\chi}_0 = 0$ by definition.

Therefore, (4.27) becomes:

$$T = \frac{\bar{\Phi}}{\lambda_\alpha} = \frac{\bar{\chi}}{\lambda_\beta} \tag{4.29}$$

This means that in the $(\bar{\Phi}, \bar{\chi})$ plane, the trajectories are straight lines, and intervals can be marked as a linear scale, either along a trajectory or along a vertical or horizontal axis, since time is linear with either variable.

On the other hand, (4.25) means that any straight line in the (x,y) plane is also a straight line in the (Φ,χ) plane.

From (4.25), it is clear that the transformations depend on the region and trigger indices $\nu\mu$. This can be indicated by attaching these indices to Φ, χ, and also to $\bar{\Phi}$ and $\bar{\chi}$, i.e., (4.25) becomes:

$$\left.\begin{aligned} \Phi_{\nu\mu} &= \frac{1}{\lambda_{\beta\nu\mu} - \lambda_{\alpha\nu\mu}} \left[+\lambda_{\beta\nu\mu}\cdot(x - x_{\nu\mu}) - y\right] \\ \chi_{\nu\mu} &= \frac{1}{\lambda_{\beta\nu\mu} - \lambda_{\alpha\nu\mu}} \left[-\lambda_{\alpha\nu\mu}\cdot(x - x_{\nu\mu}) + y\right] \end{aligned}\right\} \qquad (4.30)$$

Also (4.27) becomes:

$$T_{\nu\mu} = \frac{1}{\lambda_{\alpha\nu\mu}} \ln \frac{\Phi_{\nu\mu}}{\Phi_{\nu\mu 0}} = \frac{1}{\lambda_{\beta\nu\mu}} \ln \frac{\chi_{\nu\mu}}{\chi_{\nu\mu 0}} \qquad (4.31)$$

And, of course, (4.28) becomes:

$$\left.\begin{aligned} \bar{\Phi}_{\nu\mu} &= \ln \frac{\Phi_{\nu\mu}}{\Phi_{\nu\mu 0}} \\ \bar{\chi}_{\nu\mu} &= \ln \frac{\chi_{\nu\mu}}{\chi_{\nu\mu 0}} \end{aligned}\right\} \qquad (4.32)$$

And finally, from (4.29):

$$T_{\nu\mu} = \frac{\bar{\Phi}_{\nu\mu}}{\lambda_{\alpha\nu\mu}} = \frac{\bar{\chi}_{\nu\mu}}{\lambda_{\beta\nu\mu}} \qquad (4.33)$$

Now, for each value of $\nu\mu$ that occurs in the problem (this must be known):

a) Draw, on a linear graph paper, with $\Phi_{\nu\mu}$ and $\chi_{\nu\mu}$ axes marked on it, the lines corresponding to the following phase plane lines:

(i) The coordinate x axis with a scale on it.

(ii) The direction of the vertical lines.

b) On a log-log graph paper, mark the coordinate $\bar{\Phi}_{\nu\mu}$ and $\bar{\chi}_{\nu\mu}$ axes, and the direction of the trajectory lines, as well as a time scale, and also the scaled curve corresponding to the x axis.

c) Given a trigger amplitude W, draw the corresponding lines $x = \pm \frac{1}{\gamma}$ in the linear graphs where $\mu = 1$, and from these graphs, draw the corresponding curves in the log-log graph, by means of a point-by-point transportation.

d) The log-log graphs representing the various $(\bar{\Phi}_{\nu\mu}, \bar{\chi}_{\nu\mu})$ planes provide a means for very fast calculation of times over the trajectory corresponding to the given trigger amplitude.

e) The set of log-log papers plus the linear graphs allow a fast calculation of trajectory times for any trigger amplitude (within the bounds of the graph papers, of course).

It is clear that this method is advantageous mostly in the case where several calculations must be performed for the same system.

4.4.2 A Simple Method on the (x,y) Plane

This is a less accurate, but faster method, and more versatile in solving problems for several different trigger amplitudes. It will be called "the phase plane method A."

It consists in approximating the system phase plane portrait with four straight line segments, under the following assumptions:

a) We assume that, in regions I and III, P moves in a straight line towards the corresponding singularity $x_{\nu\mu}$, ν = I, III; μ = 0, 1; and that in region II it moves parallel to and in the same direction of the asymptote nearest to it.

b) The discontinuities of y at $x = -\frac{1}{\gamma}$ and at $x = +\frac{1}{\gamma}$ can be calculated by equations (3.61a.i) and (3.61b.i) respectively.

c) As a very fast method at the cost of obtaining a somewhat poorer accuracy, these discontinuities of y at the boundaries of region II (i.e., at $x = \pm\frac{1}{\gamma}$) can be completely ignored.

d) So, as illustrated in Fig. 23, we take a linear graph paper, mark on it the scaled x and y axes, vertical lines $x = \pm\frac{1}{\gamma}$, and singular points $X_{\nu 0}$, and also the direction of the asymptotes related to the saddle point of region II.

Then, given a trigger amplitude W, we mark the points $X_{\nu 1}$ and also P_0. Suppose a I to III transition; then $P_0 = P{:}(x_{I0}, y_0)$.

(i) Draw the segment of the line $\overline{P_0 X_{I1}}$ contained in region I.

(ii) The intersection of this line with $x = -\frac{1}{\gamma}$ is y_a.

(iii) Find y_b by (3.61a.i).

(iv) From y_b draw, inside region II, a line segment with slope $\lambda_{\beta II}$ (the positive asymptote slope); its intersection with $x = +\frac{1}{\gamma}$ is y_c.

(v) Find y_d by (3.61b.i).

(vi) Consider $P_d{:}(+\frac{1}{\gamma}, y_d)$; draw the line $\overline{P_d X_{III1}}$. Let λ_d be the slope of this line, and call it λ_d line.†

† In the descriptions of these graphical methods, references to a line shall, in general, be made using the symbol for its slope.

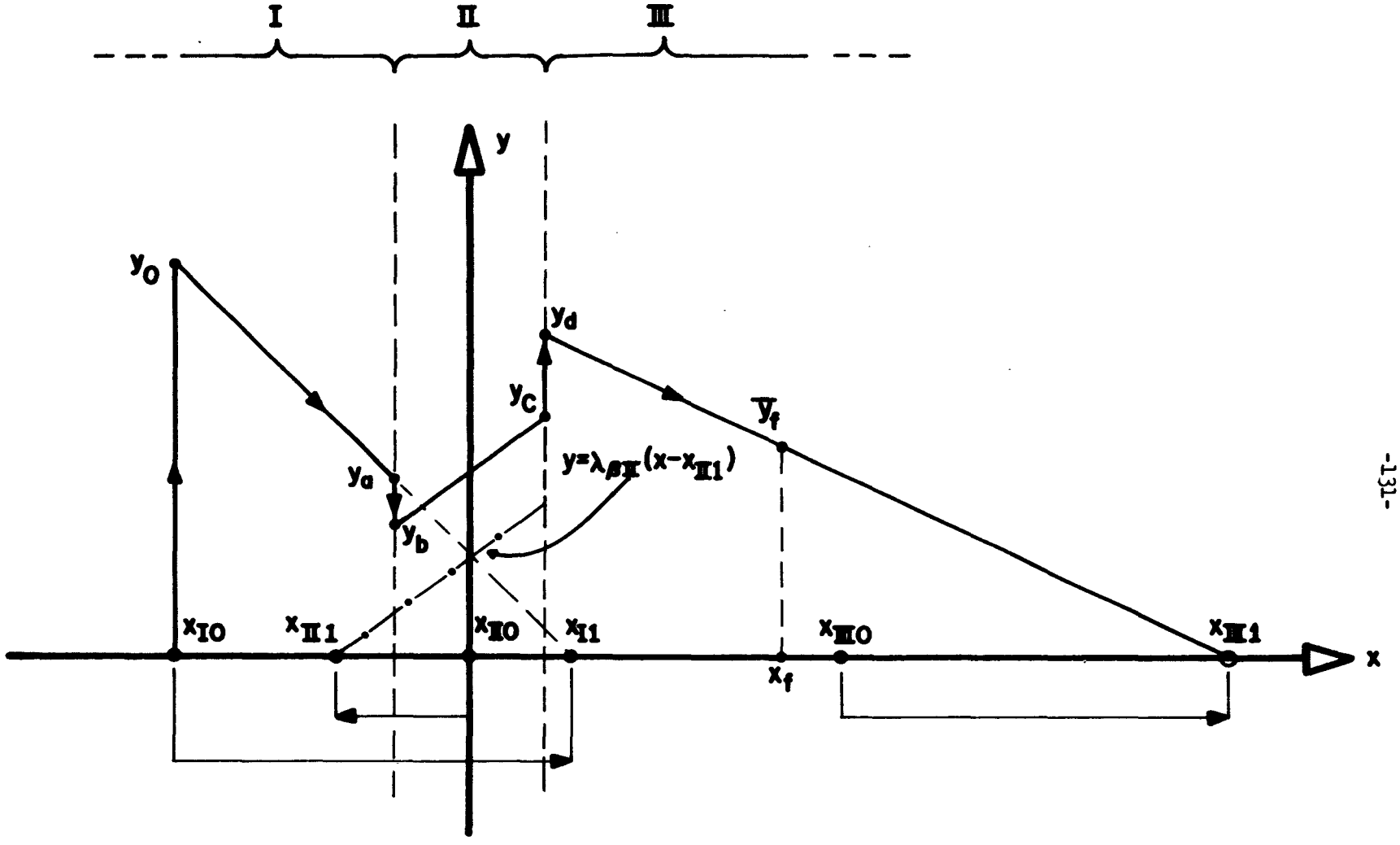

FIGURE 23: APPROXIMATE GRAPHICAL METHOD A OF TRAJECTORY CALCULATION ON THE PHASE PLANE. A LONG TRIGGER IS ASSUMED IN THIS EXAMPLE.

(vii) Consider $P_f:(x_f,\bar{y}_f)$ be the intersection of lines $\overline{P_dX}_{III1}$ and $x = x_f$.

(viii) Calculate $T'_{Of} = T_{Oa} + T_{bc} + T_{df}$ by (4.21), supposing that P crosses $x = x_f$ while the trigger is ON.

(ix) Consider the trigger duration T_W, and suppose that P crosses $x = x_f$ for the second time† after the trigger is turned OFF.

(x) Find

$$\bar{y}_e = y_d e^{\lambda_d[T_W-(T_{Oa}+T_{bc})]}$$

and mark $\bar{P}_e:(x_e,\bar{y}_e)$, the point immediately before trigger turn-off occurs.

(xi) Find $y_e = \bar{y}_e - y_O$, and mark $P_e:(x_e,y_e)$, the point immediately after trigger turn-off.

(xii) Draw the line $\overline{P_eX}_{IIIO}$, and mark point $P_f:(x_f,y_f)$ of intersection of the lines $\overline{P_eX}_{IIIO}$ and $x = x_f$,

(xiii) Find T_{ef} by (4.21), and then in this case where P crosses $x = x_f$ after trigger turn-off,

$$T_{Of} = T_W + T_{ef}$$

Of course, after the obvious changes, the same algorithm can be applied to a III to I transition.

† This method does not apply with acceptable accuracy if P crosses $x = x_f$ for the first time after trigger turn-off.

4.4.3 An Approximate Method on the (x,y) Plane

This is a slightly more sophisticated method then method A; it will be called "the phase plane method B."

We will use the phase plane equation (3.11) which we repeat here for convenience:

$$\frac{dy}{dx} = \frac{d_{\nu\mu} - c_{\nu\mu}x}{a_\nu y} - \frac{b_{\nu\mu}}{a_\nu}, \qquad d_{\nu\mu} = d_\nu + \mu n W \tag{3.11}$$

To plot a I-III transition in the phase plane, we do as follows:

(i) Find y_0, and $x_{\nu\mu}$, for all $\nu\mu$ conditions.

(ii) Draw the lines $y = \lambda_\beta(x - x^*)$ for x_{I1}, x_{III}, x_{III0}, and x_{III1}, and call them, respectively, the β_{I1}, β_{III}, β_{III0}, and β_{III1} lines.

(iii) By (3.11), we find $\frac{dy}{dx}$ at $P_C:(x_{I0}, y_0)$, and call λ_0 this derivative.

(iv) Draw a line with slope λ_0 through P_0, and call this the λ_0 line.

(v) Check if the λ_0 line intersects the β_{I1} line inside region I.

If this is so, call the intersection $P_1:(x_1, y_1)$ and call $P_a:(-\frac{1}{\gamma}\Big|_-, y_a)$ the intersection of the lines β_{I1} and $x = -\frac{1}{\gamma}$.

Otherwise, ignore the intersection of lines λ_0 and β_{I1}, and call $P_a:(-\frac{1}{\gamma}\Big|_-, y_a)$ the intersection of lines β_0 and $x = -\frac{1}{\gamma}$.

(vi) Find $y_b(x = -\frac{1}{\gamma}\Big|_+)$ by (3.61a.i)

(vii) Find $y_c(x = +\frac{1}{\gamma}\Big|_-)$ by the iterative numerical procedure using, for example, one of equations (4.4), or, instead, assume the trajectory in region II is a straight line of slope $\lambda_{\beta II}$. (The choice depends entirely on a compromise between accuracy and computation time.)

(viii) Find $y_d(x = +\frac{1}{\gamma}\Big|_+)$ by (3.61d.i).

(ix) By (3.11), calculate the slope $\frac{dy}{dx}$ at $P_d:(+\frac{1}{\gamma}\Big|_+, y_d)$ (for region III), and call β_d this derivative.

(x) Draw a line with slope λ_d through point P_d and call it the λ_d line.

(xi) Find the intersection $P_3\cdot(x_3, y_3)$ of lines λ_d and β_{IIII}.

The trajectory in region III with a very long trigger is taken as segments $\overline{P_dP_3}$ and $\overline{P_3X}_{IIII}$ of lines λ_d and β_{IIII}. Call this the line $\overline{P_dX}_{IIIf}$.

(xii) Do as directed in (vi) to (xiii) of method A, but modify instruction (x) of that method to:

(x) Find $\bar{P}_e:(x_e, \bar{y}_e)$, the point immediately before trigger turn-off occurs by:

$$\begin{cases} \bar{y}_{e1} = y_d e^{\lambda_d[T_W-(T_{0a}+T_{bc})]} \\ \bar{y}_{e2} = \bar{y}_{e1} e^{\lambda_{\beta IIII}[T_W-(T_{0a}+T_{bc}+T_{d3})]} \end{cases}$$

$$\begin{cases} \bar{y}_e = \bar{y}_{e1}, & \text{if} \quad \bar{y}_{e1} > y_3 \\ \bar{y}_e = \bar{y}_{e2}, & \text{if} \quad \bar{y}_{e1} < y_3 \end{cases}$$

Again, after the obvious modifications, this applies to a III to I transition.

An illustrative example is presented in Chapter 6.

Obs.: Notice that this Method B can be a hybrid numerical and graphical method. Various such combinations can be made and we feel that, some of these combinations may be good compromises between speed and accuracy.

4.5 Approximate Analysis of Waveforms

One of the most important aspects of transition waveforms is the time duration of the various phases of a transition as defined in section 4.2. The exact shapes of a particular variable (voltage or current) as a function of time is less important than its general characteristics, such as delay time, rise time, average form in each region, minimum and maximum values, etc. The exact shape is important insofar as it influences the calculations of these characteristics, especially the various time intervals elapsed between the definite changes in character of the curve, generally described by changes in the values of the pair of indices $\nu\mu$.

Furthermore, even if we do have the exact (analytic) solution of (2.103), it will not do us much good.

We can solve the problem for the waveforms of all variables based on the solution of (2.103). But then--besides the fact that (2.103), and therefore any solution based on it, is already an approximation to the real problem--the important general characteristics of the waveforms are hidden in a fairly cumbersome analytical formula, which would take a considerable time of tedious labor to plot.

Our aims consist mostly in analyzing and evaluating an existing flip-flop or improving its design, selecting a better trigger or loading circuits,

determining optimum trigger duration and better waveforms, and better understanding the operation of bistable circuits.

For these purposes, an approximate plot of the several variables which could be obtained in a reasonably short time would be far more useful.

In this section we will suggest some methods by which such graphs can be obtained.

4.5.1 Collector and Base Currents

Assume that an approximation to $y(x)$ (phase plane) has been obtained, consisting of four line segments, one for each value of $v\mu$ (three line segments in the case of optimum trigger duration).

This can be obtained either by the second graphical method described in section 4.4.2, or, if time durations are extremely important, by calculating time durations with one of the iterative techniques described in section 4.3, and then using (4.21) and (4.22) to determine the position of line segments which would result in the same trajectory time intervals.

a) With (4.21), several points can be marked over this approximate trajectory constituting indeed a (nonlinear) time scale.

b) Or else, considering that $x(t)$ has the form

$$x = A + Be^{\lambda t}\Big|_{v\mu} \tag{4.34}$$

A, B and λ can be found for each value of $v\mu$.

By a) or b) above, or any equivalent method, plot $x(t)$ and $y(t)$.

(i) Collector Currents

If (2.93) is assumed, an approximate graph of the collector current variables w_k, $k = 1, 2$, is immediate for they will be constants outside region II

(either 0 or 1, whatever the case may be) and will be linear functions of x inside region II, so that, by just assigning new scales, the two curves $w_k(t)$ can be obtained.

More accurate curves can be obtained by using equations (2.56) and (2.57), which will yield results in closer approximation to the real transistor currents, than the model represented by equation (2.103). Use of a graph of the tanh x would allow a completely graphical procedure.

(ii) Base Currents

Here use of equation (2.94) yields graphs of z_k, k = 1, 2, with almost equal ease. The first term is directly proportional to the corresponding collector current w_k, and the second term is proportional to y(t) in every region, since $\varphi'(x)$ is a constant in every region.

In this case, use of (2.58) and (2.59) to improve accuracy would hardly be justified.

4.5.2 Collector Voltages

By inspection of Fig. 24 we get immediately:

$$v_{o\ell} = v_k + R_{ik}C_{ik}\frac{dv_k}{dt'} - R_{ik}(i_k + i_{Bk} + I_{Bk}); \quad \begin{cases} k = 1, 2 \\ \ell = 1, 2 \\ \ell \neq k \end{cases} \qquad (4.36)$$

where t' is the nonnormalized time variable. Normalizing as before and setting

$$u_j = \frac{1}{2}\eta v_{oj}, \quad j = 1, 2 \qquad (4.37)$$

we get:

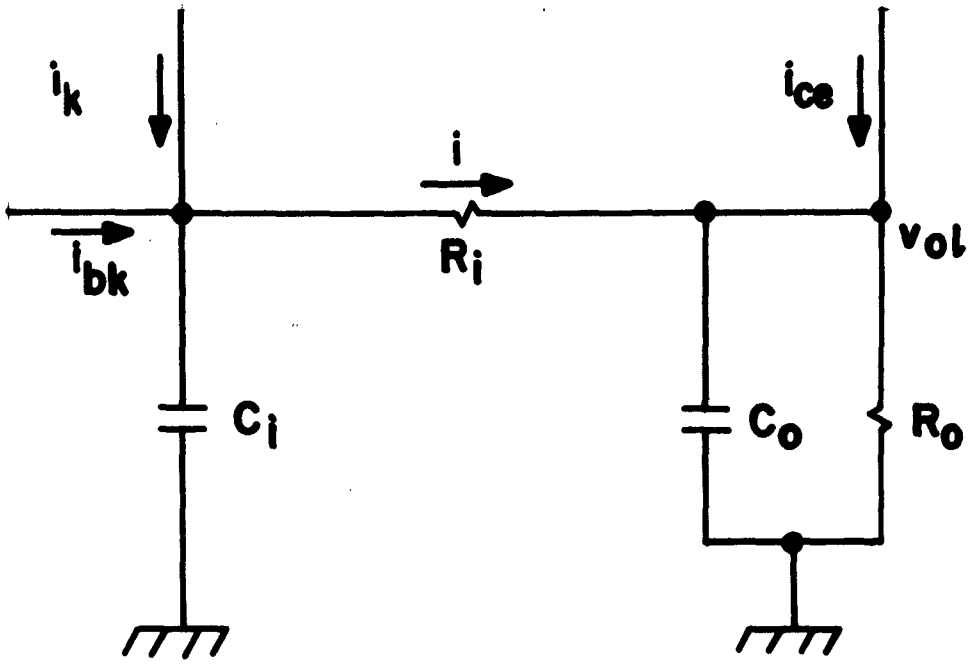

FIGURE 24: PASSIVE NETWORK YIELDS THE EQUATION FOR THE OUTPUT VOLTAGE.

$$u_\ell = x_k + \frac{\tau_i}{\tau} \overset{o}{x}_k - 2p_k \frac{R_{ik}}{R_{ok}} (\theta_k + z_k) - 2p_k \frac{R_{ik} I_{Bk}}{R_{ok} \alpha I_E} \qquad (4.38)$$

with $k = 1, 2$; $\ell = 1, 2$; $\ell \neq k$. As before, we can interpret θ_k in terms of an equivalent current source of strength s_k and a parallel conductance G_k, according to (2.79), repeated here for convenience. Assuming a rectangular trigger, and making use of the index $\mu = 0, 1$:

$$\theta_k = s_k - \frac{G_{k\mu} R_{ok}}{2p_k} x_k, \quad k = 1, 2 \qquad (4.39)$$

Substituting (4.39) into (4.38), and using $y_k = \overset{o}{x}_k$, we get:

$$u_\ell = (1 + R_{ik} G_{k\mu}) x_k + \frac{\tau_{ik}}{\tau} y_k - 2p_k \frac{R_{ik}}{R_{ok}} (s_k + z_k) - 2p_k \frac{R_{ik} I_{Bk}}{R_{ok} \alpha I_E} \qquad (4.40)$$

with $k = 1, 2$; $\ell = 1, 2$; $\ell \neq k$.

This equation is very general, and allows one to find both collector voltages of a general Eccles-Jordan flipflop (symmetrical or nonsymmetrical) if x_1 and x_2 are known and also holds for the asymmetrical flipflop, by dropping the indices k and ℓ.

For the moment we shall focus our attention on the asymmetric flipflop and on the symmetric Eccles-Jordan.

In the first case (asymmetric flipflop) we get:

$$u = (1 + R_i G_\mu) x + \frac{\tau_i}{\tau} y - 2p \frac{R_i}{R_o} (s + z) - 2p \frac{R_i I_B}{R_o \alpha I_E} \qquad (4.41)$$

And in the latter case (symmetric flipflop) we get by subtraction, and setting

$$u = u_2 - u_1 \dagger \tag{4.42}$$

$$u = (1 + R_1 G_\mu)x + \frac{\tau_1}{\tau} y - 2p \frac{R_1}{R_o} z - 2p \frac{R_1}{R_o} \mu W + \left(\frac{I_{B1} - I_{B2}}{\alpha I_E} \right) \tag{4.43}$$

with

$$\mu = \begin{cases} 0, & \text{if trigger is OFF} \\ 1, & \text{if trigger is ON} \end{cases}$$

These equations immediately suggest the procedure for obtaining the collector voltage variable u(t) from x(t), y(t), z(t) and W; it is clearly a very easy graph to obtain from the preceding ones, since, in each region, it consists of a constant plus a linear combination of the previous curves, with only the constant and possibly the coefficient of x(t) having different values for the two distinct trigger states.

4.6 The Influence of Parameters on Transition Times--Simplified Equations

We would like to have some qualitative notion about the effects of the various parameters upon the overall transition time. We are also interested in learning something about the total charge fed into and removed from transistor bases and capacitors, and their relation, if any, with transition times. Besides that, some characteristics of waveforms, such as maximum, minimum and settled levels of collector voltages and peak base currents also interest us.

At this point we must stress that we are searching for more qualitative criteria, i.e., first order approximation formulae which could help considerably

---

† Notice that $x = x_1 - x_2$, i.e., the order of the indices is reversed in the two definitions.

in the evaluation and understanding of flipflops, and not for exact (or good) engineering design formulae. In this respect the character of this section is entirely different from the general character of this dissertation.

4.6.1 The Optimum Flipflop

Let us assume (since it is possible in principle) that a flipflop has been constructed such that, if the trigger duration is optimum, i.e., if $x_e = x_{III0}$, then $y_e = 0$, where x_e and y_e are the coordinates of P_e, the position of P immediately after trigger turn off.

For this flipflop, we can say that, in a first order approximation, the transition time is given by:

$$T_{TR} = \frac{x_{I1} - x_I}{y_0} \ln \frac{x_{I1}}{x_{I1} - x_{I0}} + \frac{x_{III1} - x_{III0}}{y_0} \ln \frac{x_{III1}}{x_{III1} - x_{III0}} \quad (4.44)$$ †

Let us assume that $x_{III1} - x_{III0} = x_{I1} - x_{I0} = \Delta x$. Then

$$T_{TR} = \frac{\Delta x}{y_0} \ln \frac{x_{I1} x_{III1}}{(\Delta x)^2} \quad (4.45)$$

From Table II:

$$\Delta x = \frac{p}{1 + R_s G_1} \left[n'W + \left(1 - \frac{1 + R_s G_1}{1 + R_s G_0} \right) (J + H\Psi) \right] \quad (4.46)$$

$$x_{I1} \cdot x_{III1} = \left(\frac{p}{1 + R_s G_1} \right)^2 [(n'W + J)^2 - (H\Psi)^2] \quad (4.47)$$

† This comes from assuming a straight line approximation to the trajectory, neglecting the active time, and using equations (4.23) and (4.24) in regions I and III. Notice that state symmetry is not required for this approximate equation to be valid.

So,

$$\frac{x_{I1} \cdot x_{III1}}{(\Delta x)^2} = \frac{\left[n'W + \left(1 - \frac{1 + R_s G_1}{1 + R_s G_0}\right)(J + H\Psi)\right]^2}{(n'W + J)^2 - (H\Psi)^2} \qquad (4.48)$$

where:

a) $n' = 2\frac{R_s}{R_o}$

b) $\varphi_k = [1 + 2B_k + \rho]$

c) $\Psi = 1 - \frac{(1 - \alpha)}{\alpha} \cdot \frac{R_s}{R_o}$

d) $J = \begin{cases} \varphi, & \text{if it is an asymmetric flipflop} \\ \Delta\varphi = \varphi_1 - \varphi_2, & \text{if it is a symmetric flipflop} \end{cases}$

e) $H = \begin{cases} 1, & \text{if it is an asymmetric flipflop} \\ 2, & \text{if it is a symmetric flipflop} \end{cases}$

Assume: $a_I = a_{III} = a$, and $m_I = m_{III} = m$.

$$y_o = \frac{m_I}{a_I} W = \frac{m}{a} W \qquad (4.49)$$

where a and m are given in Table I:

a) $m = 2p\frac{\tau_{io}}{\tau}$

b) $a = \frac{\tau_i \tau_o}{\tau^2}$

And therefore

$$y_0 = \frac{2p\tau}{\tau_{0i}} W = \frac{2p\tau}{R_o C_i} W \tag{4.50}$$

So:

$$\frac{\Delta x}{y_0} = \frac{R_o C_i}{\tau(1 + R_s G_1)} \left[\frac{R_s}{R_o} + \left(1 - \frac{1 + R_s G_1}{1 + R_s G_0}\right) \frac{J + H\Psi}{2W}\right] \tag{4.51}$$

It is clear that

$$\Psi \approx 1, \quad \text{if} \quad (1 - \alpha)R_s \ll \alpha R_o$$

so that $H\Psi \approx H$.

And assumption of state symmetry eliminates biasing from the formula:

$$J = 0$$

From (4.48) and (4.51) we get:

$$T_{TR} = \frac{R_o C_i}{\tau(1 + R_s G_1)} \left[\frac{R_s}{R_o} + \left(1 - \frac{1 + R_s G_1}{1 + R_s G_0}\right) \frac{J + H\Psi}{2W}\right] \cdot \ln \frac{4W^2 \left[\frac{R_s}{R_o} + \left(1 - \frac{1 + R_s G_1}{1 + R_s G_0}\right) \frac{G + H}{2W}\right]^2}{\left(2 \frac{R_s}{R_o} W + J\right)^2 - (H\Psi)^2} \tag{4.52}$$

And, if $\Psi \approx 1$ and $J = 0$, we get

$$T_{TR} = \frac{R_o C_i}{\tau(1 + R_s G_1)} \left[\frac{R_s}{R_o} + \frac{HK}{2W}\right] \cdot \ln \frac{\left[\frac{R_s}{R_o} + \frac{HK}{2W}\right]^2}{\left(\frac{R_s}{R_o}\right)^2 - \left(\frac{H}{2W}\right)^2} \tag{4.53}$$

where

$$K = 1 - \frac{1 + R_s G_1}{1 + R_s G_o}$$

As a final simplification, if

$$G_o = G_1 \qquad \text{(equivalently, } K = 0\text{)}$$

we get:

$$T_{TR} = \frac{R_s C_i}{\tau(1 + R_s G_1)} \ln \frac{1}{1 - \left(\frac{HR_o}{2R_s W}\right)^2} \tag{4.54}$$

Let us suppose that we have a fairly large trigger, and that p is also sufficiently large† so that

$$\left(\frac{HR_o}{2R_s W}\right)^2 \ll 1 \tag{4.55}$$

Then taking the first two terms of the series expansion of the argument of the natural logarithm, and then taking the first term of the series expansion of the logarithm itself, we obtain:

---

† These conditions are not a property of flipflops. In fact $HR_o/2R_s W$ close to 1 is practical, since $W \approx 10^{-1}$ is practical. However, we assume that W has been chosen large to speed up the transition.

$$T_{TR} = \frac{H^2 R_o \tau_{oi}}{4R_s \tau (1 + R_s G_1) W^2} \tag{4.56}$$

Equation (4.56) should be an acceptable first order approximation for the transition time whenever the flipflop and trigger satisfy all of the assumptions leading to it. Observe that there is a hierarchy of equations with more and more restrictive assumptions; all of them assume the optimum flipflop described before. Then:

Equation (4.52) is very general; the only assumption is that the flipflop is either symmetric or asymmetric;

Equation (4.53) assumes, further, that $\psi = 1$, and $J = 0$;

Equation (4.54) assumes, still further, that $G_0 = G_1$, i.e., that $K = 0$;

Equation (4.56), besides the above, assumes (4.55) to be valid.

Also remember that all times are normalized with respect to τ, so that nonnormalized times would not include τ in the denominator. For example, (4.56) would read:

$$T'_{TR} = \frac{H^2}{4(1 + R_s G_1) W^2} \cdot \frac{\tau_{oi}^2}{(\tau_i + \tau_{oi})} \tag{4.57}$$

Remembering that $W = \frac{I_E}{\alpha I_E}$, we get:

$$T'_{TR} = \frac{H^2 \cdot (\alpha I_E \tau_{oi})^2}{4R_s C_i (1 + R_s G_1) I_t^2} \tag{4.58}$$

Another expression for T_{TR} can be obtained as follows: Consider that the charge variation Δq_i of C_i between the two stable states is given by (see (4.69)):

$$\Delta q_i = (v_{III0} - v_{I0}) \cdot C_i = \frac{H(x_{III0} - x_{I0})C_i}{\frac{1}{2}\eta} \approx \frac{2pHC_i}{\frac{1}{2}\eta(1 + R_s G_0)} = \frac{H\alpha I_E \tau_{oi}}{(1 + R_s G_0)} \dagger \tag{4.59}$$

Therefore,

$$T'_{TR} = \left(\frac{H\Psi\Delta q_i}{2I_t}\right)^2 \cdot \frac{(1 + R_s G_0)^2}{(1 + R_s G_1)} \cdot \frac{1}{R_s C_i} \tag{4.60}$$

If $G_0 = G_1 = 0$ (i.e., the trigger circuits are perfect current sources), and if $\Psi \approx 1$,

$$T'_{TR} = \left(\frac{H\Delta q_i}{2I_t}\right)^2 \cdot \frac{1}{R_s C_i} \tag{4.61}$$

This equation should give us a somewhat crude but satisfactory first approximation to the transition time.

We insist that use of (4.59) should always be cautious, since some of the assumptions made in its derivation are somewhat vague, and others, if ligitimate, will seldom be fulfilled. So, (4.59) is usable for estimating results, i.e., as a kind of figure of merit; it is definitely not a design formula.

---

† This approximation is made under our assumptions: $\varphi = 0$, $\Psi = 1$, $G_0 = G_1$, so there is a cancelling out in the second term of (4.60).

At first glance it seems strange that the transition time does not depend on τ in a first approximation. In other words, it seems strange that τ is not a factor of prime importance in the transition time. The following discussion should account for this observation.

First of all, since the beginning, we have completely ignored the active region, and second, we have assumed that y_d, the ordinate of P when entering region III, would be such that $y_e = 0$. Of course, if τ has some influence in the active region, it will determine the value of y_d; in assuming y_d to have a convenient value, we have ignored the effects of the transistors, or in a better way, we have assumed that there is a relationship between the transistors and the passive network such that the optimum flipflop assumption is verified. In this sense, τ should be related to τ_{oi}, and therefore (especially if this relation were found to be linear) τ_{oi} could be replaced by its expression in terms of τ. Then τ would be the prime factor in all those equations, and τ_{oi} would not appear at all. We could also have a linear combination of both parameters. That we have started using τ_{oi} was a question of convenience; the assumptions made establish a certain relationship between τ_{oi} and τ. We conclude that, after all, τ is a very important factor in the transition time.

Even more important than the approximation of T_{TR} furnished by these formulae in the case of an optimum flipflop, is the following consideration:

(i) Even if the flipflop is not optimum, the transition time should not be substantially different from the results obtained by the use of these formulae. They would be, at any rate, a first order approximation to the transition time.

(ii) They would certainly be true in a qualitative sense, i.e., as indications of the relative effects of the various parameters, as well as the order of magnitudes and directions of change.

4.6.2 The Total Charge Interchanged Between the Transistor Bases†

These were established in Chapter 2, equations (2.20) as

$$q_{Bk} = \tau i_{Ck}, \quad k = 1, 2 \tag{4.62}$$

Therefore, the total charge variation is

$$\Delta q_B = H\tau\alpha I_E \tag{4.63}$$

Some relations can be established here, such as:

$$H\alpha I_E = \frac{\Delta q_B}{\tau} = \frac{\Delta q_i}{\tau_{oi}} (1 + R_s G_0) \tag{4.64}$$

But let $G_1 = G_0$; then, from (4.60)

$$T'_{TR} = \left(\frac{H}{2I_t}\right)^2 \cdot \frac{\Delta q_i \cdot \Delta q_B \cdot \tau_{oi}}{R_s C_i \tau} \cdot \frac{(1 + R_s G_0)}{(1 + R_s G_1)} \tag{4.65}$$

Also,

$$T'_{TR} = \left(\frac{H\Delta q_B \tau_{oi}}{2I_t \tau}\right)^2 \cdot \frac{1}{(1 + R_s G_1) R_s C_i} \tag{4.66}$$

† Since the charge that enters one base is equal to the charge that leaves the other, we can talk about the charge transferred between the bases, though this transference is really only a mathematical cancellation, not physical transference.

If $G_1 = 0$,

$$T'_{TR} = \left(\frac{H\Delta q_B \tau_{oi}}{2I_t \tau}\right)^2 \cdot \frac{1}{R_s C_i} \tag{4.67}$$

Also, it is clear that, if $G = 0$,

$$\tau \cdot \Delta q_i = \tau_{oi} \cdot \Delta q_B \tag{4.68}$$

which is very illustrative of the type of condition relating the transistor parameter, the passive network parameters, and the two stable states.

Notice that for the symmetric flipflop,

$$\left.\begin{aligned} q_B &= q_{B1} - q_{B2} \qquad \therefore \Delta q_B = \Delta q_{B1} - \Delta q_{B2} \\ q_i &= q_{i1} - q_{i2} \qquad \therefore \Delta q_i = \Delta q_{i1} - \Delta q_{i2} \end{aligned}\right\} \tag{4.69}$$

$W = W_1 - W_2$ but the triggers W_1 and W_2 are assumed to occur simultaneously

4.6.3 Collector Voltages--Maximum, Minimum and Settled Values

$$\left.\begin{aligned} &\text{(i) Maximum:} && v_{Ckmax} = V_{Ck} + R_o(I_{t\ell} + \alpha I_E) \\ &\text{(ii) Minimum:} && v_{kmin} = V_{Ck} + R_o(I_{t\ell} + (1 - \alpha)I_E \\ &\text{(iii) Settled:} && v_{C1IO} = V_{C1} + R_o \alpha I_E \\ &\text{(iv)} && v_{1IIIO} = V_{C1} + R_o(1 - \alpha)I_E \\ &\text{(v)} && v_{C2IO} = V_{C2} + R_o(1 - \alpha)I_E \\ &\text{(vi)} && v_{C2IIIO} = V_{C2} + R_o \alpha I_E \end{aligned}\right\} \tag{4.70}$$

where: $k = 1, 2;\ \ell = 1, 2;\ \ell \neq k$

v_{Ckv0} = collector voltage of transistor T_k when $x = x_{v0}$

V_{Ck} = collector supply voltage of transistor T_k

In case of the asymmetric flipflop, drop the indices k and ℓ, and $v_{C1v0} = V_{C1}$.

4.6.4 Peak Values of Base Current

Considering the optimum flipflop, and the approximate model whose equation is (2.103), it is clear that the peak base current would be given by:

$$\left.\begin{aligned} z^*_{peak} &= \gamma y_d \\ y_d &= y_0 \cdot \frac{x_{IIII}}{\Delta x} \end{aligned}\right\} \qquad (4.71)$$

$$\text{with } z^* = \begin{cases} z_1^*, & \text{if the flipflop is asymmetric} \\ z_1^* - z_2^*, & \text{if the flipflop is symmetric} \end{cases}$$

and the symbol "*" means the component of the current corresponding to base charge variation

The approximate form of $\frac{y_0}{\Delta x}$, from, say, (4.54), and the approximate form of x_{IIII}, yield:

$$y_d = \frac{\tau(1 + R_s G_1)}{R_s C_i} \cdot \frac{nW}{(1 + R_s G_1)} \quad \dagger \qquad (4.72)$$

so that:

† Notice that $n = pn'$.

$$z_{peak} = 2\frac{\tau}{\tau_{oi}}\gamma W \qquad \text{or} \qquad i_{Bpeak} = 2\frac{\tau}{\tau_{oi}}\gamma I_t \tag{4.73}$$

We stress that this value of z_{peak} refers to, not only the approximate model of equation (2.103), but to this model with all the restrictions implicitly imposed in the evaluation of y_d.

Therefore, such an expression is specially meant to give us an acceptably close idea of the values of the base current in any given case, when just a fast estimate is required.

4.7 The Problem of Circuit Optimization

Whenever one tries to state a problem of optimization, besides a clear statement of what is to be optimized, two basic questions must be answered.

First: "Under what criterion?"

Second: "What are the constraints?"

The amount of material written on these optimization questions is very large. We shall not try to find complete answers here, but rather, to open the discussion by some pertinent approximations.

The first question is what characteristics we could wish to optimize: trigger duration and amplitude (if not its waveform!), circuit parameters, or the transistor characteristics.

This first question being decided, we could go on to the second question, and try to be specific about stating an optimization criterion, i.e., an interpretation of the word "improvement!"

Of a host of possibilities, we can state the following three as examples:

a) The time interval between the moment when the trigger is turned ON and the moment the collector voltage is settled (under what criterion to decide this?) is to be minimized. Call this time the "collector voltage switching time," T_{CS}.

b) The time interval between the moment when the trigger is turned ON and the moment the base (or base-to-base) voltage is settled, that is, the "base voltage switching time," T_{BS}, is to be minimized.

c) Instead of minimizing switching times, one might wish to have a given delay time and a minimum active time, or a minimum switching time with a given delay.

And so on! The above illustrates the point.

We have already attempted to approach question number one, in a very tentative way, with respect to the variable x (see 3.5d and e) in defining, for a special purpose, a concept of "optimum trigger duration," which was related to the minimization of a defined "transition time" T_{TR}, for the variable x. The difficulties were apparent and that discussion stands as a good example of the issues involved.

The second question is usually easier to settle, since constraints are naturally stated either as inequalities or as relations between the variables, or some other mathematical statement. To incorporate constraints in an optimization algorithm is still another thing; but it has been done successfully for several problems, and, once stated, there is no a priori reason to expect the problem to be intractable. The theory presented so far suggests a number of techniques to approach optimization problems, once they are stated in a mathematical form.

As a last observation, it is worth reminding ourselves that problems of optimization tend to raise questions of existence of solutions (realizability)

and that nothing has been said, for example, about the realizability of our hypothetical "optimum flipflop" so liberally used (as an approximation device) throughout this Chapter 4.

4.8 Summary

After defining a nomenclature for time intervals over a phase plane trajectory, we have presented some methods for the calculation of points and time intervals for a given trajectory.

An iterative numeric procedure allows the exact calculation of $y_b(x_b)$ and $t_b(x_b)$ if $y_a(x_a)$ and $t_b(x_b)$ are known, for any given pair of abcissae x_a and x_b.

Similarly, a fairly sophisticated graphical construction using two variable transformations, $(x,y) \rightarrow (\Phi,\chi) \rightarrow (\bar{\Phi},\bar{\chi})$, was also presented, and shown to yield accurate results, given the limitations of a graphical construction.

A more naive construction on the phase plane was described, which yields somewhat less accurate results, but is extremely simple to apply.

It was also suggested that some hybrid constructions graphical and numeric, might be ideal for accuracy and practicability of use.

A graphical procedure to obtain fairly good plots of collector and base voltage and current waveforms was described.

Engineering interest in simple-minded formulae which can work as rules of thumb for the rapid evaluation of circuit characteristics has led us to discuss, by means of an ultra-simplified model, a set of such relationships.

Finally, the optimization problem was proposed in a first approach discussion.

5. EXTENSION OF THE THEORY

5.1 Introduction

We have, so far, confined ourselves to the asymmetric and the symmetric flipflops subjected to a rectangular trigger, and also we have implicitly assumed that neither C_i, C_o or τ is zero.

In this chapter we shall discuss the problems involved in applying this theory to other situations, and indicate the methods and modifications involved.

5.2 Case When τ Is Negligible

This is a very unlikely possibility, but it may happen. In case it does, we can take $\tau = 0$ as a good approximation. Then, the coefficients of the equilibrium differential equations apparently are meaningless!

However, looking back to how these equations were established, we will see that τ was used only as a convenient time normalization constant. Of course, if it is too small (or too large, as we shall see!) it ceases to be convenient, and some other time interval $\bar{\tau}$ (such as τ_{oi}, for example) could be used as a time normalization constant.

In performing this renormalization of time, we replace τ with $\bar{\tau}$ in equation (2.34) and on all related equations from then on. By letting $\tau = 0$ in equations (2.29) and (2.30), $\overset{o}{i}_{c1}$ and $\overset{o}{i}_{c2}$ disappear from the expressions for i_{B1} and i_{B2}.

The result of this is that the charge storage in the base along with its related current will be negligible, and only the recombination component of the base current needs to be considered. Then, the equilibrium equations will not contain terms like z_0 and $\overset{o}{z}_0$. Except for this, the theory is exactly the same, and applies exactly in the same way.

5.3 Case of Negligible External Capacitances

Again we have a possible, although unlikely situation, which becomes important especially because it can be solved in a special way, i.e., not just an extension of the general theory.

By making τ_i, τ_{io}, τ_{oi} and τ_o all zero in equations (2.87), (2.88) and (2.90), we would get, respectively:

For the asymmetric flipflop, from (2.87)

$$y = \frac{R_o}{R_s}\left\{(1 - \rho)\tanh x - \frac{1}{p}(1 + R_s G_\mu)x + (1 + 2B + \rho) + 2\frac{R_s}{R_o}s\right\}\cosh^2 x \tag{5.1}$$

For the symmetric Eccles-Jordan flipflop, we get from (2.88)

$$y = \frac{R_o}{R_s}\left\{(1 - \rho)\tanh x - \frac{1}{2p}(1 + R_s G_\mu)x + (B_1 - B_2) + \frac{R_s}{R_o}s\right\}\cosh^2 x \tag{5.2}$$

For the nonsymmetric Eccles-Jordan flipflop, i.e., the most general case, directly from (2.90):

$$(1 + R_{sk}G_{k\mu})x_k = p_k\left\{(1 + 2B_k + \rho_k) - (-1)^k(1 - \rho_k)\tanh x + (-1)^k\frac{R_{sk}}{R_{ok}}y\,\mathrm{sech}^2 x + 2\frac{R_{sk}}{R_{ok}}s_k\right\} \tag{5.3}$$

so that, since $x = x_1 - x_2$, we get:

$$x = \frac{p_1}{(1 + R_{s1}G_{1\mu})}\left\{(1 + 2B_1 + \rho_1) + (1 - \rho_1)\tanh x - \frac{R_{s1}}{R_{o1}}\, y\,\mathrm{sech}^2 x + 2\,\frac{R_{s1}}{R_{o1}}\, s_1\right\}$$

$$- \frac{p_2}{(1 + R_{s2}G_{2\mu})}\left\{(1 + 2B_2 + \rho_2) - (1 - \rho_2)\tanh x + \frac{R_{s2}}{R_{o2}}\, y\,\mathrm{sech}^2 x + 2\,\frac{R_{s2}}{R_{o2}}\, s_2\right\} \tag{5.4}$$

with the result that:

$$y = \frac{\cosh^2 x}{\dfrac{p_1 R_{s1}}{(1 + R_{s1}G_{1\mu})R_{o1}} + \dfrac{p_2 R_{s2}}{(1 + R_{s2}G_{2\mu})R_{o2}}} \cdot \left\{\left[\frac{p_1(1 - \rho_1)}{1 + R_{s1}G_{1\mu}} + \frac{p_2(1 - \rho_2)}{1 + R_{s2}G_{2\mu}}\right]\tanh x - x\right.$$

$$\left. + \left[\frac{p_1(1 + 2B_1 + \rho_1)}{1 + R_{s1}G_{1\mu}} - \frac{p_2(1 + 2B_2 + \rho_2)}{1 + R_{s2}G_{2\mu}}\right] + 2\left[\frac{p_1 R_{s1} s_1}{(1 + R_{s1}G_{1\mu})R_{01}} - \frac{p_2 R_{s2} s_2}{(1 + R_{s2}G_{2\mu})R_{02}}\right]\right\} \tag{5.5}$$

So, in every case we have $y = f_\mu(x)$; of course we are assuming that $s(t)$ is a rectangular function. Therefore, we can find $x(t)$, or better $t(x)$, by the formula:

$$t - t_0 = \int_{x_0}^{x} \frac{1}{y_\mu(\xi)}\, d\xi, \quad \text{where} \quad y_\mu(\xi) = f_\mu(\xi) \tag{5.6}$$

and we mean that, if μ changes, at a certain point, we must find its abcissa x_a, and continue the integration after x_a with the new function of x.

It is easy to see from equations (2.87) and (2.88) that these cases are still exactly solvable even if only $C_{ok} = 0$ and $C_{ik} \neq 0$, in the same way as when $C_{ik} = C_{ok} = 0$. The only difference is that, in (5.1) and (5.2), instead of $\frac{R_o}{R_s}\cosh^2 x$ as a factor on the right-hand side, we shall have the following modifications:

For the asymmetric case, from (2.87), replace,

$$\text{in (5.1)}, \frac{R_o}{R_s}\cosh^2 x \quad \text{by} \quad \frac{1}{R_s\left(\frac{\operatorname{sech}^2 x}{R_o} + \frac{C_i}{\tau}\right)} \tag{5.7}$$

For the symmetric case, from (2.88), replace,

$$\text{in (5.2)}, \frac{R_o}{R_s}\cosh^2 x \quad \text{by} \quad \frac{1}{R_s\left(\frac{\operatorname{sech}^2 x}{R_o} + \frac{C_i}{2\tau}\right)} \tag{5.8}$$

Note in (2.90) that, if $C_{ok} = 0$, even the nonsymmetric case is considerably simplified, since it will be reduced to a second order case, i.e., two first order equations. Then, if $R_{s1} = R_{s2}$, the system can be exactly solved, just like the symmetric case. Otherwise it would be approximately solvable, like the nondegenerate symmetric system.

5.4 Nonsymmetric Eccles-Jordan Flipflops

The difficulty in the case of the nonsymmetric Eccles-Jordan flipflop is that there is no way (except for some extremely fortunate coincidence) to reduce the two equations (2.74) in x_1 and x_2 into a single equation. The fact is that this circuit has one more degree of freedom and there is no possible reduction to the previous cases. Nevertheless, we can do something about solving the system. Suppose that we carry out an approximation of equations (2.74), taking $\varphi(x)$ instead of $\tanh x$ just as we have done to obtain equation (2.103). The result will be the pair of equations expressed by (2.104), whose coefficients are shown in Table I.2, and which is repeated below for convenience:

$$a_{kv}\overset{oo}{x}_k + b_k\overset{o}{x} + c_k x = a'_{kv}\overset{oo}{x} + b'_{kv}\overset{o}{x} + c'_{kv}x + d_{kv}$$

$$+ f_k(\overset{o}{x})[\delta(x + \tfrac{1}{\gamma}) - \delta(x - \tfrac{1}{\gamma})] + m_{kv}\overset{o}{s}_k + n_k s_k \qquad (2.104)$$

with

$$k = 1, 2$$

These two equations are coupled only in the active region II (here the three regions are still defined in terms of the base-to-base voltage variable $x = x_1 - x_2$). Except for region II, each equation is of the same form as (2.103)!

Thus, we can define another plane where x_1 and x_2 are represented independently but on the same horizontal axis. Call it the x_k axis.

In this plane, y_1 and y_2 would also be represented independently but on the same vertical axis. Call it the y_k axis.

We will still divide this plane into three regions, but the region boundaries will be determined on the (x,y) plane, rather than on the (x_k,y_k) plane.

That is to say: If x is in region I or III of the (x,y) plane then x_1 is in its region I_1 or III_1 and x_2 is in its region I_2 or III_2 of the (x_k,y_k) plane.

If x is in region II of the (x,y) plane, then both x_1 and x_2 will be in their respective regions II_1 and II_2 of the (x_k,y_k) plane.

Therefore, region II, which is nothing but the representation of the active region of both planes, in the case of the (x_k,y_k) plane, will correspond to two regions, one for x_1 and another for x_2. These regions are determined by the values of x_1 and x_2 when $|x_1 - x_2| = \frac{1}{\gamma}$ (see Fig. 25).

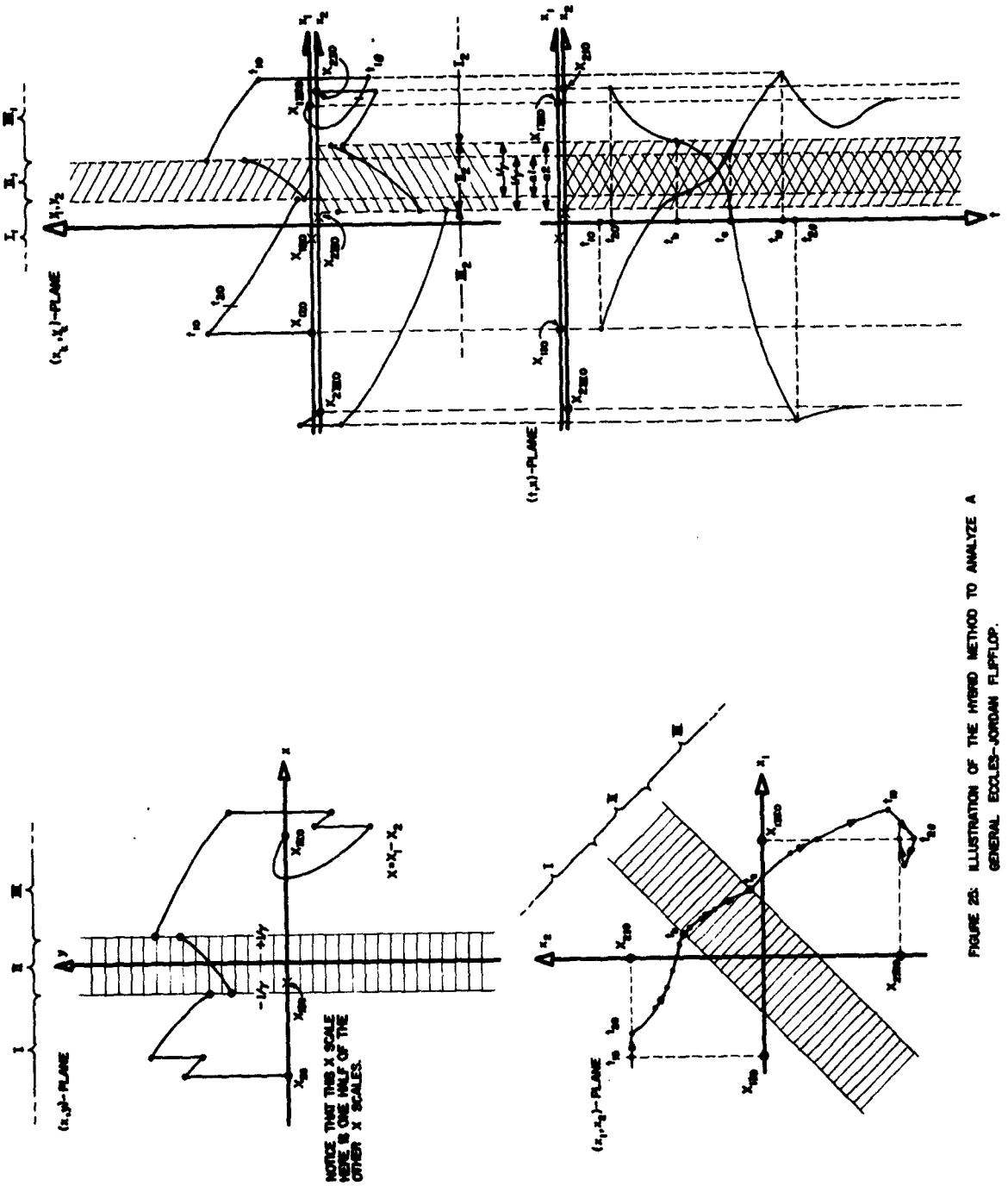

FIGURE 25: ILLUSTRATION OF THE HYBRID METHOD TO ANALYZE A GENERAL ECCLES-JORDAN FLIPFLOP.

In turn, these values depend only on how they start, i.e., the relative values of their respective initial ordinates y_{10} and y_{20}, and which one starts first (receives a trigger first). So, the regions for x_1 may not coincide at all with the regions for x_2, and besides they have a certain configuration only for a given transition: i.e., in the (x_k, y_k) plane the region configuration is a function of the system and of the triggers.

Another plane is very helpful, and can be used. It is the (x_1, x_2) plane, in which the active region is a strip of parallel lines going through the origin, intersecting the coordinate axes at points $(\pm \frac{1}{\gamma}, \pm \frac{1}{\gamma})$ thus bisecting the first and third quadrants. The representative point Q of the system is the point of coordinates (x_1, x_2), and it is a simple matter to go from the time scaled trajectories of the two points P_1 and P_2 in the (x_k, y_k) plane to the trajectory of Q in the (x_1, x_2) plane.

Use of the (x_1, x_2) plane makes it easier for us to find the points (x_{1a}, y_{1a}) and $(x_{2\bar{a}}, y_{2\bar{a}})$ where $(x_{1a} - x_{2\bar{a}}) = \pm \frac{1}{\gamma}$ (the sign $\pm$ according to the direction of the transition), i.e., the points where x enters or leaves the active region.

Now, inside the active region, equations (2.104) form a system of two linear second order differential equations in $x_k(t)$, k = 1, 2. We can easily solve this system of equations for $x_1(t)$ and $x_2(t)$, $y_1(t)$ and $y_2(t)$, and so, $x(t) = x_1 - x_2$ and $y(t) = y_1 - y_2$ can be found, and from these, the points (x_{1c}, y_{1c}), $(x_{2\bar{c}}, y_{2\bar{c}})$ where x comes out of the active region.

From then on, the equations (2.104) are again independent, and the remaining trajectories $y_1(x_1)$ and $y_2(x_2)$ can be found. Figure 25 illustrates this discussion.

The case where both C_{ik} and C_{ok} or just C_{ok} are negligible has already deserved special mention in the previous section, for it is exactly solved by equations (5.1) to (5.8).

5.5 Other Types of Trigger

5.5.1 Introduction

We have concentrated our efforts on a theory using a rectangular trigger for two main reasons: the wave form can often be approximated by a rectangular form, and a rectangular trigger lends itself easily to a phase plane treatment.

We feel, however, that some comments are necessary on the most common nonrectangular trigger waveforms, such as those mentioned in 2.4.

5.5.2 Impulse Trigger

A trigger can be considered as an impulse if the two approximate conditions hold:

$$\left.\begin{array}{ll} \text{(i)} & W_{av} \gg W_{min} \\ \text{(ii)} & q_t \approx \Delta q_i + \Delta q_B \end{array}\right\} \qquad (5.9)$$

where:

(i) W_{av} = average trigger current variable

(ii) W_{min} = minimum rectangular trigger amplitude necessary for a transition

(iii) $q_t = W \cdot T_t$, is the charge transported by the trigger

(iv) T_t = trigger duration, assumed here to be well defined

(v) Δq_i, Δq_B, as defined in (4.6.2), are the total variations of charge between the two states, of, respectively, the input capacitors C_{ik} and the base storages.

(vi) To simplify matters, we shall reason only with the asymmetric or symmetric flipflops in this section.

If conditions (5.9) are met, there are two ways to compute transition times (in the case of an impulse trigger the transition waveforms are meaningless); we will assume that $T_t = T_{TR}$.

As the crudest possible transition time evaluation, assume a rectangular trigger of amplitude W_{av} and duration $T_t = T_{TR}$. Then

$$y_0 = \frac{m}{a} W_{av} = \frac{2p\tau}{\tau_{oi}} W_{av} \tag{5.10}$$

$$T_{TR} = \int_{x_{I0}}^{x_{III0}} \frac{dx}{y_0} = \frac{a(x_{III0} - x_{I0})}{mW_{av}} \tag{5.11}$$

We find T'_{TR} from its normal form T_{TR}:

$$T'_{TR} = \frac{H\tau_{oi}}{(1 + R_s G_0)W_{av}}, \quad \text{if} \quad T_t = T_{TR} \tag{5.12}$$

As a less crude method, assume the transition is complete when the charge fed by the trigger into the input capacitances and the bases is equal to the total charge variation between the stable states:

$$q_t = \Delta q_B + \Delta q_i \tag{5.13}$$

We are implicitly assuming that the charge lost through both recombination inside the bases and the input resistances during the transition is small compared to the variation of stored charge. The trigger duration is again assumed to be optimum.

From (4.64),

$$\Delta q_B = H\tau\alpha I_E \tag{5.14}$$

$$\Delta q_i = H\tau_{oi}\alpha I_E(1 + R_s G_0) \tag{5.15}$$

$$q_t = \alpha I_E W_{av} T_t' = \alpha I_E W_{av} T_{TR}' \tag{5.16}$$

From (5.43), after denormalizing T_{TR} into T_{TR}',

$$T_{TR}' = \frac{H}{W_{av}} [\tau + \tau_{oi}(1 + R_s G_0)], \quad \text{if} \quad T_t = T_{TR} \tag{5.17}$$

where H = 1, 2, is the symmetry factor.

Further simplification in (5.12) and (5.17) is possible if $G_0 = 0$. We get from (5.12):

$$T_{TR}' = \frac{H\tau_{oi}}{W_{av}} \tag{5.18}$$

and from (5.17)

$$T_{TR}' = \frac{H}{W_{av}} [\tau + \tau_{oi}] \tag{5.19}$$

And we see that assumption of a constant value y_0 of $y(x)$ is equivalent to neglecting the transistor's collector time constant τ with respect to τ_{io}, which may be warranted or not. From (5.19), we conclude that

$$T_{min}' = \frac{H\tau}{I_t} \alpha I_E \tag{5.20}$$

is the minimum transition time that can be obtained from the given transistors and trigger (by making $C_i = 0$). As a result, we can use

$$q_B = \tau\alpha I_E \tag{5.21}$$

as a figure of merit of a transistor for use in switching circuits.

And for the flipflop and trigger we have:

$$I_t T'_{min} = Hq_B \tag{5.22}$$

5.5.3 Exponential or Sinusoidal Triggers

Here the trigger waveforms are continuously changing functions of time, and therefore phase plane treatment is not indicated, since the time variable appears explicitly in the differential equation(s) and cannot be eliminated.

We have to work either in the time domain or in the frequency domain by means of integral transforms. It is, in general, easy to solve, directly or, for instance, by Laplace transforms, the three region second order linear differential equation under an exponential or sinusoidal forcing function, so that, in any given problem, a numerical solution can always be found for waveforms, transition times, etc.

A theory covering these and other time-varying trigger waveforms, i.e., finding analytical expressions, relationships, approximate formulae and methods for the fast calculation of transition times, waveforms, etc., would be an entirely new proposition altogether, and clearly outside the scope of a phase plane theory of flipflops such as the present work proposes to be.

5.6 Use of Integral Transformations

In any of the three regions, (2.103) is a linear second order differential equation, and (2.104) is a system of two linear second order differental equations.

Therefore integral transform--or operational methods--except for other reasons--can be used, with whatever advantage one might have from them. In particular, Laplace transform methods could be used. The main advantage of these transform methods is that they simplify the solution of the differential equation under an arbitrary transformable forcing function, in our case, the arbitrary trigger. One added advantage of these methods is that they make it easy to solve (2.104) for x, which is the system's state variable.

The results are presented below, for completeness:

From (2.103) one gets:

$$\text{with} \begin{cases} W_t(\sigma) = \mathcal{L}[s(t)] \\ x(\sigma) = \mathcal{L}[x(t)] \\ \sigma = \sigma_r + j\sigma_i \text{ is a complex variable} \end{cases}$$

$$X(\sigma) = \frac{m_\nu \sigma^2 + n\sigma + d_\nu}{\sigma(a_\nu \sigma^2 + b_{\nu\mu}\sigma + c_{\nu\mu})} \cdot W_t(\sigma) + \frac{x_0\sigma + y_0}{\sigma^2} \qquad (5.23)$$

where $P_0:(x_0,y_0)$ is the initial point under each $\nu\mu$-condition.

From (2.104) one gets:

$$\text{with} \begin{cases} W_{tk}(\sigma) = \mathcal{L}[s_k(t)] \\ X_k(\sigma) = \mathcal{L}[x_k(t)] \end{cases}$$

And also:

$$x = x_1 - x_2 \qquad \therefore \begin{cases} x_0 = x_{10} - x_{20};\ y_0 = y_{10} - y_{20} \\ X = X_1 - X_2 \end{cases}$$

Parameters are as given in Table I.2.

$$X(\sigma) = \frac{(m_{1\nu}\sigma^2+n_1\sigma+d_{1\nu})(a_2\sigma^2+b_{2\mu}\sigma+c_{2\mu})W_{t1}(\sigma) - (m_{2\nu}\sigma^2+n_2\sigma+d_{2\nu})(a_1\sigma^2+b_{1\mu}\sigma+c_1\mu)W_{t2}(\sigma)}{\sigma\{(a_1\sigma^2+b_{1\mu}\sigma+c_{1\mu})(a_2\sigma^2+b_{2\mu}\sigma+c_{2\mu}) - [(a'_{1\nu}-a'_{2\nu})\sigma^2 + (b'_{1\nu}-b'_{2\nu})\sigma + (c'_{1\nu}-c'_{2\nu})]\}}$$

$$+ \frac{x_0\sigma + y_0}{\sigma^2} \qquad (5.24)$$

where $P_0:(x_0,y_0)$ is the initial point under each $\nu\mu$ condition.

This makes it obvious why the approximate and graphical methods are important!

We can also find $X_1(\sigma)$ and $X_2(\sigma)$, by:

$$X_k(\sigma) = \frac{(a'_k\sigma^2 + b'_{k\nu}\sigma + c'_{k\nu}) \cdot (\sigma^2 X(\sigma) - x_0\sigma - y_0) + \sigma \cdot (m_{k\nu}\sigma^2 + n_k\sigma + d_{k\nu}) \cdot W_{tk}(\sigma)}{\sigma^2(m_{k\nu}\sigma^2 + n_k\sigma + d_{k\nu})}$$

$$+ \frac{x_{k0}\sigma + y_{k0}}{\sigma^2} \qquad (5.25)$$

where $P_{k0}:(x_{k0},y_{k0})$ is the initial point under each $\nu\mu$ condition.

Since $X(\sigma)$ would have to be found first, this makes it doubly obvious why the approximate and graphical methods are important.

5.7 Summary

In this chapter we have shown how two degenerate cases ($\tau = 0$ and $C_{ik} = C_{ok} = 0$) relate to the theory presented so far. The case of $\tau = 0$ was shown to be essentially included in the theory, since τ has been used as a normalization constant for no other reason than that of convenience. The other case of $C_{ik} = C_{ok} = 0$, or $C_{ok} = 0$, have been shown to be exactly solvable, the first even for the nonsymmetric flipflop, and the second for at least the

asymmetric and symmetric flipflops, and possibly (if $R_{s1} = R_{s2}$) for the nonsymmetric case which, at any rate, is reduced to a system of the second order.

A phase plane method suitable for the general nonsymmetric Eccles-Jordan flipflop was given, and a discussion showed that there are areas where the nonsymmetric flipflop is equivalent to two independent asymmetric flipflops (regions I and III); the trajectories in the active region (region III) must be found by solution of the system in the time domain.

Finally, we have discussed other types of trigger waveform. Besides the almost trivial impulse trigger, for which some relationships have been established, the other cases, such as exponential or sinusoid, cannot be treated by a phase plane theory. They can be treated analytically or numerically; however no general results are available. The equations must be solved in each specific case.

Approximations (2.103) and (2.104) are also important in allowing a phase plane treatment of the most important cases (second order), besides allowing treatment in the time domain (directly) or in the frequency domain (integral transforms) for any case.

Finally, we have briefly discussed the application of Laplace transform methods to (2.103) and (2.104), and presented special formula (5.23) and entirely general formula (5.24), thus covering all possibilities.

6. EXPERIMENTAL EXAMPLES

6.1 Introduction

The present chapter has a double purpose. We wish to illustrate the application of some of the described procedures, and also to test the accuracy of the theoretical results as compared to experimental fact. No extensive program of experimentation is intended; only a few examples were treated which should suffice to provide some feeling for the quality of the theory.

The experiments we have carried out consist in triggering a flipflop with a rectangular current trigger from what was practically a current source, i.e., the collector of a transistor. The trigger had a reasonably good waveform but we did not attempt to obtain an exceptionally good rectangular shape.

As for the flipflops themselves, we took two classes: one was a slowed-down flipflop where relatively large capacitors were paralleled with the T_1 base-to-ground and T_2 collector-to-ground terminals; the other had just parasitic capacitances, which were carefully measured. Only the asymmetric structure was used. In each case transition times and waveforms were measured and recorded for different values of trigger amplitude and various values of R_i and R_o.

Corresponding calculated values were found and comparisons between theoretical and experimental values are presented in the tables. The transistors used were the same for all flipflops, 2N1309's.

6.2 Measurement of τ, C_i and C_o

The collector time constant τ determines the influence of the base current terms upon the solution of the flipflop equation.

Whenever τ is negligible compared to the other time constants of the system, it becomes irrelevant and the base current terms may be ignored, as

in Chapter 5. But if τ is comparable to the other system time constants, it becomes critical and must be carefully measured.

The system used here was as follows:

a) The transistor pair whose collector time constants (assumed equal) are to be measured were assembled into a switching amplifier, with no collector lead, and a current of 1 ma fed into the parallel emitters.

b) A (periodically repeated) step voltage with amplitude just enough to switch the current from one transistor to another was applied to the base of T_1, and the base current of T_2 was recorded and integrated with respect to time (see Fig. 25).

c) Since there is only a negligible voltage variation at the base of T_2 (grounded lead) the parasitic capacitances have only a negligible effect on the measurement. Recombination current can also be neglected in comparison to the storage current.

From Fig. 25 we obtain by integration

$$\tau = 15.1 \text{ nsec} \qquad (6.1)$$

The parsitic capacitances have to be measured in situ. This can be done by measuring the time constants of voltage curves under applied step currents. So, Figs. 27 and 28 yield C_i and C_o in all regions.† C_i is found to vary slightly from one region to another (Figs. 6.5a and 6.5b) but C_o remains essentially the same in all regions. In calculating C_o it is necessary to subtract the injected current time constant (τ_I = 15 nsec) from the total collector voltage time constant (τ_T = 61 nsec) in order to obtain the true collector circuit time constant ($\tau_o = R_o C_o$ = 46 nsec).

† C_i is the base-to-ground capacitance of T_1; C_o is the collector-to-ground capacitance of T_2 (see Fig. 3 and also Fig. 5 for comparison).

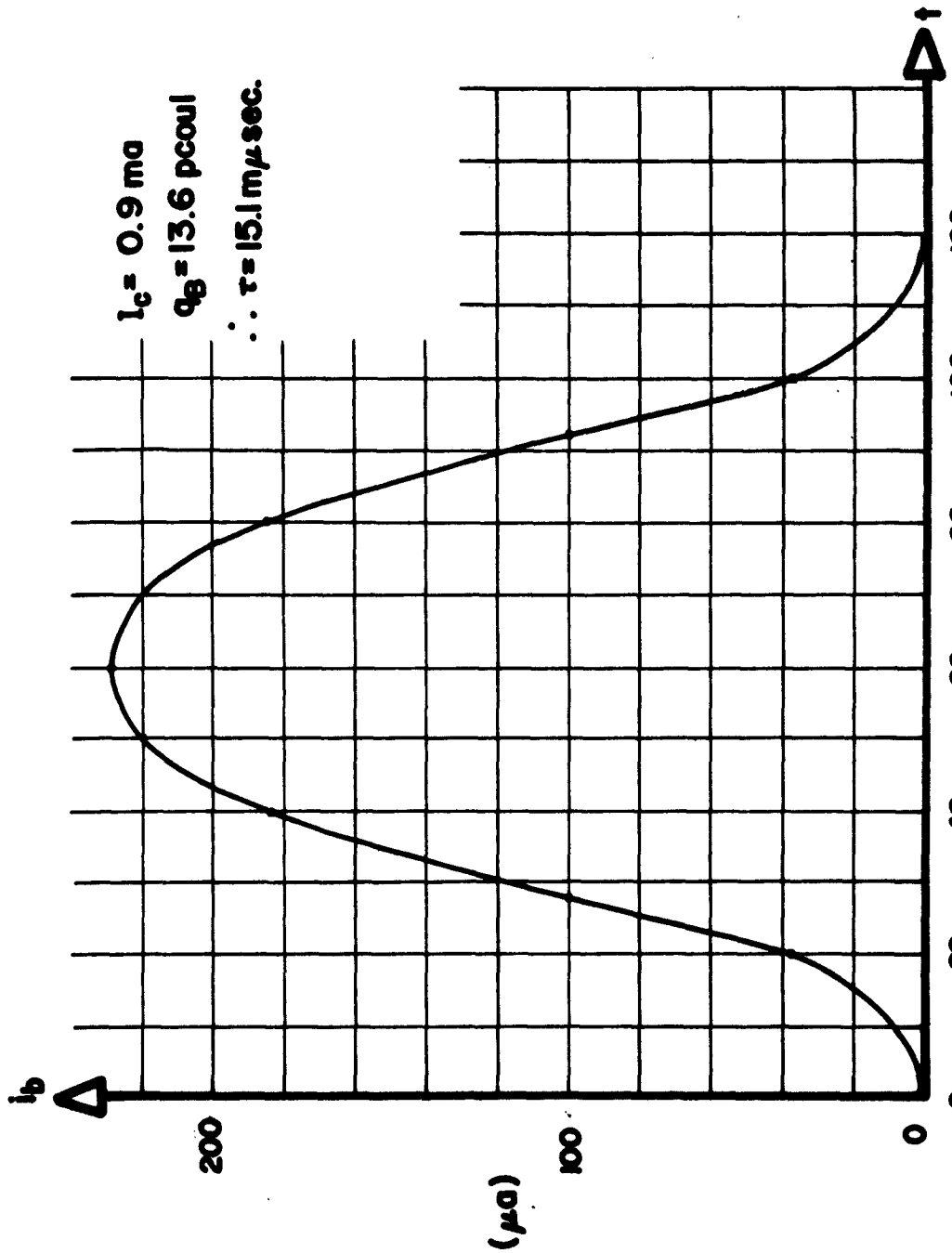

FIGURE 26: BASE CURRENT DUE TO CHARGE STORAGE.

a: T_1 BASE VOLTAGE RISE IN REGION I (T_1 ON)

Curve: v_b vs. t, I_c = 0.9 ma;
$R_s C_i$ = 170 mμsec

b: T_1 BASE VOLTAGE RISE IN REGION III (T_1 OFF)

Curve: v_b vs. t, I_c = 0;
$R_s C_i$ = 200 mμsec

FIGURE 27: T_1 BASE VOLTAGE RISE

Scales: Ord.: 0.5 v/div
Abs.: 100 mμsec/div

Parameter: R_s = 3 KΩ

Results: C_i = { 56.7 pf in region I
66.7 pf in region III

FIGURE 28: COLLECTOR VOLTAGE RISE UNDER INJECTED CURRENT

Curve: v_c vs. t

Scales: Vert.: 90 mv/div
Horiz.: 20 nsec/div

Total time constant: τ_T = 61 nsec

Time constant of the injected current:† τ_I = 15 nsec

Time constant of the collector circuit:
$R_o C_o = \tau_o$ = 46 nsec

Since R_o = 1 KΩ, C_o = 46 pf

† Not shown here.

This is not done in the measurement of C_i, since in normal operation the trigger circuit does contribute to C_i, whereas it does not contribute to C_o.

We get the values presented in (6.4).

By way of approximation we have used as a value of C_i in region II the average of its values in regions I and III, although in reality it is a continuously changing value.

6.3 Equation Parameters

We have considered two possibilities:

1. A flipflop loaded with relatively large capacitors.
2. A flipflop with only parsitic capacitances.

For case 1 we used

$$C_i = 0.02\ \mu f \quad \text{and} \quad C_o = 0.01\ \mu f \tag{6.2}$$

and had

$$R_i = 2\ k\Omega \quad \text{and} \quad R_o = 1\ k\Omega \tag{6.3}$$

In case 2 there are only parasitic capacitances:

$$C_i = \begin{cases} 56.7 \text{ in region I} \\ 61.7 \text{ in region II} \\ 66.7 \text{ in region III} \end{cases} \quad \text{and} \quad C_o = 46.0\ pf \tag{6.4}$$

The two resistors were chosen to be

$$R_i = 2\ k\Omega \quad \text{and} \quad R_o = 1\ k\Omega \tag{6.5}$$

Besides this we had:

$$\text{Case 1: } I_B = 3 \text{ ma; } I_E = 1 \text{ ma}, \quad p = 10$$
$$\text{Case 2: } I_B = 5 \text{ ma; } I_E = 0.9 \text{ ma}, \quad p = 10 \tag{6.6}$$

with the values of p calculated on the assumption that $\frac{q}{kT} = 40\ v^{-1}$.

In both cases the value of E_c was adjusted to make the system state symmetric, i.e., to have the stable values of the base voltage of T_1 symmetric with respect to ground.

Table XI presents these parameter values in a convenient form.

The equation coefficients are obtained from Tables I and II, and presented in Table XII.

Notice that all three cases are normalized with respect to τ.

6.4 An Illustrative Example

In order to illustrate some of the techniques described in the previous chapters, we shall consider case 2, under a rectangular current trigger of amplitude

$$W = 0.667, \quad \text{i.e.,} \quad I_t = 0.6 \text{ ma}$$

and we will calculate the delay, active, balance and transition times by three different methods, and compare the theoretical results with the experimental ones.

a) Graphical Method A: see Figs. 32 and 33

b) Approximate Method B: see Fig. 34

c) Iterative Numeric Method.

TABLE XI. PARAMETERS FOR THE TWO EXPERIMENTAL FLIPFLOPS

Parameter	Case 1	Case 2
C_i	0.02 μf	$61.7 + 5 \begin{bmatrix} -1 \\ 0 \\ +1 \end{bmatrix}$ pf
C_o	0.01 μf	46.0 pf
R_i	2 kΩ	2 kΩ
R_o	1 kΩ	1 kΩ
I_B	3 ma	5 ma
I_E	1 ma	0.9 ma
E_C	adjusted for state symmetry	
τ_i	40 μsec	$123.4 + 10 \begin{bmatrix} -1 \\ 0 \\ +1 \end{bmatrix}$ nsec
τ_{io}	20 μsec	$61.7 + 5 \begin{bmatrix} -1 \\ 0 \\ +1 \end{bmatrix}$ nsec
τ_{oi}	20 μsec	92.0 nsec
τ_o	10 μsec	46.0 nsec
τ_N	τ	τ
τ	15.1 nsec	
γ	0.7	0.7
p	10	10
$1 - \alpha$	0.007	
ψ ($\approx$)	0.979	0.979
φ ($\approx$)	0	

TABLE XII. PARAMETERS AND CONSTANTS INVOLVED IN THE EQUATIONS REPRESENTING THE TWO EXPERIMENTAL FLIPFLOPS

Coefficient	Case 1	Case 2
a_ν	$1.755 \cdot 10^6 + 10^4 \begin{bmatrix} 0 \\ 1 \\ 0 \end{bmatrix}$	$\begin{bmatrix} 22.9 \\ 29.0 \\ 26.9 \end{bmatrix}$
$b_{\nu\mu}$	$4.63 \cdot 10^3 + 86 \begin{bmatrix} 0 \\ 1 \\ 0 \end{bmatrix}$	$\begin{bmatrix} 16.6 \\ 38.3 \\ 18.0 \end{bmatrix}$
$c_{\nu\mu}$	$\begin{bmatrix} 1 \\ -6 \\ 1 \end{bmatrix}$	$\begin{bmatrix} 1 \\ -6 \\ 1 \end{bmatrix}$
d_ν	$\begin{bmatrix} -10 \\ 0 \\ +10 \end{bmatrix}$	$\begin{bmatrix} -10 \\ 0 \\ +10 \end{bmatrix}$
m_ν	$26.5 \cdot 10^3$	$\begin{bmatrix} 75.2 \\ 81.8 \\ 88.4 \end{bmatrix}$
n'	6	6
n	60	60
$f(\overset{o}{x})$	$-9.275 \cdot 10^3 \cdot y^2$	$-28.65 \cdot y^2$
y_0	$15.1 \cdot 10^3 \cdot W$	$3.28 \cdot W$
ℓ	$5.26 \cdot 10^{-3}$	0.988
$x_{\nu 0}$	$10 \begin{bmatrix} -1 \\ 0 \\ +1 \end{bmatrix}$	$10 \begin{bmatrix} -1 \\ 0 \\ +1 \end{bmatrix}$
$\Delta x_{I, III}$	$60 \cdot W$	$60 \cdot W$
Δx_{II}	$-10 \cdot W$	$-10 \cdot W$
$\lambda_{\alpha I}$	$-2.40 \cdot 10^{-3}$	-0.658
$\lambda_{\beta I}$	$-0.236 \cdot 10^{-3}$	-0.067
$\lambda_{\alpha II}$	$-3.611 \cdot 10^{-3}$	-1.46
$\lambda_{\beta II}$	$+0.913 \cdot 10^{-3}$	+0.142
$\lambda_{\alpha III}$	$-2.40 \cdot 10^{-3}$	-0.608
$\lambda_{\beta III}$	$-0.236 \cdot 10^{-3}$	-0.0610

a) Upper curve: v_i vs. t
Lower curve: v_o vs. t
Scales: { Vert.: 0.25 v/div
Horiz.: 10 μsec/div

b) v_i vs. t (Long trigger) + v_i vs. t (Optimum trigger)
v_o vs. t (Long trigger) + v_o vs. t (Optimum trigger)
Scales: { Vert.: 1.0 v/div
Horiz.: 0.5 msec/div

c) $\dot{v}_i$ vs. v_i (approximate)
{Upper curve: long trigger
Lower curve: optimum trigger
Scales: { Vert.: 12.5 (v/msec)/div
Horiz.: 0.25 v/div

FIGURE 29: TRANSITION CURVES FOR CASE 1

Comments:

Part a) illustrates the relationship between the transition curves for T_1 base voltage v_i and T_2 collector voltage v_o. Delay, active and balance times are apparent. The time duration of the transmission phases can be measured from it.

Part b) illustrates the effects of trigger duration upon the waveforms of both v_i and v_o.

Part c) is an approximate phase plane portrait of the transition, both for the long trigger (upper curve, showing the return of P from X_{I1} to X_{IO}, after trigger turn-off) and optimum trigger. Both curves are slightly tilted to the right due to imperfect differentiation of v_i.

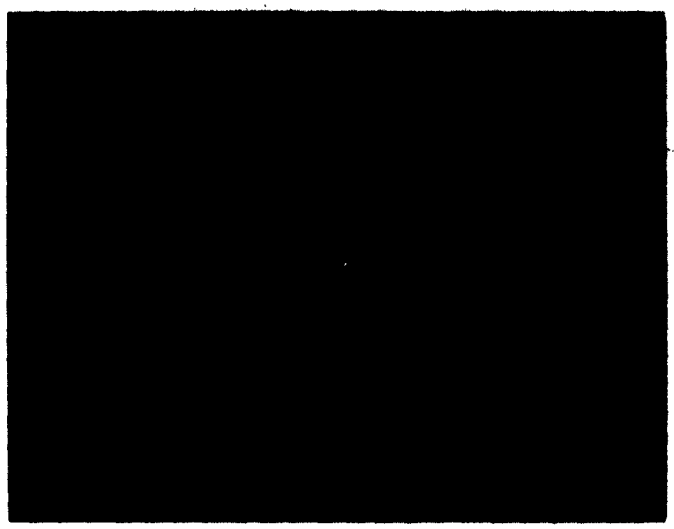

FIGURE 30: TRANSITION CURVE FOR CASE 2, WITH W = 0.445; v_i vs. t

Scales: { Vert.: 0.225 v/div
Horiz.: 20 nsec/div

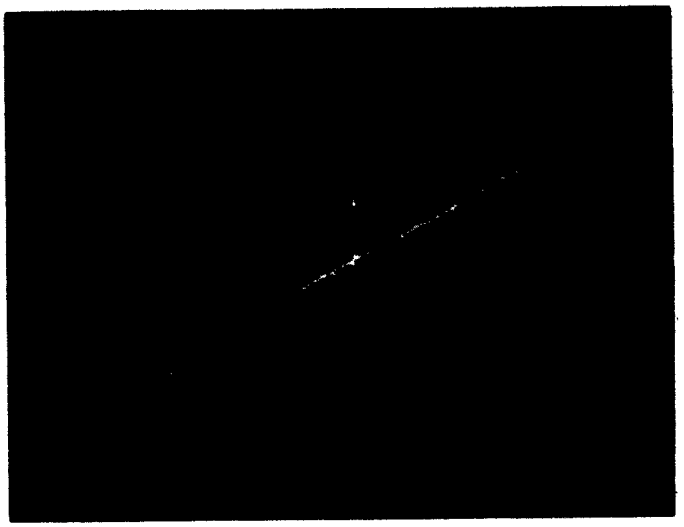

FIGURE 31: TRANSITION CURVE FOR CASE 2, WITH W = 0.667; v_i vs. t

Scales: { Vert.: 0.225 v/div
Horiz.: 20 nsec/div

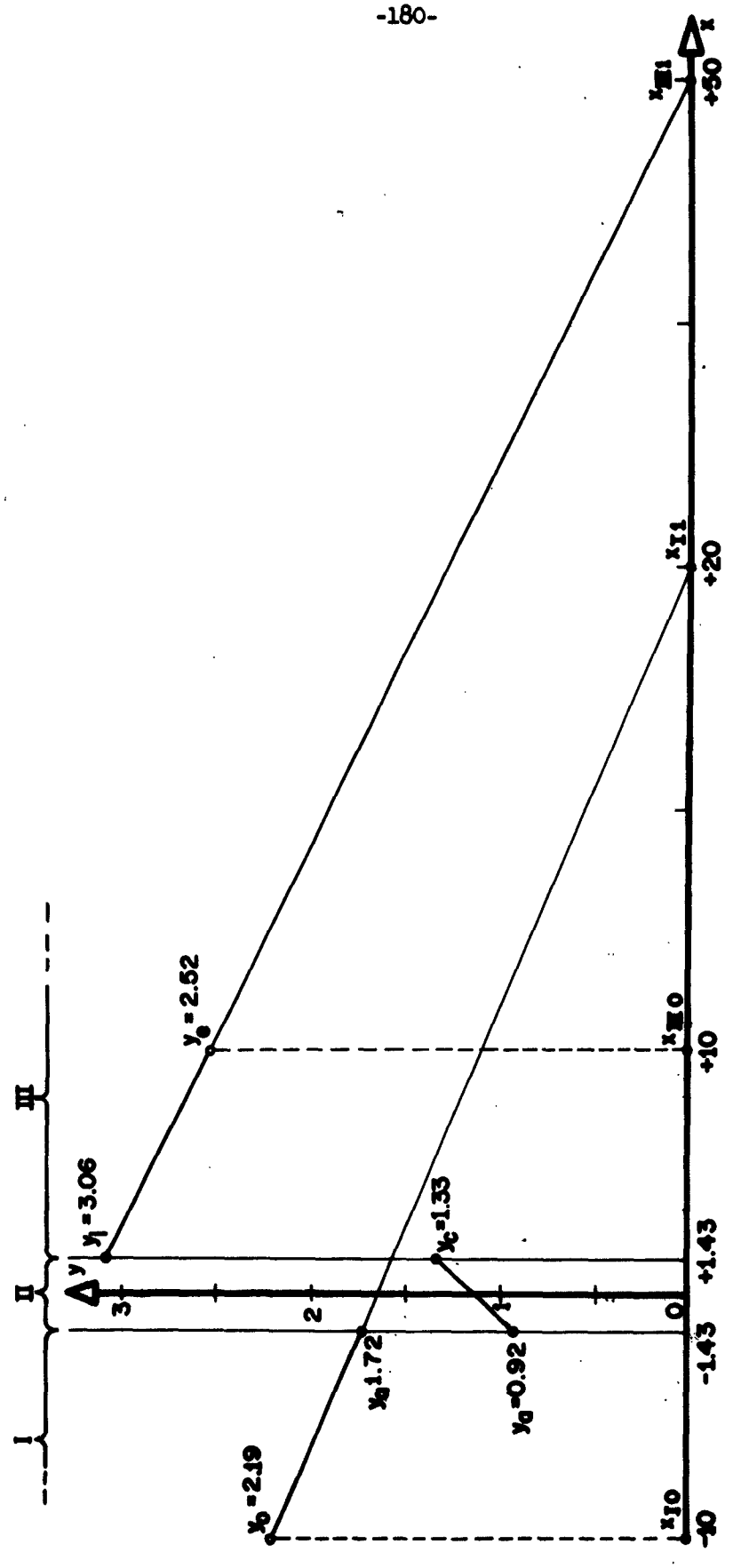

FIGURE 32: CASE 2, W=0.667 - GRAPHICAL METHOD A.

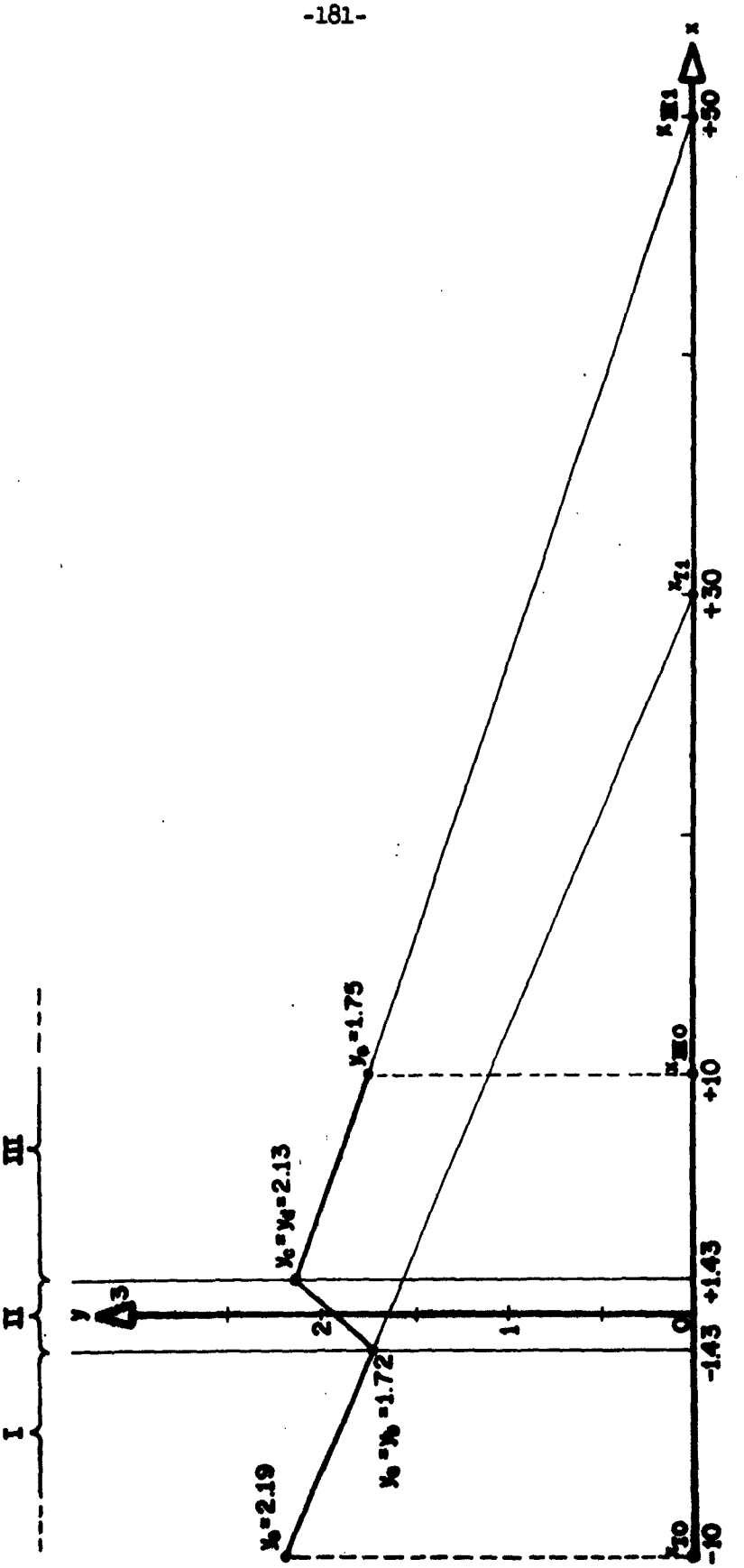

FIGURE 33: CASE 2, W = 0.667 - SIMPLIFIED GRAPHICAL METHOD A.

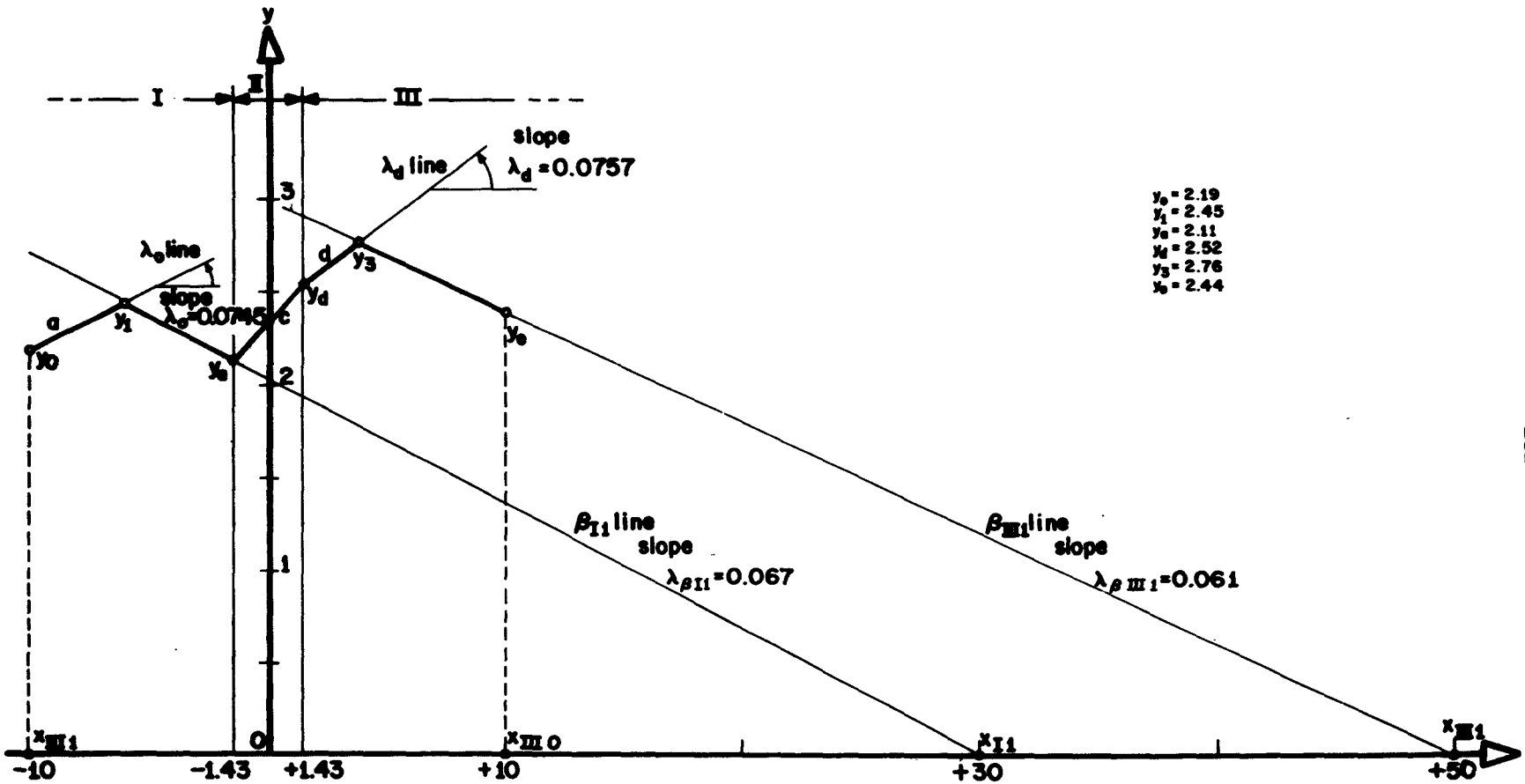

FIGURE 34: CASE 2, W=0.667-APPROXIMATE METHOD B.

6.4.1 Graphical Method A

We calculate x_{IO}, x_{IIIO}, Δx_{II}, Δx_{IIII}, x_{II}, x_{IIII} and y_0 by the formulae on Table II:

$$x_{IO} = -p \frac{Hw}{I_\mu} \approx -p = -10$$

$$\Delta x_I = nW = 40.0$$

$$x_{II} = x_{IO} + \Delta x_I = 30.0$$

$$x_{IIIO} = +p \frac{Hw}{I_\mu} \approx +p = +10$$

$$\Delta x_{III} = nW = 40.0$$

$$x_{IIII} = x_{IIIO} + \Delta x_{III} = 50.0$$

$$y_0 = \frac{m_I}{a_I} W = 2.19$$

We also need ℓ and $\lambda_{\beta II}$; we find from the note on equations (3.60):

$$\ell = \frac{m_{II}}{2a_{II}} = 0.988$$

and, obviously,

$$\lambda_{\beta II} = \frac{-b_{II} + \sqrt{b_{II}^2 - 4a_{II}c_{II}}}{2a_{II}} = 0.142$$

Then (see Fig. 34):

(i) We draw the line $\overline{P_o X_{II}}$

(ii) Intersection of $\overline{P_o X_{II}}$ with $x = -\frac{1}{\gamma}$ is P_a

$$y_a = y_o \cdot \frac{x_{II} + \frac{1}{\gamma}}{\Delta x_I} = 1.72$$

(iii) Using equation (3.61a.i) we find y_b from y_a:

$$y_b = \frac{1}{2\ell} \left(\sqrt{1 + 4\ell y_a} - 1\right)$$

We have:

$$y_a = 1.72$$

and:

$$\ell = 0.988$$

so:

$$y_b = 0.92$$

(iv) Draw, through P_b, the line of slope $\lambda_{\beta II}$, whose intersection with $x = +\frac{1}{\gamma}$ is P_c. Since

$$\lambda_{\alpha II} = 0.142$$

through

$$\Delta x = 2.86$$

causes

$$\Delta y = 0.406$$

so that

$$y_c = 1.33$$

(v) P_d is found from P_c by (3.61b.i).

$$y_d = (1 + \ell y_c) y_c$$

We have:

$$y_c = 1.33$$

and:

$$\ell = 0.988$$

so:

$$y_d = 3.00$$

(vi) (Simplified in our case) we draw the line $\overline{P_d X}_{IIII}$ and its intersection with $x = X_{III0}$ is P_e.

$$y_e = y_d \cdot \frac{\Delta x_{III}}{x_{IIII} - \frac{1}{\gamma}} = 2.52$$

The time intervals over the trajectorycan be calculated by using equation (4.21), which we repeat here, for convenience, in a slightly different, but equivalent form:

$$t_b - t_a = \frac{\Delta x}{\Delta y} \ln \frac{y_b}{y_a} \qquad (6.7)$$

Applied to region I we get:

$$T_D = \frac{\Delta x_I}{y_0} \ln \frac{y_a}{y_0} = 4.31$$

$$T_A = \frac{1}{\lambda_{\beta II}} \ln \frac{y_c}{y_d} = 2.55$$

$$T_B = \frac{\Delta x_{III}}{y_e} \ln \frac{y_e}{y_d} = 3.05$$

$$T_T = T_D + T_A + T_B = 9.91$$

Therefore,

$$T'_D = T_D \cdot \tau = 65.1 \text{ nsec}$$

$$T'_A = T_A \cdot \tau = 38.4 \text{ nsec}$$

$$T'_B = T_B \cdot \tau = 46.0 \text{ nsec}$$

$$T'_T = T_T \cdot \tau = 149.5 \text{ nsec}$$

Similarly we can find the trajectory for the other cases and fill out Table XIII.1.

Experimental values for the time durations over the trajectories are taken from Figs. 29 and 30, which are reproductions of pictures of oscilloscope images of the actual transitions.

Observe on Table XIV.1 the excellent agreement between experimental and calculated values of total transition times (T_T). Notice also that in case 1, the agreement for the partial time durations (T_D, T_A, T_B) is also excellent. But in case 2 the agreement for the partial time durations, although

TABLE XIII. DESCRIPTION OF APPROXIMATE TRAJECTORIES BY METHOD A

TABLE XIII.1

x	Case 1	Case 2	
	y	y	
	W = 0.3	W = 0.445	W = 0.667
-10	$y_0 = 4.53 \cdot 10^{-3}$	$y_0 = 1.46$	$y_0 = 2.19$
$-1.43\|_-$	$y_a = 2.38 \cdot 10^{-3}$	$y_a = 0.992$	$y_a = 1.72$
$-1.43\|_+$	$y_b = y_a$ †	$y_b = 0.626$	$y_b = 0.92$
$+1.43\|_-$	$y_c = 4.99 \cdot 10^{-3}$	$y_c = 1.032$	$y_c = 1.33$
$+1.43\|_+$	$y_d = y_c$ †	$y_d = 2.075$	$y_d = 3.06$
+10	$y_e = 3.38 \cdot 10^{-3}$	$y_e = 1.57$	$y_e = 2.52$
I_t	0.3 ma	0.4 ma	0.6 ma
$\Delta x_I = \Delta x_{III}$	18	26.7	40.0
Δx_{II}	-3.0	-4.45	-6.67
$\lambda_{\beta II}$	$0.913 \cdot 10^{-3}$	0.142	

TABLE XIII.2

Case 2 Taking $\ell = 0$	
y	
W = 0.445	W = 0.667
$y_0 = 1.46$	$y_0 = 2.19$
$y_a = 0.992$	$y_a = 1.72$
$y_b = y_a$	$y_b = y_a$
$y_c = 1.398$	$y_c = 2.13$
$y_d = y_c$	$y_d = y_c$
$y_e = 1.068$	$y_e = 1.75$
0.4 ma	0.6 ma
26.7	40.0
4.45	-6.67
0.142	

† The effects of base charge storage are negligible compared to the charge stored in C_i.

TABLE XIV. COMPARISON OF TIME INTERVALS OVER THE TRAJECTORIES OF TRANSITIONS BOTH CALCULATED BY METHOD A AND MEASURED

TABLE XIV.1

	Case 1		Case 2			
	W = 0.3		W = 0.445		W = 0.667	
	Theo.	Exper.	Theo.	Exper.	Theo.	Exper.
Region I: Delay Time T_D	38.7	32	107.0	82	66.6	52
Region II: Active Time T_A	12.2	17	53.0	34	38.4	22
Region III: Balance Time T_B	31.5	30	71.4	92	46.0	64
Transition Time T_T	82.4	79	231.4	208	151.0	138
Units	μsec		nsec			

TABLE XIV.2

Case 2 Taking $\ell = 0$			
W = 0.445		W = 0.667	
Theo.	Exper.	Theo.	Exper.
107.0	82	66.6	52
36.6	34	22.8	22
101.5	92	67.2	64
245.1	208	156.6	138
nsec			

fair, is less satisfactory. There is, however, a compensation of errors, especially between values of T_A and T_B. This seems to be a property of this approximate way of taking the base current into account. When the base current has negligible effect, as in case 1, this effect does not occur.

An apparently paradoxical fact is that we get a better agreement on partial times, although worse for the total transition time, if we take $\ell = 0$, i.e., if we completely neglect the effect of the second derivative of the base current. The graph is shown in Fig. 33, and Tables XIII.2 and XIV.2 present the ordinates and times for this very simple procedure.

This apparent paradox can be explained if we consider our type of approximation at the model level. The piecewise linear model has a behavior that differs in detail from the nonlinear real transistor pair; but the difference is such that it tends to cancel out over the different phases of a trajectory, yielding good overall results.

If an approximation at the equation level had been used, no impulses would appear.† Clearly, ignoring the impulses brings us "closer" to such a type of approximation in the sense of yielding a solution differing less from the exact one. The differences, however, although smaller, do not average out, and the overall result is, as expected, not so good.

Considering the crudeness of this graphical method B, it is an additional advantage that the results tend to be conservative, yet fairly close to the experimental values.

A last comment is necessary here. We pointed out the fact that in case 1, where we had the (in practice) exact values of all the circuit components,

† This would also be true if the approximation at the model level had a smooth characteristic (i.e., continuous with differentiable first derivative), which is not the case of the piecewise linear function $\varphi(x)$.

including known constant capacitors the agreement is as good as one can possibly have. So, we infer that part of the error obtained in case 2 should be blamed on nonconstant capacitances and the necessarily incorrect values taken for them.

6.4.2 Approximate Graphical Method B

Figure 34 and the description given in subsection 4.4.3 entirely complement each other.

$$\lambda_0 = \frac{dy}{dx}(x_{IO}) = \frac{nW}{ay_0} - \frac{b}{a} = \frac{n}{m} - \frac{b}{a} = 0.0745$$

with a, b, m, n calculated for $\nu\mu$ = Il. And

$$\lambda_d = \frac{dy}{dx}(+\frac{1}{\gamma}) = \frac{d - c/\gamma}{ay_d} - \frac{b}{a} = 0.0757$$

where $y_d = 2.52$ is obtained from the graphical construction itself.

$\lambda_{\beta Il}$ and $\lambda_{\beta IIIl}$ are given in Table XII. Observe that, in order to obtain a closer detailed approximation, we have taken $\ell = 0$.

The numerical values of the ordinates of the break points are presented together with the graph in Fig. 34 itself.

Successive application of equation (4.21) to the five branches a, b, c, d, e, of the piecewise linear approximate phase plane path yields the time intervals over these five phases of the transition.

This is certainly not true, and is actually a somewhat crude approximation, consistent with good results for two reasons: region II is relatively narrow, so this assumption affects little the value of T_A, and the error propagates only to region III, yielding poor values of T_B, but still good values of T_T.

The following variation of method B is less subject to this restriction:

a) Instead of assuming the path to be a line of slope $\lambda_{\beta III}$ inside region II, we draw the lines of slope $\lambda_{\alpha III}$ and $\lambda_{\beta III}$ through point X_{III}, and we draw, through P_a, an approximate hyperbolic arc consistent with the two asymptotes. This arc shall be taken as an approximation to the trajectory inside region II, and its intersection with the line $x = +\frac{1}{\gamma}$ determines the ordinate y_d of P_d (we take $\ell = 0$).

b) We proceed in region III as for the regular method B.

The results are presented in Table XVI, along with corresponding experimental values. Notice that this method allows us to distinguish more distinct phases of the path, i.e., one phase for each value of $\frac{dy}{dx}$ (over this approximate broken line path).

We can see that the agreement is exceedingly good for region I and II, even for the detailed shape of the curve, but it is not so good in region III.

The difficulty is mostly due to the calculation of the branch in the active region. Any small error in the calculation of point y_d is magnified throughout region III, so, even with a numerical method we should expect larger errors in region III. Even the variations of temperature would cause errors by changing the transistor-pair characteristic through $\frac{q}{kT}$ affecting especially the boundaries of region II.

So far we have assumed that the trajectory is a straight line of slope $\lambda_{\beta III}$ throughout region II.

c) Guided by the straight lines in region I and III, and by the points P_a and P_d, we draw the parabolic arcs in region I and III, and join them smoothly by a suitable arc inside region II, so that these three arcs form a curve which shall be taken to be an approximation to the real trajectory.

TABLE XV. COMPARISON OF TIME INTERVALS OBTAINED BY METHOD B WITH EXPERIMENTAL RESULTS

Time Interval (in nsec)		Over Branch
Theoretical (by Methcd B)	Experimental	
23.5	22	a
32.6	30	b
56.1	52	a and b, i.e., region I
19.0	22	c, i.e., region II
18.1	26	d
30.2	38	e
48.3	64	d and e, i.e., region III
124.3	138	Total Transition Time

TABLE XVI. COMPARISON OF TIME INTERVALS OBTAINED BY A VARIANT OF METHOD B WITH EXPERIMENTAL RESULTS

Time Interval (in nsec)		Over Branch
Theoretical (by a Variant of Method B)	Experimental	
20.1	22	a
35.2	30	b
55.3	52	a and b, i.e., region I
12.0 + 8.9 = 20.9	22	c and d, i.e., region II
23.3	26	e
30.6	38	f
53.9	64	e and f, i.e., region III
130.1	138	Total Transition

d) Now we draw a convenient piecewise linear approximation to this curve and, by repeated applications of equation (4.21) to its linear branches, we can calculate the corresponding time intervals.†

Note, in Table XVI, that the tendency persists for longer theoretical time intervals in region I, and shorter in region III, but results are somewhat better than those for plain method B. Note also that, since this method makes use of a degree of arbitrariness, results are bound to vary a little with the operator's judgment.

6.4.3 Iterative Numerical Method

The iterative numerical method offers no special difficulty. It is clear that equation (4.4b) converges in every region.†† The values of M_α, Q_α, M_β, Q_β as well as the computed ordinates y_0, y_a, y_d, and y_e are shown in Table XVII. We have again taken $\ell = 0$.

A direct application of equation (3.58) for each region yields the respective time durations, which are presented in Table XVIII.

Notice that the results are somewhat better than for the other methods, but they are not perfect. It is even worse for region II. However, this numerical method is the exact solution of the differential equation, so we conclude that an error is due:

---

† We might be tempted to use equation (3.58) but this could be disastrous. This equation is valid only for points exactly on a true trajectory, and is very critical. If the points are only approximately on a trajectory, the results obtained by use of (3.58) will probably be meaningless.

†† A rule of thumb is to work always with the large magnitude exponent $\frac{\lambda_\alpha}{\lambda_\beta}$.

TABLE XVII. PARAMETERS AND TRAJECTORY KEY ORDINATES FOR THE ITERATIVE NUMERICAL METHOD

	Region I	Region II	Region III
M_α	20.68	-11.82	24.32
Q_α	$26.32 - y_0 = 24.13$	$-7.65 - y_a = -9.716$	$29.45 - y_d = 28.24$
M_β	2.105	1.15	2.44
Q_β	$2.68 - y_0 = 0.49$	$0.744 - y_a = -1.322$	$2.955 - y_d = 1.741$
$y_0 = 2.19$	$\Rightarrow y_a = 2.066$	$\Rightarrow y_d = 1.214$	$\Rightarrow y_e = 2.294$

TABLE XVIII. COMPARISON OF TIME INTERVALS OBTAINED BY THE ITERATIVE NUMERICAL METHOD WITH EXPERIMENTAL RESULTS

Time Interval (in nsec)		Region
Theoretical	Experimental	
58.4	52	I
31.3	22	II
61.6	64	III
151.3	138	Total

a) to the piecewise linear approximation use for the most exact nonlinear differential equation.

b) to assumptions of lumped parameters, constant in each region.

c) to the measurement of circuit parameters and transistor constants.

d) possible departure of the transistor characteristics from the ideal one we have assumed.

e) the imperfection of the rectangular trigger used in the experiments.

Under the above considerations the error of about ten per cent in total transition times, along with the good agreement in waveform (in the case of method B, for example) is a satisfactory result.

7. CONCLUDING REMARKS

7.1 Summary

The purpose of this investigation was to describe in detail the operation of flipflops from a mathematical point of view, and to devise, based on this mathematical description, practical methods of analysis, design and optimization of both flipflop and triggering circuits.

The mathematical description has been accomplished with the establishment of equations (2.87), (2.88) and (2.90) in Chapter 2, and with those qualitative aspects of their piecewise linear approximations--equations (2.99), (2.100), (2.102)--which clearly apply to the original system.

Methods of analysis and design were devised by means of a detailed study on the phase plane of the piecewise linear equations, taken as approximations to the original nonlinear equations. The singularities of the system, the conditions for their existence and the dependence of their nature upon the system parameters, have been thoroughly described. The phase plane portrait of the system was described with some emphasis on separatrices, trajectories, and the influence of the singularity corresponding to a given region, whether this singularity exists in its proper region or has a virtual image in another region.

Based on this study some engineering methods of analysis and design have been described in Chapter 4, and some simplified formulae for the rapid estimate of flipflop behavior have been presented in Chapter 5.

The experimental example presented in Chapter 6 illustrates the use of some of these methods, and also, by comparing theoretical with practical results, some feeling is obtained for the adequacy of the various methods and for the type of approximations (piecewise linear at the model level) used in the theory.

7.2 Conclusions

It is apparent that we have obtained a useful and, for most practical purposes, adequate theory.

We feel, however, that there are some questions to which we do not have even unsatisfactory answers. A first question is: why is it that the best of all methods when applied to the active region yields a path which obviously differs considerably from the true path? Even the crude device of assuming the path, in region II, to be a constant equal to y_a would produce a result closer to the true one in that region!

Another question is: why is it that results are worse if the impulses (second derivatives of $\Phi(x)$) are considered than the results we get when they are ignored?

We feel that the answer lies in a more detailed study of the relationship between a nonlinear differential equation (especially of the second order!) and another equation which formally is a piecewise linear approximation to the nonlinear one. Specifically, what are the effects of

a) the break points (error in derivatives!)

b) the error itself

c) the constancy of coefficients

on the solution of the approximate equation with respect to the original one? The present investigation gives the impression that this type of approximation should be studied in detail and formalized.

7.3 Further Investigations

There are three directions for further investigation:

a) The study of approximate solutions to nonlinear differential equations by use of solvable formally approximate equations to the original one, such as

piecewise linear equations or other standard types of equations with known solutions.

b) The polishing of the present theory by considering other types of approximation, such as, for example, approximation at the equation level.

c) Application of the ideas we have described to more complex situations, for example,

(i) considering the nonlinearity of parasitic capacitances,

(ii) taking the collector-base junction capacitances into account,

(iii) considering inductances in the passive circuit,

(iv) considering the distributed nature of some of the parasitic capacitances.

Advances in one, some, or all of these directions would certainly improve the present-day techniques of switching circuit design for digital computers.

BIBLIOGRAPHY

1. Andronow, A. A. and C. E. Chaikin: Theory of Oscillations. Princeton University Press, 1949.

2. Beaufoy, R. and T. T. Sparkes: "A Study of the Charge Control Parameters of Transistors," Proc. IRE (October 1960) pp. 1696-1705

3. Bashkow, T. R.: "Stability Analysis of a Basic Transistor Switching Circuit," Proc. N.E.C., 1954

4. Cunningham, W. J.: Introduction to Nonlinear Analysis. McGraw Hill Book Company, Inc., 1958

5. Greiner, R. A.: Semiconductor Devices and Applications. New York: McGraw Hill, 1961

6. Hedvig, Thomas Ivan: "The Determination of Optimum Paths in the Phase Plane for Dynamical Systems Using Calculus of Variations Techniques." Electrical Engineering Doctoral Thesis, University of Illinois, 1961

7. Hughes, William Lewis: Nonlinear Electrical Networks. New York: Ronald Press, Co., 1960

8. Ince, E. L.: Ordinary Differential Equations. New York: Dover Publications, 19

9. Krylcff, N. M. and N. Bogoliuboff: Introduction to Nonlinear Mechanics. (Annals of Mathematics Studies, No. 11) Princeton University Press, 1943

10. Lebow, L., R. H. Baker and R. E. McMahon: "The Transient Response of Transistor Switching Circuits," Tech. Report 27, Mass. Inst. of Technology, 1953

11. Lefschetz, S.: Lectures on Differential Equations. (Annals of Mathematics Studies, No. 14) Princeton University Press, 1946

12. Liapounov, A. M.: Problème Général de la Stabilité du Mouvement. (Annals of Mathematics Studies, No. 17) Princeton University Press, 1947

13. Linvill, J. G.: "Nonsaturating Pulse Circuits Using Two Junction Transistors," Proc. IRE, vol. 43 (July 1955) p. 826

14. Liu, Ruey-Wen: "Two Dimensional Autonomous Oscillatory System Solution without Approximations by Analogy to Classical Dynamics," Electrical Engineering Doctoral Thesis, University of Illinois, 1960

15. Middlebrook, R. D.: An Introduction to Junction Transistor Theory. New York: Wiley, 1960

16. Millman, Jacob and Herbert Taub: Pulse and Digital Circuits. McGraw Hill Book Company, Inc., 1956

17. Minorsky, N.: Introduction to Nonlinear Mechanics. Ann Arbor: Edward Bros., 1947

18. Murphy, George M.: Ordinary Differential Equations and Their Solutions. Princeton (N. J.): Van Nostrand, 1960

19. Poppelbaum, W. J. and N. E. Wiseman: "Circuit Design for the New Illinois Computer," University of Illinois, Digital Computer Laboratory Report No. 90, August 20, 1959

20. Pressman, Abraham I.: Design of Transistorized Circuits for Digital Computers. New York: Rider, 1960

21. Shockley, William: Electrons and Holes in Semiconductors. Princeton (N. J.): D. Van Nostrand Company, Inc., 1950

22. Stoker, J. J.: Nonlinear Vibrations in Mechanical and Electrical Systems. New York: Interscience Publishers, Inc., 1950

23. Tillman, J. R.: "Transition of an Eccles-Jordan Circuit," Wireless Eng. (1951) pp. 101-110

24. Valdes, Leopoldo B.: The Physical Theory of Transistors. New York: McGraw Hill, 1961

25. Vallese, L. M.: "On the Synthesis of Nonlinear Systems," Proc. Symp. Nonlinear Circuit Analysis, Polytechnic Inst. Brooklyn (1953)

26. Vallese, L. M.: "A Note on the Analysis of Flip-flops," Symposium on Nonlinear Circuit Analysis, Polytechnic Inst. Brooklyn (April 25-27, 1956)

27. Vallese, L. M.: "Transient Analysis of Second Order Flip-flops," Trans. AIEE, Communications and Electronics (1957)

28. Wilf, Herbert S.: Mathematics for the Physical Sciences. New York: John Wiley, 1962